

PART I
INVESTIGATION OF THE "VAPOUR SNAKE" PHENOMENON

PART II
A COMPARISON OF THE PRODUCTION OF ACTIVE NITROGEN
by
THE ELECTRODELESS AND CONDENSED DISCHARGES
and
ITS REACTIONS WITH OXYGEN CONTAINING COMPOUNDS

by
Roger H.C. Verschingel

A thesis submitted to the Faculty of Graduate
Studies and Research of McGill University in
partial fulfillment of the requirements for
the Degree of Doctor of Philosophy

McGill University

April, 1955

Suggested Library Title

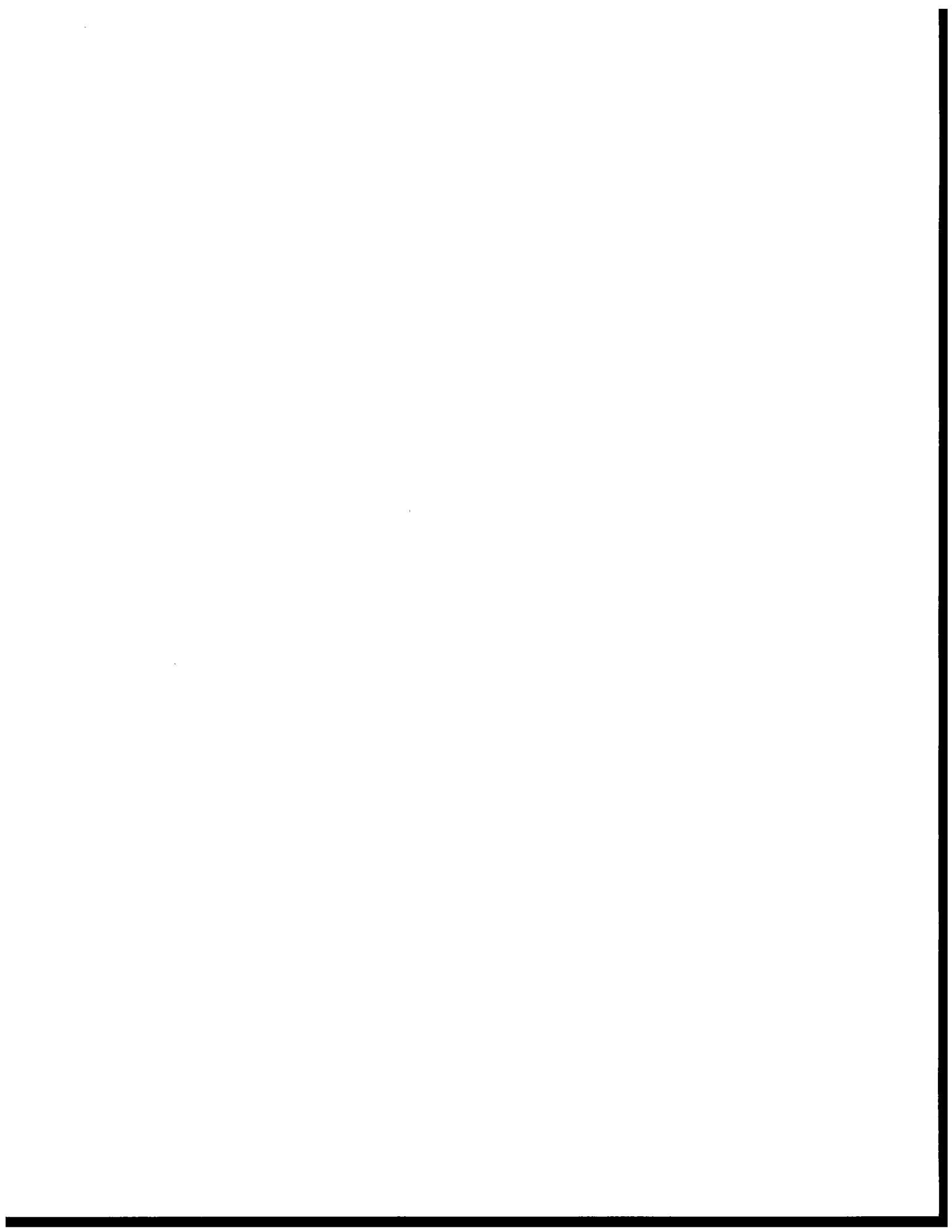
I. "VAPOUR SNAKES" - II. ACTIVE NITROGEN REACTIONS WITH OXYGEN COMPOUNDS

R. Verschingel

ACKNOWLEDGEMENTS

Appreciation is expressed to the National Research Council of Canada for the granting of two Studenships.

The author also wishes to acknowledge the advice and criticism of Dr. H. I. Schiff under whose direction this work was performed.



PART I

INVESTIGATION OF THE "VAPOUR SNAKE" PHENOMENON

TABLE OF CONTENTS

INTRODUCTION

	Page
DESCRIPTION OF THE PHENOMENON	1
PURPOSE OF THE PRESENT INVESTIGATION	7

EXPERIMENTAL

REAGENTS	8
APPARATUS	8

RESULTS

Results	11
The Role of the Crust	14
Nature of the Gas Within the Bubble and Tubule	15
Temperature Range	16
Rate of Travel of the Tubule	17
Size of the Tubule	17
Wall Thickness of the Tubule	18
Previous History of the Sample	19
Effect of Impurities	20
Appearance of the Crust	20
Presence of a Hole in the Crust	21
A Similar Phenomenon in the Vapour Region	24

DISCUSSION

PROPERTIES OF COMPOUNDS GIVING THE PHENOMENON	26
MECHANISM OF TUBULE FORMATION AND PROPAGATION	29
EXISTENCE AND ROLE OF THE VAPOUR CONDUCTION MECHANISM	32

	11
CRYSTALLIZATION VELOCITY AND THE PHENOMENON	35
<u>SUMMARY</u>	
.....	38
<u>BIBLIOGRAPHY</u>	
.....	39

INTRODUCTION

DESCRIPTION OF THE PHENOMENON

The term "Vapour Snake" was first associated with a rather unusual phenomenon by Phibbs and Schiff (1). This phenomenon was reported to occur upon the immersion of an ampule of pure degassed cyclohexane in a dry ice-acetone freezing mixture. A solid crust first formed on the surface of the liquid, while a thin sheath of glassy solid appeared below the liquid level next to the walls of the ampule - the rest of the cyclohexane remaining liquid. Then a small vapour bubble appeared directly below the crust and developed into the form of a thin snake-like tubule which extended rapidly into the liquid. The tip of the "snake" travelled throughout the liquid, changing direction upon meeting an obstacle and thereby leaving an interwoven trail. Meanwhile, the liquid gradually solidified from the walls of the ampule so that the interwoven trail of the "snake" became incased in the glassy solid.

The "snake" continued to travel as long as there was some liquid left. Visible crystallization occurred at the walls of the "snake" about 1 cm. behind its tip and extended slowly outwards to the glassy solid.

The "snake" was described as a vapour tubule defi-

nately hollow over its entire length. It travelled at a rate of about 3 cm. per second.

The phenomenon was reported to be very sensitive to slight traces of air; the introduction of a small air bubble completely destroyed the effect and resulted in spontaneous crystallization.

The occurrence of the phenomenon in a few other compounds was investigated by Phibbs and Schiff. Neopentane showed the effect but the crust was often blown off before the "snake" had travelled any distance. Some success was also obtained with benzene and tertiary butyl alcohol, but the "snake" moved much slower in both cases and crystallization occurred at other points besides the liquid-vapour interface. Straight chain hydrocarbons simply froze by crystallization, e.g. decane, and asymmetric compounds formed glasses only, e.g. 3-methyl pentane.

Seki (2) (3) has also observed the phenomenon in cyclohexanol and carbon tetrachloride. His observations were somewhat different from those of Phibbs and Schiff on two counts. First, he reported the presence of a large hole in the crust by which the tubule is in contact with the vapour above the crust. This is clearly shown in the drawings accompanying his initial communication (2). Secondly, in his description of the phenomenon he

stated that the crust formed from the periphery inwards and that the "residual gas seemed to burrow a tunnel in the liquid".

Phibbs and Schiff proposed that the unusual phenomenon be attributed to the high vapour pressure of the compound at its melting point (ca. 35 mm. for cyclohexane at 6.4°C) along with the observed fact that crystallization tended to take place only at a liquid-vapour interface in the absence of dissolved gaseous impurities. As evidence for the latter they presented the observation that only a clear, glassy solid was produced when gradual cooling was applied from the bottom or when the sample was confined in a sealed tube and subjected to a hydrostatic head of 40 mm Hg (so that no vapour could be formed).

They described the process in the following sequence. Upon cooling the sample, crystallization occurs at the surface. Further contraction of the liquid by cooling causes a vapour bubble to form below the crust and as crystals form around this bubble, heat of fusion is liberated which causes further vaporization. The increase in pressure then forces the vapour into a tubule which is propagated through the supercooled liquid by the repeated cycle of crystallization and vaporization. Since the "snake" travels rapidly through the viscous liquid it is not curved up by buoyant forces and is sharply

reflected from obstacles at any but small angles.

Due to the fact that the "snake" appeared to be propelled by a considerable force they favoured a vapour mechanism, the pressure being probably highest at the tip of the "snake" which would therefore be pushed forwards as if jet-propelled.

They concluded that the phenomenon should also occur in other symmetrical compounds which possess high vapour pressures at their melting points.

Seki (3), noting the low vapour pressure at the melting point of the two compounds (cyclohexanol and carbon tetrachloride) in which he observed the phenomenon, maintained that a high vapour pressure at the melting point is not a necessary condition and suggested a connection between its occurrence and the formation of plastic crystals. He also pointed out that by rapidly cooling these substances below their respective solid-solid transition point a polycrystalline state is obtained without intermediate "snake" formation.

In a subsequent communication a different explanation was offered by Frank (4). He agreed with Phibbs and Schiff that a high vapour pressure at the melting point is required but suggested that the fact that crystallization tends to take place at the liquid-vapour interface in the absence of dissolved gaseous impurities was not a

contributory cause of the phenomenon, but rather a parallel effect of the same cause.

Although he conceded the theoretical possibility of an oriented layer of molecules at the free surface of a liquid which should nucleate the solid more rapidly than the different kind of order in the body of the liquid, he concluded that freezing occurred more readily at the free surface because the temperature is lowest there. He then proceeded to explain the "Vapour Snake" phenomenon by a vapour heat transfer mechanism. The transfer of vapour into and through the cavity provided a mechanism of heat conduction additional to that through the solid sheath at the walls, which alone would apply when the tube is not cooled above the liquid surface.

He interpreted the sequence of the phenomenon as follows. The rapid evaporation of liquid from the free surface to the cooled upper walls causes the surface to freeze immediately. Simultaneously, a thin sheath forms at the walls: but this sheath grows in thickness less rapidly than the upper crust since the heat of solidification of the latter is carried away by vaporization to a much larger area of glass walls. Once a solid crust encloses the liquid, further freezing develops a negative pressure which nucleates a vapour bubble. The vaporization of liquid to fill this cavity with vapour removes

sufficient heat to freeze a skin of liquid $1/1000$ of its radius in thickness. In addition vapour transfer in the cavity is accompanied by a heat transfer from the warmer to the cooler points on its surface. The tubule behaves as a conductor of heat by the transfer of vapour to the crust where it condenses. The heat thus liberated at the crust is further transferred to the upper walls of the ampule by evaporation of solid at the free surface.

According to Frank, the rate of increase of the volume of the cavity is determined by the rate of removal of heat of fusion through the glass walls divided by the latent heat of fusion and multiplied by the contraction on freezing. On this basis he concluded that an ampule of different size and shape would give "snakes" of different diameter but of the same rate of increase in length.

He considered the rate of advance of the "snake" as a linear crystallization velocity, and, as such, it appeared that a "record" of 3 cm. per second in measured crystallization velocities had been established.

Frank concluded that the requirements for a well developed "Vapour Snake" phenomenon would appear to be a fairly high vapour pressure at the melting point, a high crystallization velocity, a high ratio of the latent heat of vaporization to the latent heat of fusion and an

initial temperature not high above the melting point. From this point of view he maintained that all the observations made by Phibbs and Schiff were intelligible.

PURPOSE OF THE PRESENT INVESTIGATION

This investigation was therefore undertaken with a view to determine the effect of the following factors:

- 1- symmetry of chemical structure,
- 2- vapour pressure at the melting point,
- 3- heat and entropy of fusion,
- 4- occurrence of solid-solid transitions.

In additons, experiments were devised to test the predictions derived from the previously mentioned explanations. Furthermore the phenomenon was investigated under a wide range of experimental conditions to obtain as much information as possible.

EXPERIMENTAL

REAGENTS

The reagents were obtained from various commercial suppliers. They had to be further purified before any experiments were carried out. The methods of purification varied necessarily from compound to compound and depended upon the impurities present. Standard methods of purification, described in the literature, were employed. In addition, some unavailable substances and others available in only very impure grades were obtained from the supply of pure hydrocarbons of the National Research Council at Ottawa.

APPARATUS

The apparatus consisted mainly of a gas handling manifold in which a high vacuum could be maintained. The high vacuum was necessary for complete degassing of samples. Final purification was obtained by bulb-to-bulb distillation, the initial and final portions being rejected.

Extreme care had to be taken to prevent the apparatus from contamination from solid particles such as those from drying agents or dust particles. Once these were present, the apparatus could no longer be used to prepare samples capable of producing the phenomenon.

The apparatus then had to be dismantled and thoroughly cleaned. To avoid contamination all liquids and gases were introduced through fine porosity glass fritted disks and were removed in the same fashion.

For the purification of high boiling liquids or solids a small high vacuum gas manifold was constructed in a well insulated chamber whose temperature could be raised to 300°C if necessary. These compounds could then be distilled or sublimed without localized solidification in the apparatus. The movable parts of the apparatus were lubricated by a special high temperature vacuum grease supplied by Dr. I. Puddington of the National Research Council at Ottawa.

When temperature measurements were made in the interior of the ampule a thermocouple was introduced into the system through an atmospheric leg of mercury. In this way the thermocouple could easily be moved to any desired positions within the sample without having to disturb the system. A copper-constantan thermocouple was used. It was made of No. 32 gauge wire in order to minimize the heat capacity and thermal conductivity. The portion of the fibrous insulators around the wires which had to be immersed into the compound was first thoroughly cleaned and then boiled with some of the compound in order to prevent any contamination. In addition,

since the insulator around the wires was found to allow the diffusion of air into the apparatus, a portion of the wires had to be stripped of the insulator, imbedded in wax, and placed under mercury at a point just before the wires entered the vertical leg of mercury.

RESULTS

A list of those compounds which give the phenomenon readily is given in Table I. It was observed that the higher the triple point pressure of a compound the more readily did the phenomenon occur. With none of the compounds having a triple point pressure greater than a few mm Hg was it necessary to cool the walls of the ampule above the liquid surface. Actually for those compounds having a triple point pressure greater than 50 mm Hg great care had to be taken to prevent the cooling of the upper walls. Otherwise the pressure inside the tubule under the crust became so much larger than that above the crust that the latter was violently blown off and the growth of the tubule interrupted.

In Table II a few of those compounds in which the phenomenon can only be made to occur with great difficulty are listed. For those compounds, which have a vapour pressure at the triple point in the range of 1-2 mm Hg, it was found necessary to cool the upper walls and even to pump on the sample simultaneously to obtain the phenomenon. Along with those compounds are listed a sufficient number of other compounds which do not show the phenomenon to illustrate clearly which of the factors previously mentioned determine its occurrence.

TABLE I

Compound	Triple point pressure mm Hg	Melting point °K	Fusion entropy eu	Transi- tion temp. °K	Transi- tion entropy eu	Comments
Hexachloro-ethane	760	460	4.35	345	7.2	Very good snakes #
Hexamethyl-ethane	710	377	4.5	148	3.2	Very good snakes #
Camphor	385	453	2.8	250	7.6	Very good snakes #
Neopentane	230	253	3.0	140	4.4	Very good snakes #
Ammonia	46	195.3	9.4	Very good snakes
2-butyne	44	240.9	9.16	153.8	2.0	Very good snakes
Bromine	42	265.9	4.87	Very good snakes
Tert.-butyl alcohol	41	298.6	3.4	Very good snakes
Cyclohexane	40	279.8	2.24	186.0	8.59	Very good snakes
Benzene	35	278.7	8.46	Very good snakes
Tert.-butyl chloride	24	244.7	2.0	219.3	3.0	Good snakes
Carbon tetrachloride	9	250.3	2.3	225.7	4.8	Good snakes
Naphthalene	7	353.4	12.75	Good snakes
Tetranitro-methane	6	286.7	Good snakes
1,1,1,-trichloro-ethane	5	240.5	4.5	224.3	5.0	Good snakes

fine temperature control required

TABLE II

Compound	Triple point pressure mm Hg	Melting point °K	Fusion entropy eu	Transi- tion temp. °K	Transi- tion entropy eu	Comments
Trichloro-acetic acid	1	332	4.2	Poor snakes #
Phenol	1	313.9	8.6	Poor snakes #
Cyclohexanol	1	297	1.4	263	7.45	Poor snakes #
Chloroform	below 1	209.6	10.8	No snake formation
1-butyne	below 1	192.9	No snake formation
Methyl-cyclohexane	below 1	146.6	11.0	No snake formation
Chloro-cyclohexane	below 1	230	2.9	218	7.8	No snake formation
Cyclohexene	below 1	169.7	4.6	138.7	7.2	No snake formation
Cyclopentene	below 1	138.1	5.8	87.1	1.31	No snake formation
Cyclopentane	below 1	179	0.8	122.4	9.6	No snake formation
Cyclohexanone	below 1	169	4.6	139	...	No snake formation
Toluene	below 1	177.9	9.3	No snake formation
Methyl alcohol	below 1	175.3	4.3	157.8	1.0	No snake formation
2,2-dimethyl butane	below 1	172.1	0.64	127.4	8.6	No snake formation

pumping and wall cooling required

The results obtained from the different specific experiments carried out will now be summarized. Unless otherwise stated these results are general in nature and not derived solely from one specific compound.

The Role of the Crust. In order to determine whether the crust is necessary for tubule formation the following experiments were performed:

1. A sample of cyclohexane was confined over mercury so that a closed volume was provided which had no vapour space. This sample was immersed into a bath whose temperature was below the freezing point of mercury. As soon as the mercury froze, a bubble formed at the top of the cyclohexane and developed into a tubule whose behavior was identical in every respect to that previously described.

2. An ampule of cyclohexane was immersed in a freezing bath in the usual manner. However, as soon as the crust had formed the ampule was quickly inverted before the bubble had a chance to form. The bubble then appeared at the top of the sample and produced a tubule which made no contact with the crust.

3. When a sample was allowed to melt after the conclusion of one experiment a vapour bubble occasionally emerged when the melting surface crossed the tubule, and rose to the surface of the liquid. On several occasions

it was possible to form a crust by reimmersing the sample in the bath just as one of these bubbles was emerging from a small amount of remaining solid. If the process was properly timed a new tubule developed from this bubble and grew in the usual manner, having no contact with the crust. At no time was it possible to have two tubules developing at the same time in the same liquid region.

Thus it appeared that the sole function of the crust is to provide a closed volume for the system. This is best illustrated by the first experiment mentioned in which no tubule developed as long as the mercury was still liquid, the contraction in volume of the cyclohexane in the ampule causing more mercury to flow in. Once the mercury solidified however, a further contraction in volume due to continued cooling resulted in the formation of a bubble which then developed into a tubule.

Nature of the Gas Within the Bubble and Tubule.

These bubbles and tubules have been identified as composed of the vapour of the compound and not of foreign gas. This was demonstrated by allowing a bubble to form in a closed volume, either under the crust or elsewhere, and then warming and cooling the sample alternatively so as to prevent the bubble from expanding into a tubule and the crust from melting. Upon warming the sample, the

liquid expanded in volume and the bubble decreased in size: when cooled the liquid contracted and the bubble again increased in size. This variation in volume of the bubble could be produced at will. Now, considering the small area of the bubble, it would be impossible to expel and dissolve foreign gases at the above rates. On the other hand the liquid could readily evaporate and vapour condense to fill or deplete the bubble.

Temperature Range. The phenomenon was found to occur at all bath temperatures from 0.1°C below the melting point to -196°C . The lower limit was of no particular significance due to radial heat conduction uncertainties.

For those compounds whose vapour pressure at the triple point is of the order of 1 to 2 mm Hg it was found necessary to use cooling baths well below the freezing point to form the crust and even some pumping on the sample. Nevertheless the tubule was shown to travel in a medium just below the freezing point by thermocouple measurements.

The tubule could travel in a liquid medium up to 10 degrees above the melting point, as indicated by thermocouple measurements, if the removal of heat was rapid. On the other hand there was never an indication of any super-cooling occurring within the liquid.

Rate of Travel of the Tubule. For a given ampule the colder the cooling bath the greater the velocity of the tubule and the smaller its diameter. At a given bath temperature a decrease in the diameter of the ampule resulted in an increase in the velocity and a decrease in the diameter of the tubule.

Velocities varying between 0.001 cm/sec and 5 cm/sec were obtained. These velocities are by no means limiting velocities since with a proper bath temperature a tubule could easily be stopped in its path for as long as ten minutes before being allowed to develop further. On the other hand the upper limit could not be determined with any accuracy since at the higher velocities the tubules tended to seal themselves. An estimate of the upper limit would be approximately 10 cm/sec. It is to be noted that the upper limit varied from compound to compound and for those compounds which gave the phenomenon only with great difficulty the tubules never travelled more than a fraction of a centimeter per second.

Size of the Tubule. The size of the tubule was governed by the rate at which it travelled, the faster the rate the smaller its diameter. In the limiting case of a bath temperature just below the freezing point the tubule grew in a spherical shape, never reaching the tubule stage, or a previously developed tubule could be

made to grow further into a spherical shape.

If the ampule was allowed to remain in a cooling bath 10 to 20 degrees below the melting point the tubule decreased rapidly in size as the velocity increased. Although the tubule would decrease from 5 to 10 times in diameter, it nevertheless did not terminate before all the liquid was solidified. From repeated experiments it appeared that the product of the velocity and cross section of the tubule remained essentially constant.

Wall Thickness of the Tubule. The sheath surrounding the bubble from which the tubule develops is initially very thin. This was observed by the ease with which the bubble could be made to migrate under the crust in experiments where the bath temperature was only a fraction of a degree below the freezing point. For lower bath temperatures the thickness of this sheath was found to increase rapidly and take on the appearance of a glass. Irrespective of the bath temperature, the sheath surrounding the bubble and tubule increased in rigidity with time and took on the appearance of a glass.

White crystals were found to start growing on the outside of the bubble sheath once the tubule is formed. A similar growth developed on the walls of the tubule at a distance of one centimeter from its tip. The white crystallization did not penetrate the glassy sheath.

The existence of the thick walls of the tubule could best be seen if the sample was warmed up after the tubule had progressed for some distance. The liquid was then forced back into the tubule by expansion, whereupon wall or sheath thicknesses up to 1 mm. could be observed. Upon reimmersing this sample into the bath the liquid was again expelled from the tubule which then continued in its previous direction. This occurred in preference to the formation of a new bubble and new tubule as long as some vapour still remained in the old tubule and if the time lapse between warming and recooling was not too great.

Previous History of the Sample. The previous history of the sample was found to have no effect upon the phenomenon. A sample of cyclohexane kept at 100°C for two months showed the same behavior as one freshly prepared or previously frozen.

One notable exception, however, was observed. When cyclohexane was kept at less than 0.1°C above its freezing point for at least one-half hour and then immersed in a bath at least 40 degrees below its freezing point no bubble and tubule developed. Instead, the crust extended downwards until the entire sample became an opaque mass of small crystals. The growth of the transparent glassy solid at the walls of the ampule was not affected

however. This may be due to some degree of orientation attained by the liquid under these conditions.

Effect of Impurities. The effect varied with the nature of the impurities. Gases such as air and nitrogen, which were not liquid at the temperature of the experiment, when introduced into the ampule at pressures in excess of 20 mm Hg prevented the occurrence of the phenomenon. The presence of small traces of these gases resulted in the formation of an opaque solid instead of the transparent, glassy solid at the walls of the ampule. More than one percent by volume of miscible liquids, even those which produce the phenomenon themselves, caused crystallization to occur throughout the sample, instead of tubule formation. The presence of small traces of liquid impurities caused an opaqueness similar to that brought about by traces of non-condensable gases.

Trace amounts of solids, irrespective of their chemical nature, invariably caused crystallization to occur without tubule formation. Under these conditions super-cooling readily occurred and then the liquid would completely solidify, the particles serving as nucleating centers.

Appearance of the Crust. The character of the crust varied according to the cooling rate. If the cooling bath was only a few degrees below the freezing point the

crust was transparent and free of polycrystalline solid at first. It appeared to be subjected to some tension, for it slowly developed cracks or fissures from which white crystallization proceeded. Rapid cooling always produced a large amount of white crystallization which grew downwards. The walls of the tubule behaved exactly as the crust. On the other hand the glassy solid formed at the walls of the ampule remained transparent during the entire course of the experiment and was never accompanied by white crystallization.

When the glassy solid was cooled at liquid air temperatures it developed numerous fissures, accompanied by sharp noises which indicated a considerable volume change. This was most noticeable when only the glassy solid was formed by cooling below the liquid-vapour level and thus preventing tubule and white crystallization from developing. This glassy solid, upon melting slowly, did not liberate gaseous bubbles as did the white solid, and its presence in the liquid did not prevent tubule formation upon further cooling.

Presence of a Hole in the Crust. In the case of benzene a small hole was noticed in the crust directly above the origin of the tubule. The size of the hole increased with increasing cooling rates. Smaller holes were also noticed in some other compounds when the rate

of cooling was sufficiently rapid. It must be pointed out here that these holes were not necessary for the occurrence of the phenomenon. This was readily demonstrated by simply shaking the ampule after the bubble had formed under the hole. The bubble would then move away from the hole to another position under the crust and the tubule could then be made to develop in the usual manner.

In the case of benzene this led to two variations of the phenomenon. It had been observed during some experiments with benzene that sometimes part of the liquid rose through the hole and flowed over the top of the crust during warming of the ampule. Upon further investigation it was found possible to reproduce this at will under specific experimental conditions.

First the crust was formed and the tubule started in the usual manner. After the tubule had developed for a few centimeters, and while its tip was still pointing downwards, its growth was interrupted by removing the ampule from the bath. Once the tip of the tubule had burst open and the liquid had started to recede back into it, the lower part of the ampule was rapidly warmed up by holding it in the hand, taking care not to warm the region near the crust. In this fashion a pressure was developed in the closed volume under the crust.

The crust being still rigid and strong, the pressure was relieved by the liquid rising through the tubule and overflowing unto the crust. Depending on the rate of warming of the lower part of the ampule, which governed evaporation under the crust, the rise of liquid proceeded slowly or like a gusher. Up to half the liquid could be made to rise above the crust at rates up to 5 milliliters per second.

The resulting system consisted now of two liquid layers interconnected by the previously formed tubule and the upper one supported by the old crust. The two layers were separated by a vapour layer for if the ampule was slightly cooled the liquid above the crust flowed back under the crust through the tubule as the pressure was decreased there. The upward flow of liquid obviously stopped when the vapour pressure above each liquid layer became equalized.

When this two liquid-layer system was immersed in a bath about 10 degrees below the freezing point two new crusts formed and under each one a bubble appeared from which a normal tubule again developed. During the entire process the first tubule remained intact.

It was even possible to repeat this procedure twice in succession on the same sample, thus obtaining four liquid layers joined by three tubules and then to develop

four tubules simultaneously, one in each liquid layer. These experiments very well illustrated the rigidity and thickness of both the crust and the walls of the tubule. They also demonstrated that any type of closed volume was sufficient to bring about the occurrence of the phenomenon, and that only one tubule developed in each closed volume.

A Similar Phenomenon in the Vapour Region. This variation was most spectacular with benzene, but could be obtained to a lesser degree with other compounds which gave the phenomenon readily.

In benzene it could readily be obtained by employing the following procedure. The ampule containing the pure degassed benzene was immersed in a bath at about -10°C until the tubule started downwards. The ampule was then immediately removed from the cooling bath and kept in air at room temperature to warm up slowly (best results were obtained if the tubule was stopped while still in its downward path). The moment the solid, formed by distillation from the liquid surface to the walls of the ampule above the crust, started to melt and flow downwards, the ampule was immediately immersed in a cooling bath at -20°C (at lower bath temperatures the phenomenon was too rapid to be observed). Then either one of two things was observed to take place:- a tubule started to travel

upwards from the hole in the crust, or the liquid simply syphoned upwards. With care, an upwards travelling tubule could be obtained on the average of about once every second trial.

The upwards travelling tubule is identical to the tubule formed in the liquid medium, except that it is originally filled with liquid instead of vapour. It always started as the hole in the crust and had rigid, transparent, glassy walls at first, although they rapidly became coated with white crystallization. It changed direction upon meeting a solid obstacle and at the end left a solid interwoven pattern above the crust.

Because of the rapid cooling rate required, the tubule could never be made to travel at a rate less than one centimeter per second. During its growth it always gained speed rapidly, ending up with velocities probably well in excess of 10 cm/sec. Greater velocities would probably have been attained if it were not for the fact that the tubule terminated between 2 to 5 seconds after starting when its tip became sealed. As much as 10 cc. of the liquid could be used up in a few seconds as indicated by the empty space under the crust at the end of the experiment. This liquid was transported through the solid tubule which was still hollow at the end of the experiment.

DISCUSSION

PROPERTIES OF COMPOUNDS GIVING THE PHENOMENON

From the observations recorded in Tables I and II it is evident that the vapour pressure at the triple point is of critical importance. Thus, compounds with a vapour pressure in excess of 50 mm Hg give the phenomenon with great ease, but the difference in pressure below and above the crust must be regulated by a fine temperature control, or the crust is simply blown off. Compounds with a vapour pressure in the range of 30-50 mm Hg give very good tubules. It is in this vapour pressure range that the second phenomenon could also be made to occur above the crust. In the vapour pressure range of 5-30 mm Hg good tubules are still obtained, but they cannot be made to travel as fast as those with compounds having higher vapour pressures.

Compounds with a vapour pressure of 1-2 mm Hg still manifest a tendency to give the phenomenon. For these, the tubule travels so slowly that in fact only a central cavity or hole is left after the upper portion of the liquid is solidified by rapidly cooling and pumping, while the volume contraction takes place. Compounds with vapour pressures below 1 mm Hg cannot be induced to form a crust under any set of experimental conditions.

This contradicts Seki's (2) (3) contention that a high vapour pressure at the triple point is not a necessary condition for the occurrence of the phenomenon. It may be pointed out that his description of the phenomenon in his first communication is similar to that found for compounds in the range of 1-2 mm Hg of vapour pressure. These compounds did not produce good tubules, irrespective of the experimental conditions.

Furthermore, it was found that there is no connection between the formation of plastic crystals and the occurrence of the phenomenon as was suggested by Seki. Plastic crystals, according to Timmermans (5), are produced only by those compounds which have low entropies of fusion and relatively high entropies of transition. However, no allotropic forms of benzene have been reported in the numerous and precise determination of the heat capacity of this compound below its freezing point. Nevertheless, benzene gives the phenomenon readily.

Upon examination of Table I it is readily seen that the compounds which have high vapour pressures at their triple point may be subdivided into two groups. The first group corresponds to those which give plastic crystals; they have relatively low entropies of fusion and high entropies of transition. The second group comprises those compounds which have high entropies of fusion,

between two to five times higher than those of the first group, and no transition points, or, if a transition point is known, the entropy of transition is low compared to the fusion entropy.

On the other hand compounds like cyclohexene, cyclopentane and others listed in Table II have transition points and form plastic crystals, but since their vapour pressures are too low they do not give the "Vapour Snake" phenomenon.

In addition to high vapour pressures at their triple point, the compounds which show the phenomenon have apparently only one other property in common. Their molecules are more or less spherical in effective volume and were given the designation of "globular molecules" by Timmermans (6) who carried out a diversified study on these molecules. Thus a high degree of physical symmetry leads to a high vapour pressure at the triple point with or without the formation of plastic crystals.

A detailed study of the physical symmetry was undertaken by van de Vloed (7). He arrived at the conclusion that a chlorine atom was identical to a methyl group in so far as similar physical properties are concerned from a study of carbon tetrachloride and tert-butyl chloride for instance. Both these compounds show a similar "Vapour Snake" phenomenon. Van de Vloed also showed

how easily this volume symmetry could be destroyed by the substitution of a methyl group or a chlorine atom for an atom of hydrogen in cyclohexane. Correspondingly it was observed that while cyclohexane gave the phenomenon, methyl cyclohexane, chloro-cyclohexane and cyclohexene did not give the phenomenon. Similarly the phenomenon occurred with benzene but not with toluene. Thus substitution of a group of different physical size destroyed the physical symmetry and lowered the vapour pressure sufficiently to prevent the occurrence of the phenomenon.

MECHANISM OF TUBULE FORMATION AND PROPAGATION

A simple mechanism for the formation and propagation of the tubule can be formulated. Removal of heat from the system causes a volume contraction. If the volume of the system is fixed, either by forming a crust above the liquid by rapid distillation or by other means, this contraction produces a negative pressure sufficiently large to yield a cavity which takes on the shape of a bubble for minimum surface energy. This bubble is immediately filled with vapour at a pressure equal to the vapour pressure of the liquid. Because of the high triple point pressures of these compounds, considerable mass transfer will occur from the liquid to the vapour phase per unit change in volume of the liquid. Since the heats of evaporation of these compounds are normal,

while their heats of fusion are low, this large mass transfer will result in solidification at the liquid-vapour interface, if the temperature of the liquid is near the freezing point. Consequently, the vapour bubble will become incased in a solid sheath.

If the cooling is rapid the contraction per unit time is large and evaporation will proceed faster. This results in a greater cooling rate at the liquid-vapour interface which leads to a much faster solidification of the sheath surrounding the bubble. In addition the transfer of vapour within the bubble from the liquid to the cold spot, whether it be the crust or the walls of the ampule, is accelerated due to the greater temperature gradient present on more rapid cooling.

As contraction of the liquid continues the bubble must grow further since it possesses a positive pressure. It is prevented from growing spherically by the acquired rigidity of the sheath and therefore develops in the direction of the weakest part of the sheath — that which has been formed last and is farthest away from the cold surface where the bubble is located. Hence, it will grow in the form of a tubule, expanding only at its tip.

It will travel at a rate governed by the rate of volume contraction and by the rate of vapour transfer within the tubule to the cold spots at the crust and on

the walls. The increasing velocity of the tubule accompanied by a decrease in its diameter during the course of its development cannot be accounted for by an increase in the rate of volume contraction. Up to a fivefold increase in the velocity of the tubule could be detected while the temperature of the liquid decreased only by a few degrees and the rate of freezing remained essentially constant.

An increase in velocity after a few seconds can be explained only by the fact that as the tubule acquires more cold spots, more vapour is condensed and solidified, resulting in an increase in the vapour transport within the tubule. The cold spots of the tubule, either at the walls or at the crust, are the only points where a large temperature gradient exists between the tip of the tubule and the cooling medium. Thus, as the vapour transfer becomes more rapid, more vaporization must occur at the tip of the tubule to maintain the pressure equilibrium between the liquid and the vapour region within the tubule. In so doing, the cooling rate at the tip of the tubule is markedly increased, causing the walls to solidify more rapidly and thereby expanding to a smaller diameter. This is in agreement with the constancy of the product of the tubule velocity and cross section observed for a given cooling rate. In addition, it points out

that the heat conduction through the liquid is negligible compared to the vapour heat conduction.

The same explanation applies in the cases where a hole was noticed in the crust, since the liquid is still confined to a closed system. The occurrence of the similar phenomenon in the vapour phase above the crust is thereby also explained, remembering that here we have liquid conduction through the tubule due to the large pressure gradient purposely developed to supply the large amount of material required to form the walls at the rates previously mentioned.

EXISTENCE AND ROLE OF THE VAPOUR CONDUCTION MECHANISM

In the formulation of a mechanism for the phenomenon it was found necessary to postulate a vapour conduction process in addition to the simple evaporation of liquid to fill the volume contraction. Simple calculations show that the thickness of the sheath which would be formed if the first process was not operative would be quite small. Thus, if we consider that the heat liberated by fusion is removed by simple evaporation we have:

$$w_s L_f = w_v L_e \quad (1)$$

where w_s and w_v are the weight of solid and vapour formed, L_f the latent heat of fusion and L_e the latent heat of evaporation.

Assuming that the simple gas law is applicable at

these low pressures, we have:

$$w_v = \frac{V_v PM}{RT} \quad (2)$$

where V_v is the volume of the vapour, P the vapour pressure, M the molecular weight of the vapour, R the gas constant and T the freezing point. Since the volume of the vapour must equal the volume of the spherical bubble, equation (2) becomes

$$w_v = \frac{4/3 \pi r^3 PM}{RT} \quad (3)$$

where r is the radius of the bubble.

Now the weight of the solid w_s equals the density of the solid, d , multiplied by the volume of the solid, V_s . The volume of the solid constitutes the volume of the sheath of the bubble, and since the volume of a thin spherical shell of thickness t is given by the formula $V_{shell} = 4\pi r^2 t$ we have:

$$w_s = 4\pi r^2 t d \quad (4)$$

Substituting the values of w_v and w_s , from equations (3) and (4) respectively, into equation (1) we have:

$$4\pi r^2 t d L_f = \frac{4/3 \pi r^3 PM}{RT} L_e \quad (5)$$

and rearranging equation (5) to obtain t we have:

$$t = \frac{r M P L_e}{3 d R T L_f}$$

The thickness of the sheath for a bubble of 1 mm. radius in cyclohexane would be 0.001 mm. For a tubule of the same radius the sheath would be even thinner. Although the sheath may be as thin as this at the tip of the tubule it is thicker a short distance behind the tip. The average thickness being somewhere between 0.5 and 1.0 mm. Since it has been shown that the liquid need not be supercooled, the tubule being capable of traveling through the liquid at or near the freezing point and even through a liquid whose temperature is as high as 10 degrees above the freezing point, additional heat cannot be removed by conduction through the liquid. The only other possibility is transport of heat by the vapour as was suggested by Frank (4). As was pointed out in the formulation of the mechanism such a heat removal process accounts for the differences observed in the phenomenon under slightly different experimental conditions.

The conduction of heat by the vapour does not necessarily have to take place to the crust and thence to the upper walls as was presupposed by Frank. The conduction may take place to any portion which is below the freezing point of the liquid and actually proceeds to more and more spots as the tubule makes more and more contacts with the walls and crust during its travels. Thus in experiments 1 and 2, described on page 14, the tubule

originated at the glass walls and did not come into contact with a crust. In experiment 3, also described on page 14, the tubule may have had a very thin sheath until it approached the glass wall where it would acquire a cold spot. When the rate of cooling was increased, by using a colder bath or a narrower ampule, the velocity of propagation increased because of the faster contraction while the diameter of the tubule decreased because of the rapid sheath or wall formation due to a more efficient heat conduction over a greater temperature gradient.

CRYSTALLIZATION VELOCITY AND THE PHENOMENON

The main discrepancy between Frank's explanation and the observations made during the course of this investigation lies in the velocity of propagation of the tubule. Frank argued that the tubule cannot travel at a rate greater than the linear crystallization velocity of the material. On this basis he predicted that a change in diameter of the ampule would not alter the velocity of the tubule. This is contrary to what was observed. In actual fact the size of the tubule for any given rate of volume contraction is governed solely by the rate at which vapour is transferred to the cold spots at the walls. This was shown by the speeding up of the tubule after several cold spots had developed while the temperature

of the liquid had decreased only by a few degrees.

Moreover he stated that the previously reported velocity of 3 cm/sec constituted a new "record" for crystallization velocities. The present observations, in the case where the tubule was made to travel in the vapour region, would on this basis better the record by at least another factor of five. Actually the present observations indicated that the true crystallization velocity was not much greater than the rate at which the crystals grew downwards from the crust or the rate at which they grew from the walls of the tubule. None of these rates ever exceeded 1 mm/sec.

The formation of crystals directly after a fresh liquid-vapour surface was produced, namely under the crust and at the walls of tubule one centimeter behind its tip, may perhaps be taken as evidence for nucleation preconditioned by a liquid-vapour interface. This could also be due to the fact that a layer of cooled liquid is formed on the outside of these solid surfaces by evaporation of liquid to form them. Crystallization would then rapidly follow the tip of the tubule but would proceed at normal rates in a perpendicular direction to the direction of propagation of the tubule. This latter growth represents the true linear crystallization velocity while the former is somewhat similar to the instan-

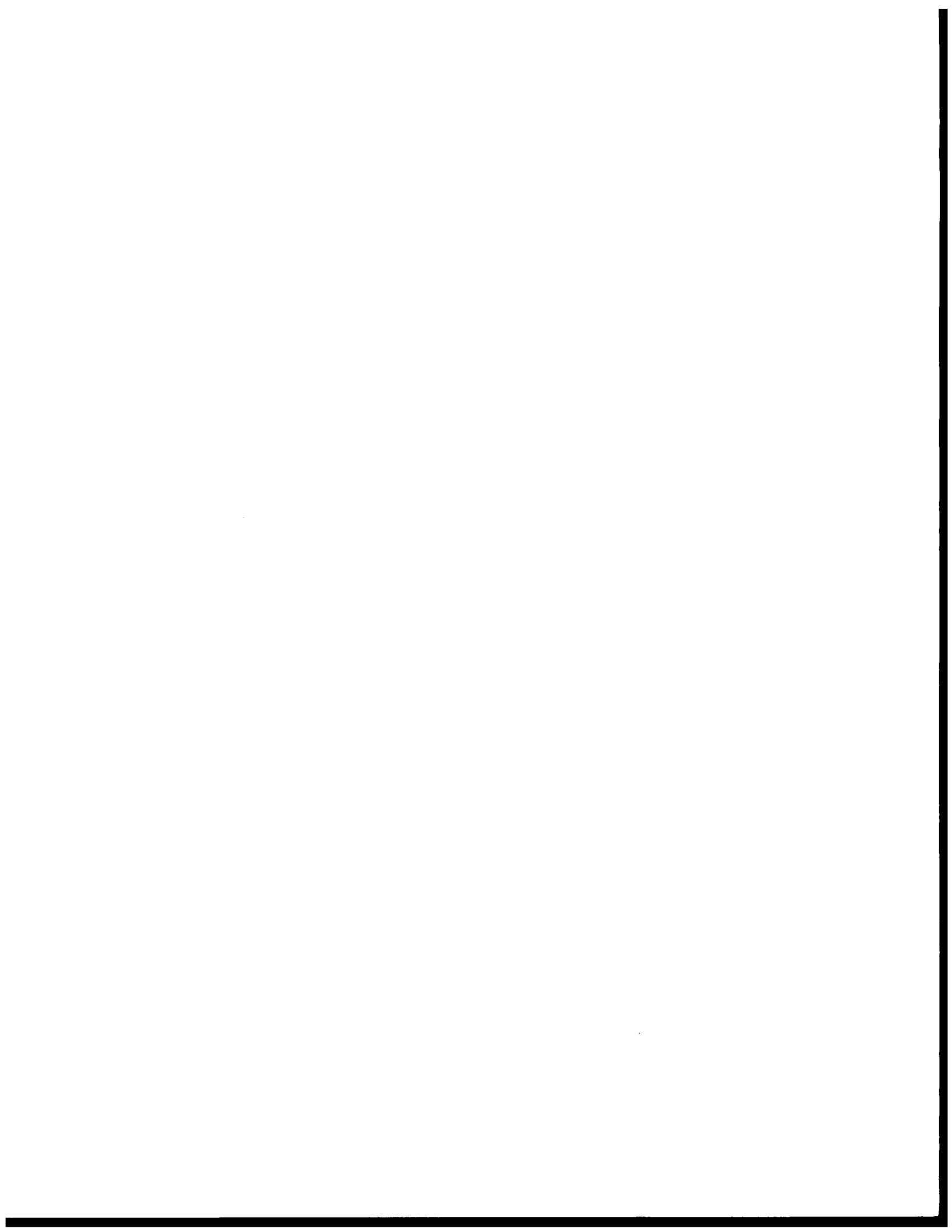
teneous crystallization obtained in a supercooled liquid, a film of supercooled liquid being formed during the rapid evaporation accompanying wall formation.

SUMMARY

- 1 - A simple mechanism was formulated for the formation and propagation of the tubule observed in this phenomenon.
- 2 - The following facts were established:
 - a) a closed volume for the system is required,
 - b) the cooling temperature must be a fraction of a degree below the freezing point or lower,
 - c) the rate and size of the tubule were shown to be governed by the rate of cooling and the size of the ampule containing the sample,
 - d) the tubule was shown to be hollow, rigid, and filled with vapour of the compound under study,
 - e) the compound had to be pure and degassed.
- 3 - The only property of compounds essential for occurrence of the phenomenon was shown to be a high vapour pressure at the triple point. This property is directly related to the degree of spherical symmetry.
- 4 - There is no apparent correlation between the rate of propagation of the phenomenon and linear crystallization velocities.

BIBLIOGRAPHY

1. M.K. Phibbs and H.I. Schiff, J. Chem. Phys. 17, 843 (1949).
2. S. Seki, Kagaku, 18, 277 (1948).
3. S. Seki, J. Chem. Phys. 18, 397 (1950).
4. F.C. Frank, J. Chem. Phys. 18, 231 (1950).
5. J. Timmermans, J. chim. phys. 35, 331 (1938).
6. J. Timmermans, J. chim. phys. 46, 546 (1949).
7. A. van de Vloed, Bull. Soc. chim. de Belgique, 48, 229 (1939).



PART II

A COMPARISON OF THE PRODUCTION OF ACTIVE NITROGEN

by

THE ELECTRODELESS AND CONDENSED DISCHARGES

and

ITS REACTIONS WITH OXYGEN CONTAINING COMPOUNDS

TABLE OF CONTENTS

INTRODUCTION

	Page
CHARACTERISTICS OF ACTIVE NITROGEN	1
Production	1
Physical Properties of the Nitrogen Afterglow	5
Chemical Reactivity of Active Nitrogen	8
THEORIES OF ACTIVE NITROGEN	10
Ionic Theory of Active Nitrogen	10
Atomic Theory of Active Nitrogen	13
Molecular Theory of Active Nitrogen	16
PURPOSE OF THE PRESENT INVESTIGATION	22
REVIEW OF CHEMICAL REACTIONS RELATED TO THIS INVESTIGATION .	23
Reaction of Active Nitrogen with the Hydrocarbons	23
Reaction of Hydrogen Atoms with Methanol and Methyl Ether	26
Reaction of Methyl Radicals with Methanol and Methyl Ether	29

EXPERIMENTAL

REAGENTS	31
APPARATUS	32
The Nitrogen Flow Control	32
The Activation and Reaction Section	34
The Product Collecting and Sampling Section	35
The Reactant Flow Control	36
METHODS OF ACTIVATION	39
Discharge Tubes	39

	Page
Electrodeless Discharge Circuit	41
Condensed Discharge Circuit	47
PROCEDURE FOR A TYPICAL EXPERIMENT	50
ANALYTICAL APPARATUS AND TECHNIQUE	52
Water Analysis	52
Hydrogen Cyanide Analysis	55
Analysis of Other Products	57
 <u>RESULTS</u>	
REACTION OF ACTIVE NITROGEN WITH METHANOL	58
Characteristics of the Reaction	58
Products of the Reaction	62
REACTION OF ACTIVE NITROGEN WITH DIMETHYL ETHER	76
Characteristics of the Reaction	76
Products of the Reaction	77
REACTION OF ACTIVE NITROGEN WITH ACETONE	84
Characteristics of the Reaction	84
Products of the Reaction	85
 <u>DISCUSSION</u>	
GENERAL COMMENTS	89
REACTION OF ACTIVE NITROGEN WITH METHANOL	91
REACTION OF ACTIVE NITROGEN WITH DIMETHYL ETHER	107
REACTION OF ACTIVE NITROGEN WITH ACETONE	112
 <u>SUMMARY</u>	
.....	116
 <u>BIBLIOGRAPHY</u>	
.....	118

LIST OF TABLES

	Page
I Hydrogen Cyanide, Water and Condensable Products Yield with Various Methanol Flow Rates - Series I	64
II Hydrogen Cyanide, Water and Condensable Products Yield with Various Methanol Flow Rates - Series II	65
III Hydrogen Cyanide, Water and Condensable Products Yield with Various Methanol Flow Rates - Series III	66
IV Maximum Hydrogen Cyanide and Water Yield with Various Nitrogen Flow Rates	70
V Hydrogen Cyanide, Water and Condensable Products Yield with Various Methanol Flow Rates - Series IV	73
VI Hydrogen Cyanide, Water and Condensable Products Yield with Various Dimethyl Ether Flow Rates - Series V	79
VII Hydrogen Cyanide, Water and Condensable Products Yield with Various Dimethyl Ether Flow Rates - Series VI ...	81
VIII Hydrogen Cyanide and Condensable Products Yield with various Acetone Flow Rates - Series VII	87
IX Series I - Calculated Data at Various Methanol Flow Rates	96
X Series II - Calculated Data at Various Methanol Flow Rates	96
XI Series III - Calculated Data at Various Methanol Flow Rates	97
XII Series IV - Calculated Data at Various Methanol Flow Rates	97

LIST OF FIGURES

	Page
1 Electronic Levels of the Nitrogen Molecule	12
2 Nitrogen Flow Control - Activation and Reaction Section - Collecting and Sampling Section	33
3 Reactant Flow Control	37
4 Discharge Tubes	40
5 Exciter Circuit	43
6 Amplifier Circuit	45
7 Relaxation Oscillator Circuit	48
8 Water Analysis Apparatus	53
9 Plot of Hydrogen Cyanide Yield as a Function of Methanol Flow Rate - Series I, II and III	67
10 Plot of Water Yield as a Function of Methanol Flow Rate - Series I, II and III	68
11 Plot of Maximum Hydrogen Cyanide and Water Yield as a Function of Nitrogen Flow Rate - Series I, II and III ..	71
12 Plot of Hydrogen Cyanide and Water Yield as a Function of Methanol Flow Rate - Series IV	74
13 Plot of Hydrogen Cyanide and Water Yield as a Function of Dimethyl Ether Flow Rate - Series V	80
14 Plot of Hydrogen Cyanide and Water Yield as a Function of Dimethyl Ether Flow Rate - Series VI	82
15 Plot of Hydrogen Cyanide as a Function of Acetone Flow Rate - Series VII	88

INTRODUCTION

CHARACTERISTICS OF ACTIVE NITROGEN

Production

During the latter part of the nineteenth century considerable work was done on the effects of the passage of high voltage sparks through gases. By means of induction coils afterglows were produced which, as the name implies, lasted for some length of time after the discharge was turned off. In 1865, Morren (1) was successful in producing an afterglow which lasted up to one minute in a mixture of nitrogen and oxygen containing traces of sulfur dioxide. Some thirty years later, Lewis (2) proved that this afterglow was a characteristic property of nitrogen by correlating its spectrum to that of pure nitrogen.

Burke (3) was the first one to show that an afterglow identical to the one obtained by the condensed discharge could be produced by an electrodeless discharge. In the following years both methods of excitation were used in numerous experiments carried out on active nitrogen. At first the electrodeless or uncondensed discharge was used very little since it produced but a feeble afterglow, but as the method was improved it became more prominent. It was used successfully by Kaplan (4) (5)

for the production of nitrogen afterglows as well as auroral afterglows. Knaus and Murray (6) later showed that the spectrum of the afterglow obtained by Kaplan was similar to the spectrum of the afterglow produced by the condensed discharge.

In 1937, Willey (7), in some studies on nitric oxide arrived at the conclusion that impulse discharges and high frequency discharges are more effective than A.C. or D.C. discharges, provided the pulses are of the proper duration so that the precursor of the active constituent, or the active constituent itself can be withdrawn from the discharge region before the next pulse. This was apparently the case for the nitrogen afterglow, since the use of a secondary weak discharge coupled with the main discharge did, according to some earlier work of Willey (8) and Strutt (9), decrease the intensity of the afterglow. Similar results have been reported by other investigators, but a thorough investigation of the problem has never been carried out.

In all the work on active nitrogen very little attention has been paid to its production. In most publications, except for a few like those of Lord Rayleigh, it is impossible to determine the way in which the nitrogen was activated, no mention being made of the type of electrical circuit used nor of the type of

vessel in which the activation was promoted. For an illustration of the possible variety in these, the reader is referred to Lord Rayleigh's publications in which abundant sketches and descriptive information are to be found.

In the early work on active nitrogen a controversy developed as to whether or not it was possible to obtain an afterglow in highly purified nitrogen. The effect of impurities, especially traces of oxygen, on the production of the afterglow received considerable attention. Lewis claimed that traces of oxygen were required for the production of the afterglow. Strutt (10), on the other hand, concluded that small amounts of oxygen were not necessary since nitrogen purified with phosphorus gave the glow. In the absence of oxygen, Koenig and Elöd (11) reported a longer and more intense afterglow. Tiede and Domcke (12), in direct contradiction, showed that the introduction of oxygen in glowless nitrogen caused the afterglow to reappear.

Even when the investigators repeated the experiments in each other's presence different results were obtained and no satisfactory explanation could be given (13). In subsequent work, Strutt (14) found that traces of oxygen were required to obtain a strong afterglow. A similar effect was observed for any foreign gas.

Sponer (15) proposed that traces of oxygen or other foreign gases act as a poison by adsorption on the glass walls as does water in the case of monatomic hydrogen. The catalytic effect of the walls was subsequently investigated by Herzberg (16). He found that the afterglow was short lived in baked out vessels and upon the introduction of foreign gases its duration was restored to normal. This was confirmed by Lewis (17). Kaplan (4) was later successful in using the adsorption of oxygen on the walls as a poison in a continuous flow system. The procedure consisted simply of maintaining an air discharge in the apparatus until the blue-green color of NO developed and then continuing the discharge for a few hours. After several repetitions a good afterglow was obtained. This method of poisoning has been used subsequently by other investigators and found satisfactory (6).

Lord Rayleigh, in later experiments (18), obtained some evidence that oxygen must act as a wall poison by showing that it definitely hindered the glow in a nitrogen stream where the wall effect was eliminated. This he demonstrated by producing an afterglow in the center of a vessel and letting it diffuse to the walls. By maintaining the pressure sufficiently high, the afterglow "streamers" were prevented from actually coming in contact with the walls. Under these conditions the introduction

of oxygen in the nitrogen stream reduced the length of the "streamers" by a factor of ten, as illustrated in his drawings, but did not destroy it completely.

In more recent experiments, Reinecke (19) has shown that the introduction of oxygen or other foreign gases, in addition to intensifying the glow, produced marked changes in the intensity distribution of the bands emitted by the afterglow. This will be discussed more thoroughly later.

Thus it appears that the foreign gases affect the afterglow in at least two ways. One being the heterogeneous conditioning of the walls and the other some homogeneous interaction with the nitrogen itself.

In the production of active nitrogen the walls are generally poisoned with sulfuric or phosphoric acid and sometimes with oxygen. Furthermore, traces of foreign gases are generally added to obtain a more intense afterglow. These steps are taken to obtain a more intense and longer lived afterglow, but are not necessary for the production of active nitrogen.

Physical Properties of the Nitrogen Afterglow

It is distinguished from other afterglows by its exceptionally long duration. Lord Rayleigh was able to maintain a visible afterglow in an isolated vessel coated with metaphosphoric acid for as long as $5\frac{1}{2}$ hours (20).

Other investigators have observed 15-minute afterglows without too much difficulty.

The increase in brightness of the afterglow upon cooling, first observed by Strutt (21) in his unsuccessful search for a new component in active nitrogen, is also remarkable. The increase in brightness is always accompanied by a shortening of its duration. On the other hand, Cario and Caplan (22) reported that the afterglow disappeared upon heating. It was later pointed out by Okubo and Hamada (23) that only very impure active nitrogen lost its afterglow completely upon heating, since pure active nitrogen, even when heated to 650°C , still glowed weakly. Okubo and Hamada also observed a decrease in the afterglow when active nitrogen was submitted to a weak secondary electrical discharge. This is in agreement with Willey's results mentioned previously.

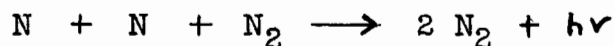
An increase in pressure produced by compressing the glowing nitrogen was observed by Strutt (24) to have the same effect as cooling. A sudden increase in pressure was shown by Knipp and Scheuerman (25) to cause a "flash" in the afterglow. This flash travelled much like a wave in the afterglow which continued to die out afterwards.

Quantitative experiments by Lord Rayleigh (26) indicated that the brightness of the afterglow, upon admission of inert nitrogen, increased roughly with the pressure of

the nitrogen. Upon compression, the brightness varied as $1/V^3$, while cooling to liquid air temperatures increased it some 80 times.

A correlation between the pressure and temperature effects was reported by Debeau (27). He observed that at low pressures excitation of the afterglow by an electrodeless discharge nearly caused a doubling of the pressure without any appreciable wall temperature increase. Upon application of liquid air to less than 1% of the area of the system the pressure returned to its normal value and the afterglow disappeared, but upon slowly removing the liquid air the glow reappeared.

The rate of decay of the afterglow was investigated by Kneser (28) using a simple photometric method. He found that under different experimental conditions such as walls, pressure, and dilution with argon his results agreed with a three body collision mechanism. The brightening of the glow upon introduction of nonactive particles, he maintained, quantitatively confirmed this. The glow emission process was represented by



Similar experiments carried out by Willey (29) also favored a third order reaction. In addition, he attributed the strong wall effect to adsorption and heterogeneous recombination of nitrogen atoms.

The concept of two species in active nitrogen, one being responsible for the afterglow and the other for the chemical reactivity, of which mention will be made later, was first suggested by Saha and Sur (30). Willey (31) later proposed that a low energy species was responsible for the chemical reactivity, while a high energy species was responsible for the afterglow. The existence of a chemically reactive, glowless or dark modification of active nitrogen was supported by the experiments of Cario and Caplan and those of Willey, experiments which however have been disputed by Okubo and Hamada as was previously mentioned.

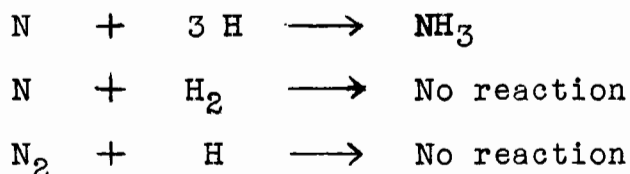
Thus considerable contradiction, which has not been resolved to date, exists in the early work on the physical properties of active nitrogen.

Chemical Reactivity of Active Nitrogen

The term "active nitrogen" came into use in connection with the afterglow phenomenon because of its chemical reactivity. As early as 1911, Strutt (32) called it a chemical, active modification of nitrogen. He found it to react with NO to give NO₂ and with organic radicals to give HCN which was detected by direct chemical analysis as well as by the brilliancy of the CN spectrum. It was also found to form nitrides with metals and nonmetals (10). The reactivity towards NO

was later often used to determine the activity of the glowing nitrogen.

Since active nitrogen had previously been shown not to react with hydrogen (21), the problem was investigated further by Lewis (33). He was able to obtain traces of ammonia only when active nitrogen was made to react with atomic hydrogen, his results being summarized by the following equations:



where N is used to represent active nitrogen. Similar results were obtained by Ewart and Rodebush (34) who synthesized ammonium bromide by simultaneously passing nitrogen and hydrogen bromide through an electrical discharge. Attempts to find an oxidizable form of active nitrogen which would react with ozone were also unsuccessful (35) (36).

Numerous reactions of active nitrogen with organic compounds had been reported in a qualitative manner by 1938. This led Howard and Hilbert (37) to investigate the use of this method as a means of synthesizing nitrogen containing compounds. They reacted a few aromatic compounds obtaining hydrogen cyanide as a major product. Other nitrogen containing compounds were also obtained

in appreciable amounts, but since these generally were present in a polymerized form, their identification could not be made.

For a decade following this work the investigation of the chemical activity of the glowing nitrogen was not pursued any further. A systematic investigation of the reactions of active nitrogen with the simple hydrocarbons, saturated and unsaturated, as well as other aliphatic compounds was started recently by C. A. Winkler and co-workers (38) (39) (40). In their experiments they also observed the predominance of hydrogen cyanide formation and the lack of ammonia formation. In addition they obtained some cyanogen. Mechanisms for the reactions were postulated. This was made possible by the detection of a variety of additional products in these reactions. More detailed mention of this work will be made later.

THEORIES OF ACTIVE NITROGEN

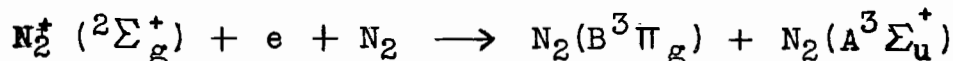
Three main theories have been put forward in an attempt to explain the nitrogen afterglow. They are: the ionic theory, the atomic theory and the molecular theory. These will now be discussed separately in that order.

Ionic Theory of Active Nitrogen

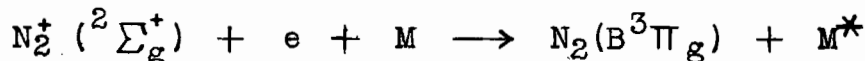
In the formation of active nitrogen the role of positive ions as precursors of atoms is indicated by

Okubo's and Hamada's (41) electron impact experiments. In these they observed that the production of active nitrogen suddenly increased when the accelerating potential of the electrons attained 16 volts, the first ionization potential of the nitrogen molecule, and increased gradually afterwards. Willey (42) pointed out that neutralization of the N_2^+ ions could readily give rise to atoms or excited molecules. The excited molecules might be reactive.

In the ionic theory of Mitra (43), the N_2^+ ions were considered to be the active centers. The main reactions proposed were:



where the ordinary nitrogen molecule acts as a third body or,



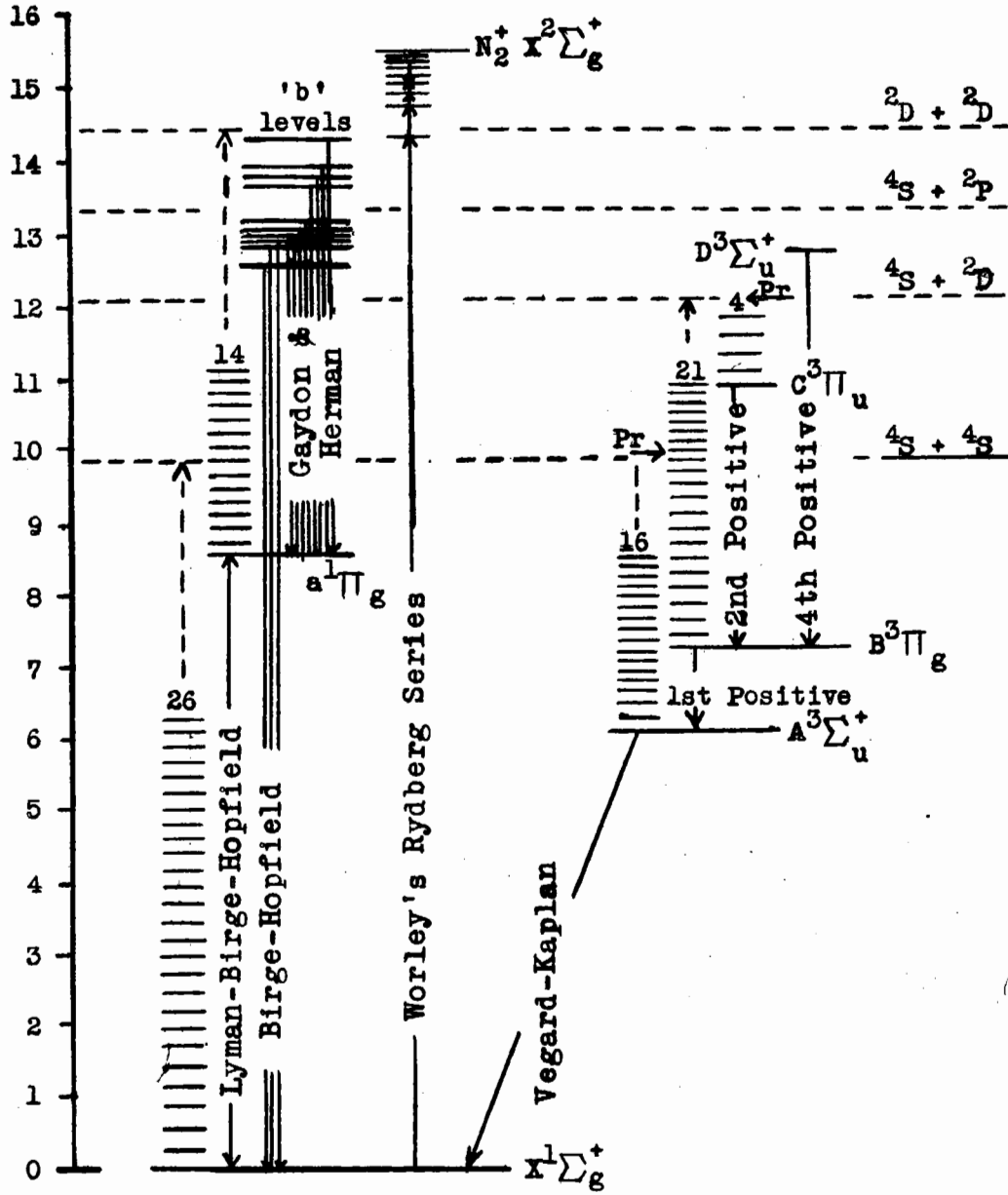
in which case the energy is dissipated at the walls

A diagram showing the electronic levels of the nitrogen molecular states is given in Figure 1.

This theory requires the slow neutralization of the ions, to explain the observed lifetime of the afterglow, which is rather improbable. Furthermore, careful removal of all charged particles was shown by Willey and Stringfellow (44) and other investigators not to have any effect on the activity of the nitrogen.

FIGURE 1

Electronic Levels of the Nitrogen Molecule



Worley (45) pointed out that if nitrogen ions were the active centers they should be present in large concentrations. The N_2^+ bands have never been detected in the absorption spectrum of the afterglow, indicating that this is not the case. Benson (46), using a sensitive microwave technique, found the afterglow to contain electrons but no positive ions.

Atomic Theory of Active Nitrogen

The recombination of atoms has long been postulated as a source of the afterglow (15) (47). However the older recombination theories, such as those of Cario and Kaplan (48) (49), cannot be reconciled with the recently determined value of 9.76 volts for the dissociation energy of nitrogen (50) (51) (52). Taking account of this, Gaydon (50) suggested that two normal atoms could recombine on a potential curve which is either repulsive or of low stability. The molecules thus formed could undergo radiationless transitions (preassociation) leading to the stable $B^3\Pi_g$ state. This mechanism would excite the 11th and 12th vibrational levels of the B state and could thus account for the intensity of these levels observed in the first positive bands of the afterglow.

The difficulty with this explanation lies in the short lifetime of a two body collision relative to the lifetime or radiation. Reinecke (19), elaborating on this

theory, discussed the possibility of a sort of three body collision in which an atom is first pictured as colliding with a molecule to form a quasi-molecule which could then react with another atom. This quasi-molecule would be held together by weak van der Waals' forces and would thus have a sufficiently long lifetime to permit recombinations to the $B^3\Pi_g$ state. Difficulty still remains, however, in explaining the relatively strong intensity observed for the 6th vibrational level of the B molecules. Moreover, it is difficult to see why the recombination of atoms by a three body collision on the ground state potential energy curve should be a very slow process. The only obvious explanation would require nitrogen molecules to be poor collision partners as was actually suggested by Reinecke in another connection.

Thus, from his studies on the effect of foreign gases on the nitrogen afterglow, he concluded that the intensity distribution of its spectrum should be interpreted as an overlapping of recombination processes in the triple collisions involving nitrogen molecules, and particularly, particles of foreign gases. As an explanation, he proposed that the quasi-molecules formed with the foreign gas molecules have a longer lifetime than those formed with the nitrogen molecules.

The presence of atoms in the discharge region has

been established. Herzberg (53) found that the atomic arc lines in the red and infra-red regions must be excited in the discharge before the afterglow can be produced. Bay and Steiner (54) showed that the intensity of the afterglow was proportional to the concentration of atoms in the discharge which in turn was proportional to its capacity. On the other hand Kichlu and Basu (55) showed that active nitrogen could be produced by an uncondensed, electrodeless discharge in which no appreciable amount of atoms could be detected spectroscopically. This renders doubtful the complete correspondence between the afterglow and the presence of atoms in the discharge.

Numerous attempts have been made to detect the presence of atoms in the afterglow by spectroscopic methods. Metastable atoms, which were required in the early recombination theories, have been shown by Herbert, Herzberg and Mills (56) to be present in too low a concentration to account for the afterglow. They also criticized the work of Jackson and Broadway (57) who claimed to have detected only $^2P_{\frac{1}{2}}$ metastable atoms by a Stern-Gerlach experiment. Anand, Kalia and Ram (58) were unable to detect atomic absorption lines in the Schuman region. However, E. Inn (59) has recently obtained absorption lines in the vacuum ultra-violet region in the nitrogen afterglow. Jackson and Schiff (60), using

a mass spectrometric method, obtained evidence for the presence of atoms as well as excited molecules in the afterglow. The concentration of atoms estimated from the results obtained by these last two methods was less than two percent.

On the other hand Wrede (61), using a differential diffusion gauge, claimed to have observed concentrations of atoms up to 40%. Considerable doubt has been placed on this method due to the proximity of the high energy discharge and the possibility of temperature gradients across the capillary. Winkler and co-workers (38) (40) have also reported concentrations up to 40% based on the extent of reaction with various hydrocarbons. This estimate was based on the assumption that atoms are the sole reactive species.

Thus it appears that although high concentrations of atoms can be detected in a condensed discharge no unequivocal evidence for their presence in the afterglow in concentrations greater than a few percent has been obtained.

Molecular Theory of Active Nitrogen

The earlier molecular theories resulted from the fact that the positive bands, mainly the first and second, were strongly enhanced in the nitrogen afterglow as observed in the spectrographic experiments of Lord Rayleigh

(62) and Duffieux (63). In his investigation of the characteristics of discharges leading to the production of the afterglow, Herzberg (53) observed the appearance of the fourth positive bands, if the excitation was maintained sufficiently long. These bands were also detected by Kaplan (64). In some later work, Kaplan (65) was able to excite the fourth positive bands by subjecting the afterglow to a mild, secondary electrical discharge. Since the mild discharge by itself was unable to excite the D level of the nitrogen molecule, the source of the fourth positive bands, he concluded that some excited, metastable molecules were present.

Of all the excited molecular levels involved in the above transitions only those of the lower triplet state, the $A^3\Sigma_u^+$ state, could have been metastable, since its transition by radiation to the ground state was shown by Kaplan (66) to occur only under special conditions. On the other hand the A state, being the lower state involved in the emission of the afterglow, could not easily be considered as its source. It has recently been pointed out by Muschlitz and Goodman (67) that, although metastable, the A state is short lived, thus rendering it incapable of explaining the long lifetime of the afterglow. Even though the probability of the triplet states being the cause of the long lifetime of the afterglow is

small, the numerous singlet states still remain to be considered.

The singlet states lie mostly in the range of 12.5 to 15.5 volts above the ground state and are very difficult to analyse, as was pointed out by Janin (68) and Worley (69). A mechanism in which neutral molecules above the first ionization limit may play a vital part was discussed by Worley (45) who, in previous work, had observed the existence of such states in the far ultraviolet absorption spectrum of active nitrogen. In addition some transitions from the lowest singlet state, the $a^1\Pi_g$ state, to the triplet states have been reported by Meyerott (70).

A molecular theory in agreement with the above experiments and based on additional evidence has been tentatively proposed by Nicholls (71). In controlled electron experiments on the emission of the triplet bands of molecular nitrogen two assumptions have usually been made. First, that the transitions to the upper levels of the band systems came about directly as the result of collisions of the first kind between ground state molecules and fast electrons; and secondly, that the energy values of these states are the voltages at which they respectively appear upon excitation by the electron beam of controlled energy. These assumptions would place the

triplet levels about 2 volts higher than the accepted values based on reliable spectroscopic evidence (72).

If, on the other hand, the primary excitation by collisions of ground state molecules and electrons is considered to result in the population of the singlet levels of the $a^1\Pi_g$ and 'b' states, population of the triplet levels could then come about by intercombination due to collisions of the second kind between slow electrons and the excited singlet levels. The 'b' states are the upper states of the Birge-Hopfield systems and the Gaydon and Herman singlet systems. The latter appear as eight progressions, probably due to eight independent systems, all involving transitions to the $a^1\Pi_g$ state as shown in Fig. 1.

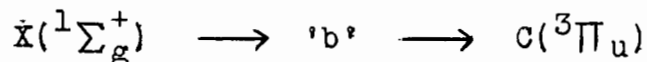
This mechanism is suggested from comparative arguments between the energies of the singlet levels with the electron energies at which the triplet bands appear. The appearance potential of the first positive bands, after correction by extrapolating to the (0,0) band, is about 9.5 volts, which is the value for maximum excitation probability of the $a^1\Pi_g$ level. The appearance potential of the second positive bands is approximately 13 volts which is also near the maximum excitation probability of the 'b' levels. Since the first positive system appears at about 9.5 volts and is not fully developed until the

second positive bands appear at 13 volts and reaches a maximum with them, it appears that the primary population of the $B^3\Pi_g$ levels below the $a^1\Pi_g$ level is due to collisions of the second kind between slow electrons and the $a^1\Pi_g$ molecules. The secondary population of the $B^3\Pi_g$ levels, especially those lying above the $a^1\Pi_g$ level, seems to result from the emission of the second positive bands. Some of the molecules in the 'b' levels, by collisions of the second kind, could also contribute to the formation of the upper $B^3\Pi_g$ levels. The fourth positive system appears at 15 volts when certain of the 'b' levels which lie above the $D^3\Sigma_u^+$ level become populated and reaches a maximum intensity at 20 volts.

Such a mechanism adequately accounts for the observed excitation potentials in terms of the known levels of nitrogen. The initial excitation is also in accord with the Frank-Condon principle and does not involve a change in multiplicity. Furthermore, the g symmetry of the $a^1\Pi$ state recently proposed by Herzberg (73) (74) renders that level metastable, making collisions of the second kind more probable. Although the metastability renders excitation less probable, the fact that only singlet bands, and no singlet-triplet bands, appear in absorption shows that it has a much greater probability than the excitation of the triplet states. Herzberg (73) pointed

out that the long path required for this absorption provides experimental evidence for the metastability.

Preliminary experiments by Nicholls (75), in which he studied the above mechanism, showed that since the energy involved in excitation of the $C^3\Pi_u$ state is of the order of the separation between the ground state and the 'b' levels rather than between the ground state and $C^3\Pi_u$ levels the indirect mechanism



is the most probable.

This mechanism does not preclude the existence of atoms which could come about by predissociation. Predissociation in the $a^1\Pi_g$ state has recently been observed by Herman (76) and confirmed by Herzberg (74).

Thus electron bombardment experiments designed to produce the positive bands seem to involve the singlet systems of excited molecules. Nicholls (75) has suggested that this method of excitation is also the most probable one in the case of glow discharges. Kaplan (4), in some previous experiments, had observed that glow discharges had a similar spectrum to that of the afterglow. In his experiments only the first positive bands were observed in the discharge with a structure similar to that in the afterglow. The second positive bands, which are strong in the condensed discharge, were almost completely missing

from the glow discharge.

There still remains the question as to whether the condensed discharge afterglow arises from the same mechanism. At present this mechanism offers no explanation for the observed high intensity of the 11th and 12th levels of the B state. Moreover, additional information will be required on the metastability of the $a^1\Pi_g$ state or of the 'b' states before it can account for the lifetime of the afterglow.

In summation then, it appears that the afterglow does not contain positive ions, does contain excited molecules and also atoms in at least small concentrations. Various theories have been successful in explaining the observed emission of the afterglow, the temperature and pressure effects, but the question of the long lifetime of the afterglow still remains unanswered.

PURPOSE OF THE PRESENT INVESTIGATION

The investigation was undertaken with three main objectives in mind:

1. To try to establish the mode of attack of active nitrogen, produced by a controlled high frequency electrodeless discharge of known and fixed frequency, on organic molecules.
2. To establish differences, if any, between the chemical reactivity of active nitrogen produced by the

electrodeless discharge and that produced by the condensed discharge method.

3. To study the reactions of a new class of compounds, namely, those containing oxygen, which have up to now not been considered even in a qualitative manner.

Since this thesis reports the results of the chemical reactions between some oxygen containing compounds and active nitrogen produced by the electrodeless discharge a brief review will be given of the work done with active nitrogen produced by the condensed discharge method. In addition, a summary of the action of hydrogen atoms and methyl radicals on methanol and dimethyl ether, the compounds under investigation, will be given for comparative purposes.

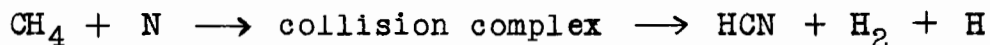
REVIEW OF CHEMICAL REACTIONS RELATED TO THIS INVESTIGATION

Reaction of Active Nitrogen with the Hydrocarbons

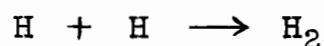
As was mentioned earlier, C.A. Winkler and co-workers have recently undertaken a series of investigations on these reactions. Mention of the reactions with methane, ethane and ethylene will be made since only these have direct bearing on the present problem. Later publications on the reactions of active nitrogen with other compounds are to be found in the Canadian Journal of chemistry after 1951.

The reactions of ethane and methane were studied by

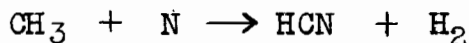
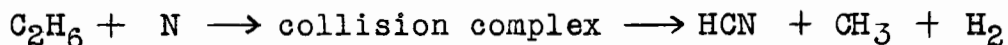
Blades and Winkler (38). In the reaction with methane, which took place to an appreciable extent only at temperatures above 300°C, the following mechanism was suggested:



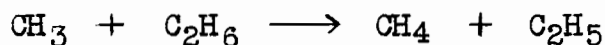
followed by



No other products were detected. Similarly, for the reaction of ethane with active nitrogen, the sole products in the temperature range 106-295°C were hydrogen cyanide and hydrogen. The suggested mechanism was



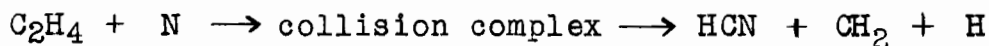
The absence of methane as a product indicated that the reaction



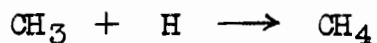
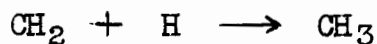
did not occur. The reaction of methyl radicals with the nitrogen atoms was considered to be very fast.

In both these reactions the primary step was postulated as an attack of a nitrogen atom on the hydrocarbon, yielding a collision complex, which then rearranged to hydrogen cyanide. The limiting hydrocarbon flow rate above which the rate of hydrogen cyanide formation no longer increased was called the clean-up point of the reaction.

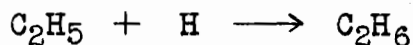
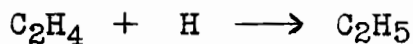
The reaction of active nitrogen with ethylene was first investigated by Greenblat and Winkler (39). The products consisted of hydrogen cyanide together with smaller amounts of ethane. In addition, a large amount of a polymeric material was obtained. The reaction was re-investigated later by Versteeg and Winkler (40) after a method was devised to eliminate this large amount of polymerization. The additional products obtained in this case were cyanogen, acetylene and methane, the latter being of the same order of magnitude as the ethane. The proposed mechanism was



where it was thought that a hydrogen atom is liberated in the complex formation step. The methylene radical then reacts further with nitrogen atoms to yield more HCN or reacts with some of the hydrogen atoms to yield methane as follows



The ethane also resulting from a similar reaction,

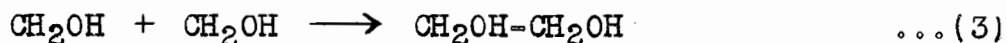
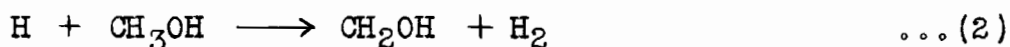
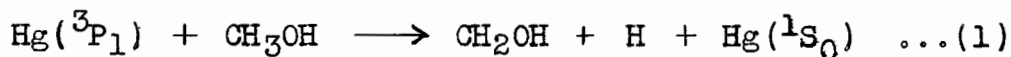


This reaction was found to proceed by clean-up of the reagent in excess, either the hydrocarbon or the nitrogen atoms.

Reaction of Hydrogen Atoms with Methanol and Methyl Ether

There is only very incomplete information available on the reaction of hydrogen atoms with methyl alcohol. Geib (77) investigated this reaction and reported H_2O , CO and CH_4 as products. Chemiluminescence also occurred, the C-H and C-O bands being emitted. Steacie (78) reviewed the question and pointed out that there appeared to be a catalytic recombination of hydrogen atoms in the presence of the alcohol. He concluded that the data are too scanty to allow any mechanism to be set up. Since no further work appears to have been carried out on this reaction only indirect evidence could be obtained from photolysis experiments on the alcohol.

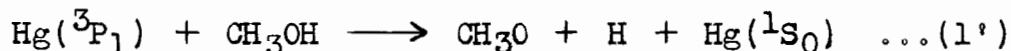
Recently the mercury photosensitization of simple organic molecules containing oxygen has been studied (79) (80). In the cases of dimethyl and diethyl ether it was found that the primary step led to the abstraction of a hydrogen atom. This work was later extended to methyl alcohol by Phibbs and Darwent (81). They postulated the following steps:



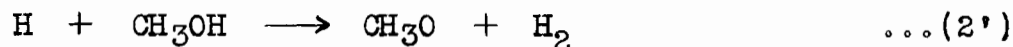
On this basis hydrogen and ethylene glycol are the only important products as was found experimentally. They

pointed out that this is in agreement with the previous work on the simple ethers, that is, there is no tendency to split the C-O bond in the initial act.

The alternate primary action



was shown to be unimportant since no ether peroxide was detected. Even if all the peroxide decomposed into CH_3OH and CH_2O the ratio of the CH_3OH used to H_2 produced should be less than two while it was found to be 2.28 in agreement with (1). They also excluded reaction (1') on the basis that when CH_3OD was used, only small amounts of HD were produced and not the large amount expected for reaction (1'). The small amounts detected may have been due to some CH_2DOH in the starting material. For similar reasons the alternate to reaction (2)

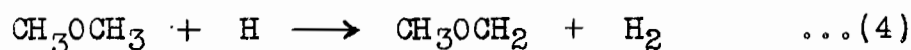


must also be unimportant. An explanation for the predominance of reactions (1) and (2) over (1') and (2') may be due to the difference in strength of the C-H and O-H bonds. The average O-H bond in water is 110 kcal. and by analogy the one in the alcohol should at least be this large, thus making it 10 kcal. stronger than the C-H bond which is approximately 100 kcal.

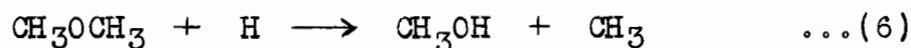
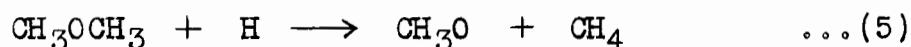
The same should hold true for hydrogen atoms produced by discharge excitation and thus reaction (2) may

be taken as the best probability for the action of hydrogen atoms on methanol.

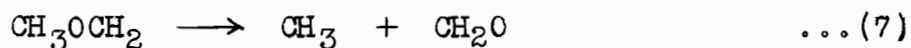
The reaction of hydrogen atoms with dimethyl ether has been investigated by Trost, Darwent and Steacie (82). As in the photochemical decomposition, the primary step is the abstraction of a hydrogen atom as follows:



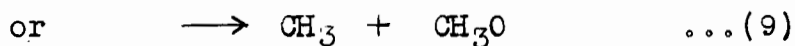
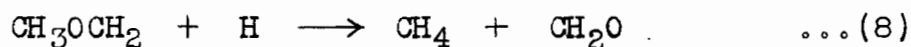
The alternate primary steps



were assumed to occur only slightly since reaction (5) could not account for the high deuterization of methane in experiments with deuterium atoms, while the absence of methyl alcohol as a product discredited reaction (6). Since the products formed were CH_4 , CO and H_2O the secondary reactions proposed were the decomposition of the radical formed in (4)

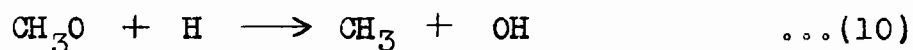


or atomic cracking reactions such as



Reaction (7) was ruled out since it has a high activation energy and reaction (8), since it could not account for the high deuterization of methane. This leaves reaction (9) as the main secondary reaction.

The mechanism accounted for the production of large amounts of CH_4 , smaller amounts of CO and traces of HCOH. The authors pointed out that the main difficulty of the speculative mechanism is the formation of water, which they could only account for by a reaction of CH_3O



followed by reactions of OH which led to water formation.

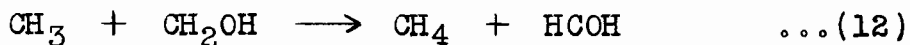
The above facts clearly show that the action of hydrogen atoms on methanol and dimethyl ether can best be explained by the initial abstraction of hydrogen atoms.

Reaction of Methyl Radicals with Methanol and Methyl Ether

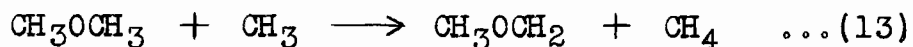
The reaction of methyl radicals, produced by the decomposition of CH_3NNCH_3 , on methyl alcohol has been shown to proceed by an initial rate controlling step, which involves the abstraction of a hydrogen atom as follows (83)



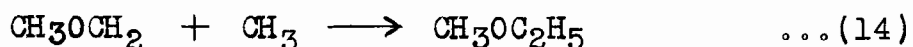
followed by



The mode of attack of methyl radicals on dimethyl ether was also shown to be hydrogen abstraction in the initial step (80) (84)



accompanied by the usual recombination step



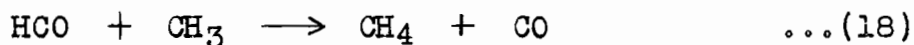
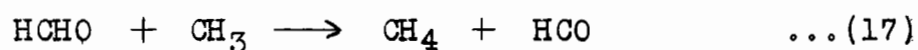
as well as the breakdown of the methyl ether radical



and further decomposition of some of the formaldehyde



The aldehyde formed has been postulated to be decomposed by the two fast reactions (83) (84)



Although a completely satisfactory mechanism for these reactions has not been found it appears that methyl radicals like hydrogen atoms react with the compounds by initial hydrogen abstraction.

The reactions of these compounds with active nitrogen will be described.

EXPERIMENTAL

REAGENTS

Methyl alcohol of 99.5% purity (by volume) was obtained from Mallinckrodt Chemical Works. It was submitted to a simple bulb to bulb distillation in which the first and last fractions were rejected. This procedure was repeated until the water content, determined by the Karl Fischer method, was shown to be negligible. Mass spectrometric analysis failed to reveal the presence of any other impurities.

Commercial dimethyl ether was obtained from the Ohio Chemical and Manufacturing Company. It was found to contain some ethyl methyl ether and ether peroxides as impurities. In order to remove these, repeated bulb to bulb distillations were carried out, each time rejecting the first and last fractions. The product from each distillation was analyzed on the mass spectrometer and the procedure repeated until the dimethyl ether was shown to be free of all foreign constituents.

Acetone labelled "Certified Reagent" was obtained from Fisher Scientific Company. It was also submitted to simple bulb to bulb distillation until no further changes in its mass spectrum could be detected.

Commercial, water-pumped nitrogen was purified by

passing it over 0.5 mm. copper turnings at 450-475°C. The copper turnings were thoroughly degreased before being closely packed into a 25-mm pyrex glass tube. A heating mantle, 40 cm. in length, was then fitted around the tube. At 15 cm. from both ends of the mantle a thermocouple was inserted between it and the glass tube. The temperature of the furnace was adjusted by means of a variable transformer controlling the wattage of the heating coil. In order to obtain maximum efficiency at all times from the furnace, the copper oxide formed was periodically reduced back to copper by passing hydrogen through it. Following its passage over the hot copper, the oxygen-free nitrogen was led through a dry ice-alcohol trap to remove water and any traces of organic materials.

APPARATUS

The apparatus used was of the continuous flow type. It consisted of four main sections: the nitrogen flow control, the activation and reaction section, the product collecting and sampling section, and the reactant flow control.

The Nitrogen Flow Control

The nitrogen was introduced under a pressure slightly greater than atmospheric at N, Figure 2, so that a continuous stream of nitrogen slowly escaped through the mercury bubbler MB. The mercury bubbler was adjusted to

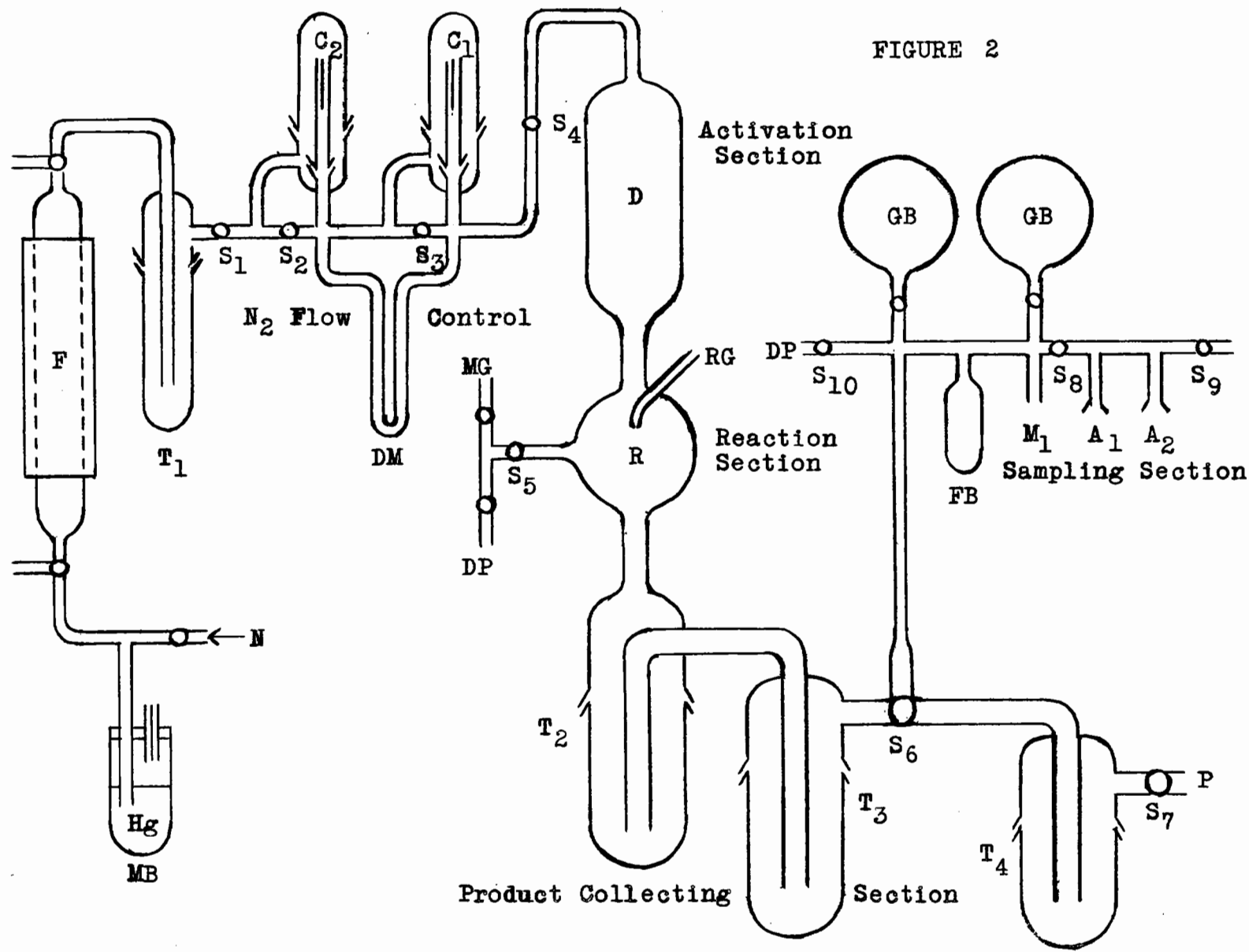


FIGURE 2

Product Collecting Section

give only slight variations in pressure, less than 1%. The nitrogen was purified as described above by passage through the furnace F and the trap T₁. A three-way stopcock was located at each end of the furnace so that hydrogen could be passed through it without passing it through the rest of the flow system.

The purified nitrogen was then introduced into the discharge vessel through a capillary flow meter, which consisted of two capillaries, C₁ and C₂ in series, across which was inserted a differential manometer DM. Any desired flow rate of nitrogen could be obtained by varying the size of the capillaries. For each flow rate the differential pressure was recorded. The flow meter could be isolated from the furnace and discharge vessel by closing stopcocks S₁ and S₄ respectively, and could be by-passed by opening stopcocks S₂ and S₃.

The Activation and Reaction Section

The nitrogen from the flow meter was passed directly into the electrodeless discharge vessel D, which consisted of a pyrex glass tube 7.5 cm. in diameter and 28 cm. in length. The excited nitrogen entered the reaction vessel R through a 25-mm pyrex tube. The reaction vessel was a one-liter pyrex flask chosen to minimize the surface to volume ratio, since no wall poisoning was used in these reactions.

The reactant gas entered the vessel through the small jet RG, 2 mm. in diameter, located in the center of the nitrogen flow.

The pressure in the reaction vessel was measured by means of the McLeod gauge MG upon opening stopcock S₅. The system could be thoroughly evacuated, whenever required, by means of the diffusion pump DP through the same stopcock.

The effluent gases passed through two 45-mm traps, T₂ and T₃, which were immersed in liquid nitrogen. The noncondensable gases were pumped out of the system by means of an Edwards S-150 high capacity vacuum pump at P. Active nitrogen was prevented from reacting with the pump oil by passage over copper turnings placed in trap T₄.

The Product Collecting and Sampling Section

The condensible products were transposed by slow distillation from traps T₂ and T₃ to the freezing bulb FB through stopcock S₆. The stopcock was then turned back to the flow position. The freezing bulb was allowed to warm up to room temperature and the pressure of the products in the accurately known volume GB was measured. Two 5-liter bulbs were required in order to obtain a pressure reading, on manometer M₁, which was large enough to be read accurately but small enough to justify appli-

cation of the perfect gas law.

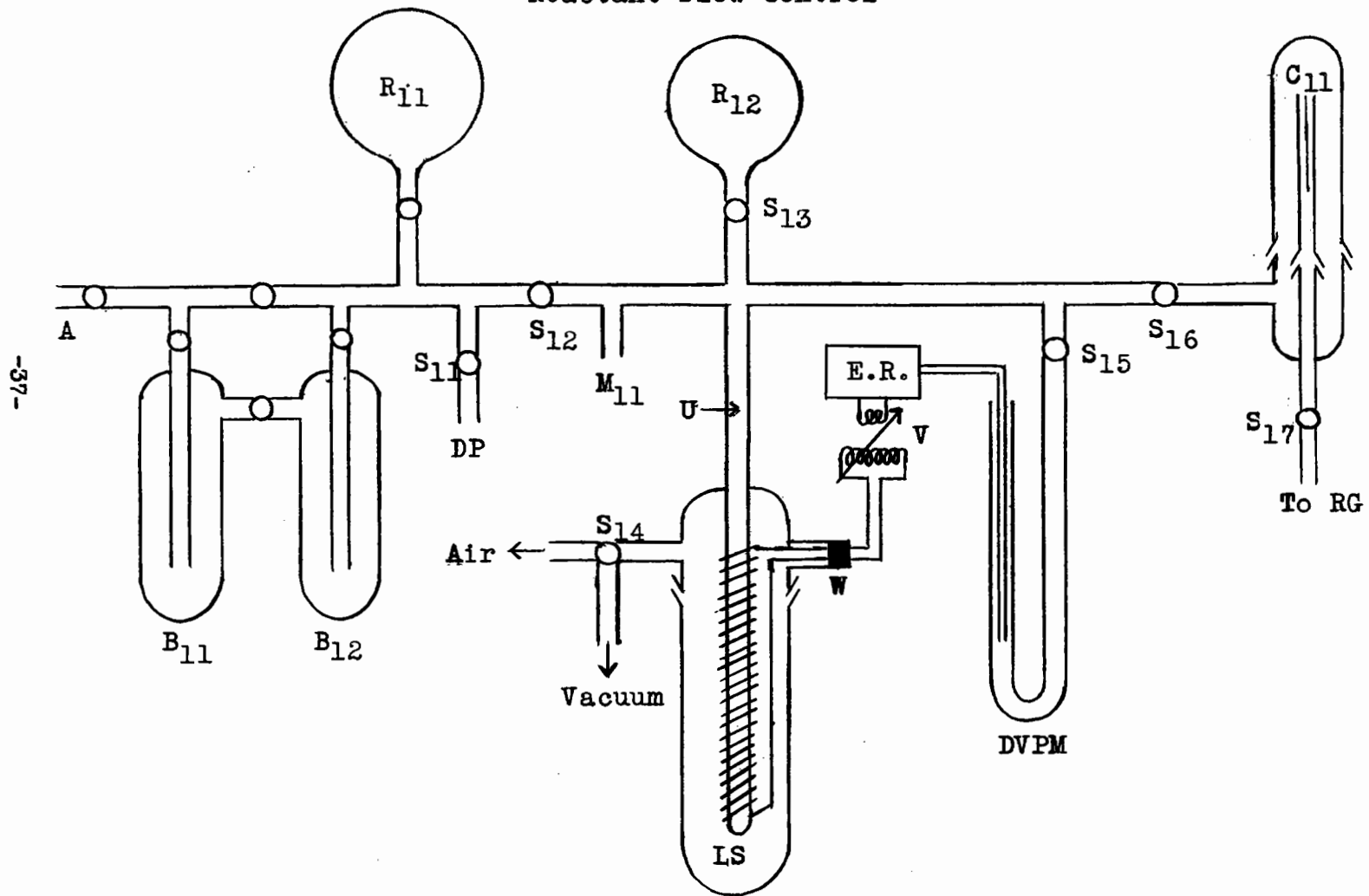
The two bulbs permitted the products to be separated into two portions, one for water analysis, and one for hydrogen cyanide analysis. These portions were transferred into sample bulbs at A_1 and A_2 through stopcock S_8 . Stopcock S_9 permitted the manifold to be brought to atmospheric pressure to facilitate removal of the sample bulbs. The manifold could be evacuated by means of a diffusion pump DP, also used to evacuate the flow system as previously mentioned, through stopcock S_{10} .

The Reactant Flow Control

This part of the apparatus is illustrated in Figure 3. The reactant was introduced at A and purified by bulb to bulb distillation (bulbs B_{11} and B_{12}) as described previously. After purification it was stored in bulb R_{11} . This part of the system could be thoroughly evacuated through stopcock S_{11} with a diffusion pump DP.

Any required amount of reactant could be introduced in the bulb R_{12} , and the constant vapor column U, by opening stopcocks S_{12} and S_{13} and closing stopcocks S_{15} and S_{16} . The amount could then be calculated from the recorded pressure on manometer M_{11} after stopcock S_{12} was closed, since the total volume thus enclosed had been previously calibrated. The gas was then frozen in the column U and stopcock S_{13} closed.

FIGURE 3
Reactant Flow Control



The contacts in the vapor pressure control manometer DVPM were then adjusted so that the desired flow rate could be obtained. The reactant gas entered the reaction vessel through stopcock S₁₆, capillary C₁₁ and stopcock S₁₇.

A uniform flow rate of reactant was provided by maintaining the pressure constant before the capillary. The column U constituted part of a modified LeRoy (85) fractionating column LS. A heating coil made of loosely wound No 30 B & S constantan wire surrounded the tube U. The heater had a resistance of 10 ohms and its leads entered the outer jacket through the tube W, into which they were sealed by Dekhotinsky cement. The space between the tube U and the removable, outer jacket could be evacuated to any pressure found suitable to give the proper heat balance between the refrigerant surrounding the outer jacket and the heating coil.

Since it was found to be very difficult to determine the proper heating rate beforehand and since this varied from experiment to experiment an automatic heating control was used. This was done by connecting one end of a U-tube to the system through stopcock S₁₅ so it could be isolated when not required. This U-tube was filled with sufficient mercury to enable the use of pressures up to one atmosphere. In the open end of the U-tube tungsten

leads of a make-and-break electrical relay ER, were introduced. This relay activated a variable transformer delivering the power to the heating coil. After roughly adjusting the heating rate the automatic control was switched on. By varying the depth of the leads in the tube any desired pressure could be maintained in the system. If the pressure became too high, contact was made through the mercury, the relay tripped, and heating was discontinued. If the pressure was too low the reverse occurred. In this way the pressure could be controlled to within 3%.

METHODS OF ACTIVATION

Discharge Tubes

The types of discharge tubes used in the electrodeless and the condensed discharge methods of excitation are drawn to the scale 1:4 in Figure 4.

The dimensions of the electrodeless discharge tube have already been given. The primary coil P.C. was located between the two sections of the split secondary coil S.C. The variable condenser which formed the remaining part of the coupling circuit was located near these coils. Energy was transmitted from the amplifier to the coupling circuit by means of coaxial cable.

The condensed discharge tube was made of a 60-cm length of 25-mm pyrex tubing bent in the form of a

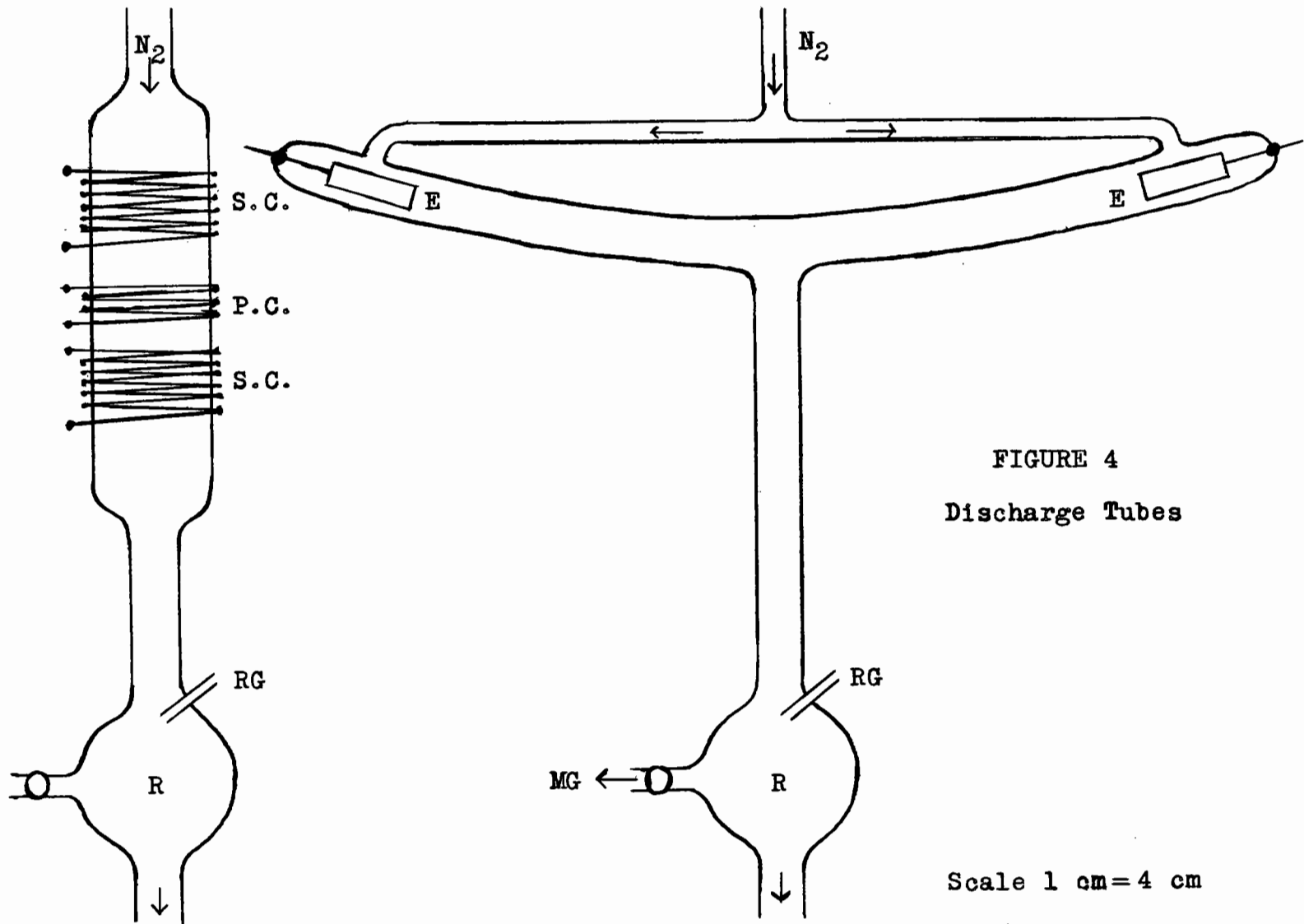


FIGURE 4
Discharge Tubes

Scale 1 cm = 4 cm

gentle U. The electrodes were hollow aluminum cylinders, 6 cm. long, 1 cm. in diameter and 2 mm. in wall thickness. The tungsten leads were sealed through the ends of the discharge tube and were connected to the electrodes by hammered connections.

The nitrogen was introduced over each electrode so that the gas flowed from the electrodes towards the center of the tube. The excited gas was withdrawn from the center of the discharge and entered the reaction vessel through a length of 25-mm pyrex tubing.

Both discharge tubes were so located that the distance between the reaction vessel and the center of the discharge was 30 cm. This distance was found sufficient to prevent back diffusion of the reactant gas into the discharge region.

Electrodeless Discharge Circuit

The electrodeless discharge was excited by a high frequency oscillator. The oscillator consisted of a push-pull 813 amplifier controlled by a 40-watt exciter. The exciter and amplifier were well shielded to prevent the escape of unwarranted radiation. Similarly, the activation coil and the circuit by which the effective load of the discharge tube was matched to the impedance of the oscillator were also shielded. The high frequency energy was transmitted from the oscillator to the coupling .

circuit by coaxial cable. The oscillator was designed to operate at several frequencies but since better coupling was obtained at 14 Mc. with the type of discharge tube used, this frequency was adopted throughout the experiments.

The exciter circuit is given in Figure 5. The circuit is identical to the one described in the Radio Amateur's Handbook (86) and has the advantage of requiring only one tuning control.

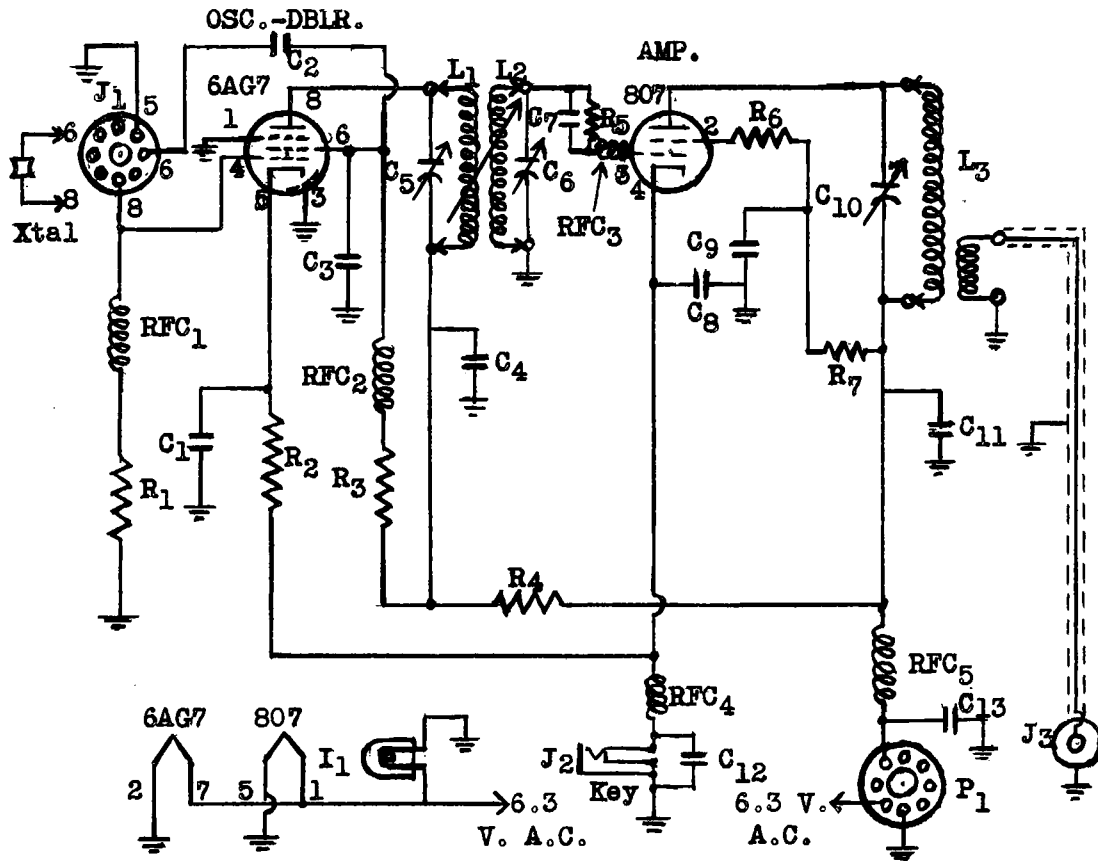
The crystal oscillator uses a modified Pierce circuit. The crystal frequency of 7.231 Mc. was doubled by the oscillator to give the 14 Mc. bands used. The coupling between the oscillator and the 807 amplifier of the exciter was adjusted to give the narrow band response required and fixed in that position. The use of inductive band-pass couplers served to reduce v.h.f. harmonics.

The coupling coils, L_1 and L_2 , were wound on the same form, $1\frac{1}{2}$ inch in diameter, $\frac{1}{2}$ inch apart. Each coil consisted of 9 close-wound turns of No. 20 d.s.c. wire. The output stage is a conventional 807 amplifier working straight through on the output frequency of the crystal oscillator.

The unit was operated from a single power supply, and both stages were keyed simultaneously. Keying of the oscillator was only used in a few specific experiments.

FIGURE 5

Exciter Circuit



- C₁, C₈, C₉ — 0.01 μ fd. disc ceramic.
- C₂ — 0.005 μ fd. disc ceramic.
- C₃ — 25 μ fd. mica.
- C₄, C₁₂, C₁₃ — 0.001 μ fd. disc ceramic.
- C₅, C₆ — 3-30 μ fd. air-dielectric trimmers.
- C₇ — 100 μ fd. mica.
- C₁₀ — 300 μ fd. transmitting variable.
- C₁₁ — 0.001 μ fd. mica, 1200 v.d.c. working.
- R₁ — 47,000 ohms, $\frac{1}{2}$ watt.
- R₂ — 330 ohms, 1 watt.
- R₃ — 47,000 ohms, 1 watt.
- R₄ — 10,000 ohms, 5 watts wire-wound.

- R₅ — 22,000 ohms, 1 watt.
- R₆ — 47 ohms, $\frac{1}{2}$ watt carbon.
- R₇ — 20,000 ohms, 5 watts, wire-wound.
- L₁ — See text.
- L₂ — See text.
- L₃ — Plate coil, for 807 stage, National AR-17-10E.
- I₁ — 6.3 volt pilot lamp.
- J₁ — Octal socket, ceramic.
- J₂ — Closed-circuit jack.
- J₃ — Coaxial connector, female.
- P₁ — Octal plug, panel mounting.
- RFC₁, RFC₂ — 2.5mh. r.f. choke.
- RFC₃ — 1.8 μ h. r.f. choke.
- RFC₄, RFC₅ — 7 μ h. r.f. choke.

The exciter was connected to the amplifier by a four-foot length of coaxial cable.

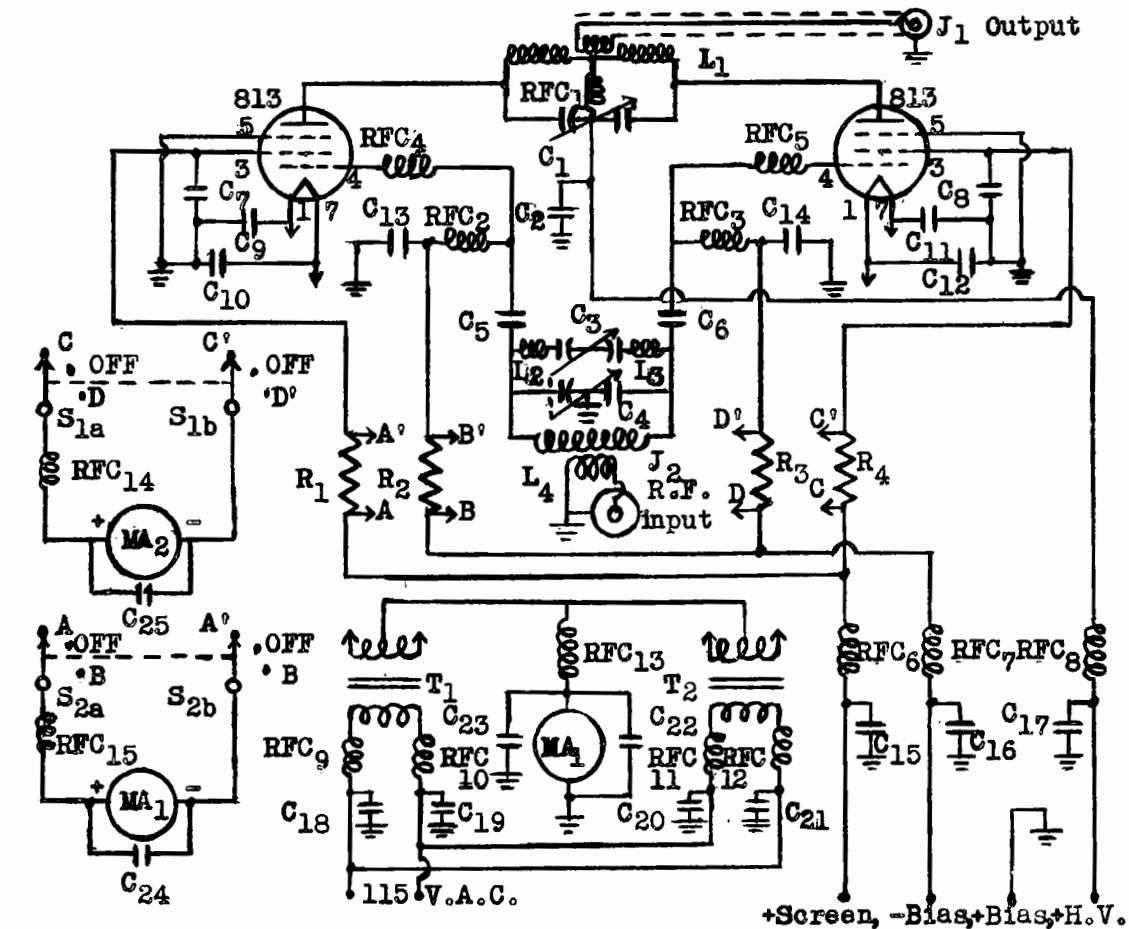
The circuit for the amplifier is given in Figure 6. The 900-watt amplifier was constructed as described in the Radio Amateur's Handbook (87), except for the omission of the neutralization condensers. A multiband tuner, eliminating the need for access to the grid circuit, permitted complete shielding for greater stability.

A commercial, National Type MB-40L tuner was used as the multiband tuner without modification. It consists of the coils L_2 , L_3 and L_4 and the condensers C_3 and C_4 in the grid circuit. With this tuner the grid tank circuit could be resonated to the frequency of the exciter with the adjustment of only one control which was then fixed in position.

A 1000-ma. d.c. meter measured the total cathode current while two 50-ma. d.c. meters registered the individual grid or screen currents of each tube. The latter permitted a ready comparison of the currents to check the balance of the amplifier. All supply leads and leads running to the meters were shielded.

In the output circuit a Baker and Williamson's Type 20HDVL coil, coil L_1 Fig. 6, was used for the 14 Mc. bands. An identical coil was also used as the activation coil wound around the electrodeless discharge tube.

FIGURE 6
Amplifier Circuit



C₁ — 100 μ fd. per-section-variable, 0.077-inch spacing.
 C₂ — 0.001 μ fd. 5000 v.d.c. working, mica.
 C₃, C₄ — See text.
 C₅, C₆ — 0.001 μ fd. mica.
 C₇, C₈ — 0.001 μ fd. 1000 v.d.c. working, mica.
 C₉₋₁₂ — 0.0047 μ fd. mica.
 C₁₃, C₁₄ — 100 μ fd. mica.
 C₁₅ — 470 μ fd. mica.
 C₁₆ — 500 μ fd. 1000 v.d.c. working, mica.
 C₁₇ — 500 μ fd. 5000 v.d.c. working, mica.
 C₁₈₋₂₅ — 470 μ fd. mica.
 R₁₋₄ — 100 ohms, $\frac{1}{2}$ watt.

L₁ — See text.
 L₂, L₃ — See text.
 L₄ — See text.
 J₁, J₂ — Coaxial connector.
 MA₁, MA₂ — 50-ma. d.c. milliammeter.
 MA₃ — 1000-ma. d.c. milliammeter.
 RFC₁ — 800-ma. r.f. choke (National R-175).
 RFC₂, RFC₃ — 2.5-mh. r.f. choke.
 RFC₄, RFC₅ — 1 μ h. 300-ma. r.f. choke (National R-33).
 RFC₆₋₁₅ — 7 μ h. r.f. choke.
 S₁, S₂ — 2-section-3-position ceramic rotary.
 T₁, T₂ — Filament transformer: 10 volts, 5 amp.

A power supply was designed which allowed the amplifier to deliver any desired amount of energy. This was made possible by connecting the primary of the plate voltage transformer to a 0-120 volt variable transformer and by inserting a two-section, multiple position switch in the screen and bias voltage circuits so that the proper screen and bias voltages could be simultaneously applied for any given plate voltage. The power switches were arranged in series so that the lower voltages were turned on before the higher ones. A time-delay relay was inserted in the power circuit to insure that no plate or screen voltages were turned on before the amplifier tubes were properly warmed up.

The energy was transmitted from the oscillator to the activation circuit by means of a 12-foot length of coaxial cable. The activation circuit was identical to the tank circuit of the 813 amplifier in construction, this being the easiest way of attaining good coupling with the amplifier. All experiments were carried out at a plate voltage of 1500 volts. The corresponding screen and bias voltages were 300 volts and -75 volts. The total cathode current was always set at 250 milliamps, this being the value for proper loading of the oscillator. The individual screen currents varied between 14-16 ma. and the grid currents between 18-20 ma., indicating proper balance.

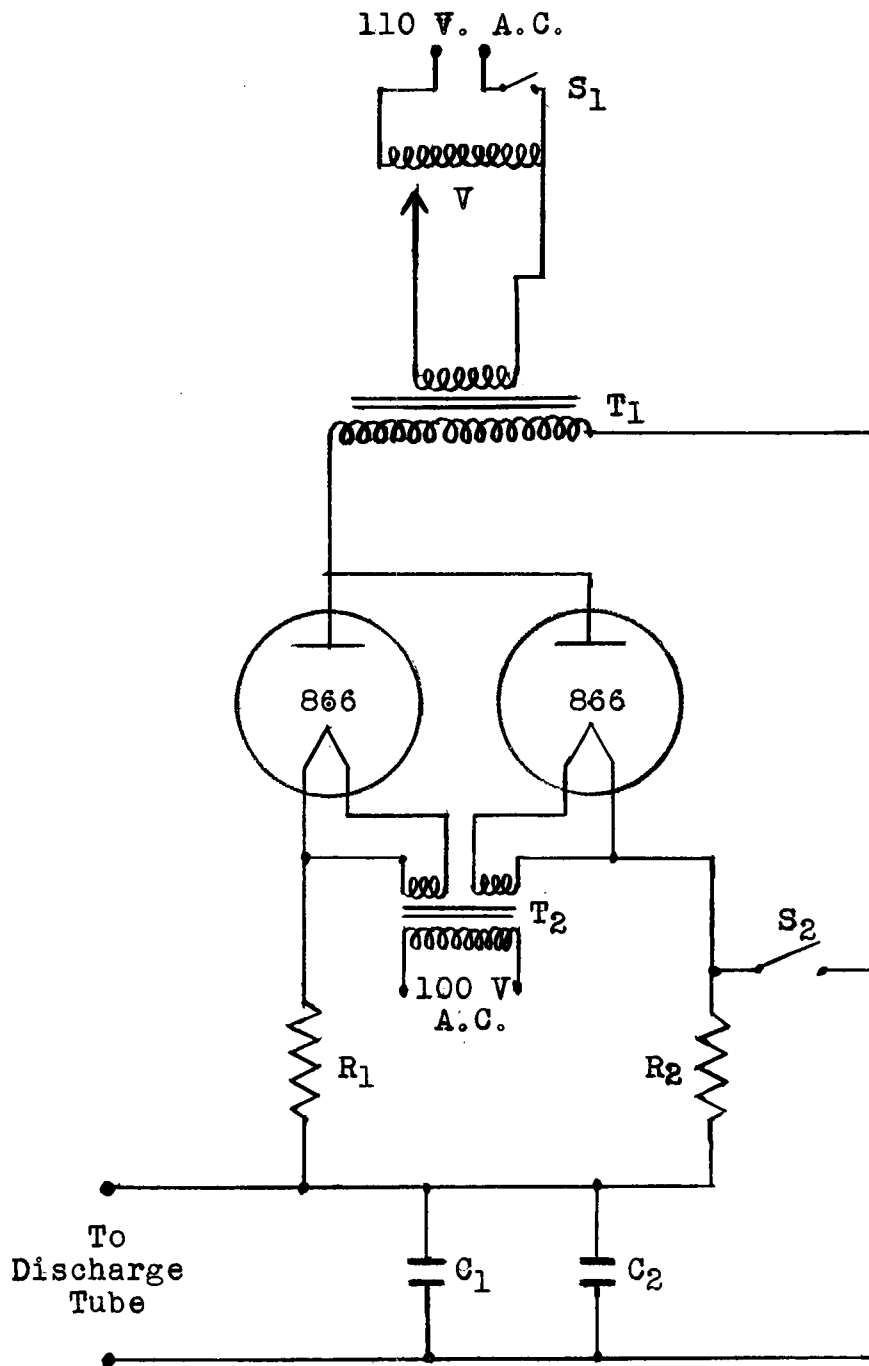
Condensed Discharge Circuit

The condensed discharge was excited by means of a relaxation oscillator whose circuit is given in Figure 7. The oscillator consisted of a 5000 V. transformer T_1 whose voltage was regulated by connecting its primary coil to a variable, 0-120 V. transformer V . One side of the secondary coil of the power transformer was connected directly to the charging condensers, C_1 and C_2 , each having a capacity of 2 microfarads. The other side was connected to the plates of two 866 mercury rectifier tubes in parallel. The filament voltages were supplied to each tube individually by the split winding of the filament transformer T_2 .

The condensers were charged up through the two 5000 ohms resistors R_1 and R_2 . The power was led from the condensers to the discharge tube by means of high voltage leads. A d.p.d.t. switch, represented here as S_1 and S_2 , was inserted so that at the end of an experiment the condensers could be discharged and the power supplied to the circuit cut off simultaneously. Resistor R_2 was used as a bleeder when the switch was closed.

The operation of the oscillator is very simple. A potential is built up on the condensers till it reaches a value greater than the break down potential of the gas in the tube. When this occurs the condensers discharge

FIGURE 7
Relaxation Oscillator Circuit



across the tube until the voltage is reduced below the value required to maintain the discharge which is then interrupted. Since a fairly constant current is delivered to the condensers, these are charged up again and the cycle repeats itself. It is obvious that the rate of discharge pulses is governed solely by the rate at which the condensers are charged up. In the present case the rate was varied by controlling the voltage delivered to the primary of the power transformer.

The pulsating rate chosen was the one which by inspection gave the most activation. It must be pointed out that the striking voltage of the discharge tube depended only on its design and the pressure of the gas in it. These were fixed for any series of experiments and therefore will not be discussed here. In practice it was found that setting the variable transformer at 60-65 volts a pulsating rate of approximately 5 pulses per second was obtained and the experiments were carried out under these conditions. Minor adjustments of the voltage had to be made during each experiment since there was a slight tendency of the oscillator to drift. An estimate of the total wattage input to the oscillator gave a value of 700 watts. The wattage delivered to the discharge tube could not be estimated since the introduction of measuring instruments altered the discharge.

PROCEDURE FOR A TYPICAL EXPERIMENT

Before beginning a series of experiments the traps T_2 and T_3 were cleaned out thoroughly. They were washed with cleaning solution and rinsed several times with distilled water. The outer jackets and the inner-tubes of the traps were then flamed with a non-luminous flame to drive off the water and to check for any salt deposits. When the traps were perfectly clean they were reassembled. The reaction and discharge vessels did not have to be cleaned since carbonization was never detected after flaming; indicating that no deposits were formed. None of the walls were poisoned.

The copper furnace was reactivated before each series of experiments by passing hydrogen through it. It was then evacuated and flushed several times with nitrogen.

The system was first pumped out thoroughly and when the furnace was at the right temperature the nitrogen flow was started by opening stopcocks S_1 and S_4 , stopcocks S_2 and S_3 being closed. The nitrogen then flowed through the capillaries C_1 and C_2 and when the proper pressure difference was recorded on the differential manometer DM the flow conditions had reached equilibrium. The pressure in the system was now measured, by the McLeod gauge MG, at three-minute intervals until constant, and then recorded. Following this the discharge was

turned on and allowed to reach a steady state.

During this time a definite amount of reactant was isolated in the reactant reservoir R_{12} and its pressure recorded on manometer M_{11} . The amount of reactant was calculated from the gas law since the pressure and volume were known. The pressure was then adjusted to deliver and maintain the required flow rate of reactant across the capillary C_{11} by means of the differential manometer DVPM.

After stable pressure and discharge conditions were obtained the product collecting traps T_2 and T_3 were immersed in liquid nitrogen and allowed to cool. Stopcock S_{16} was then opened and the moment the pressure reached equilibrium again stopcock S_{17} was opened, and the time recorded. The reaction was allowed to proceed for the desired length of time, which varied between 10 and 150 minutes, depending on the flow rate of the reactant.

During the reaction the pressure was found to remain unchanged and equal to the pressure of the nitrogen gas before the reactant was introduced. The nature of the reaction flames and the behavior of the oscillator and discharge tube were checked periodically. In the case of the condensed discharge, slight adjustments had to be made from time to time to keep a constant rate of discharge across the tube. The electrodeless discharge on

the other hand was very stable and no adjustments were required.

At the end of the experiment stopcocks S₁₇ and S₄ were closed in rapid succession and the discharge was discontinued as soon as possible. The remaining nitrogen was then pumped out of the system till the pressure was below 1 mm. as indicated by the change in sound of the pump. The three-way stopcock S₆ was closed to the pump and opened to the sampling section.

After the products were transferred to the sampling system and their total amount measured as previously described two aliquots were transposed to sample bulbs for subsequent analysis.

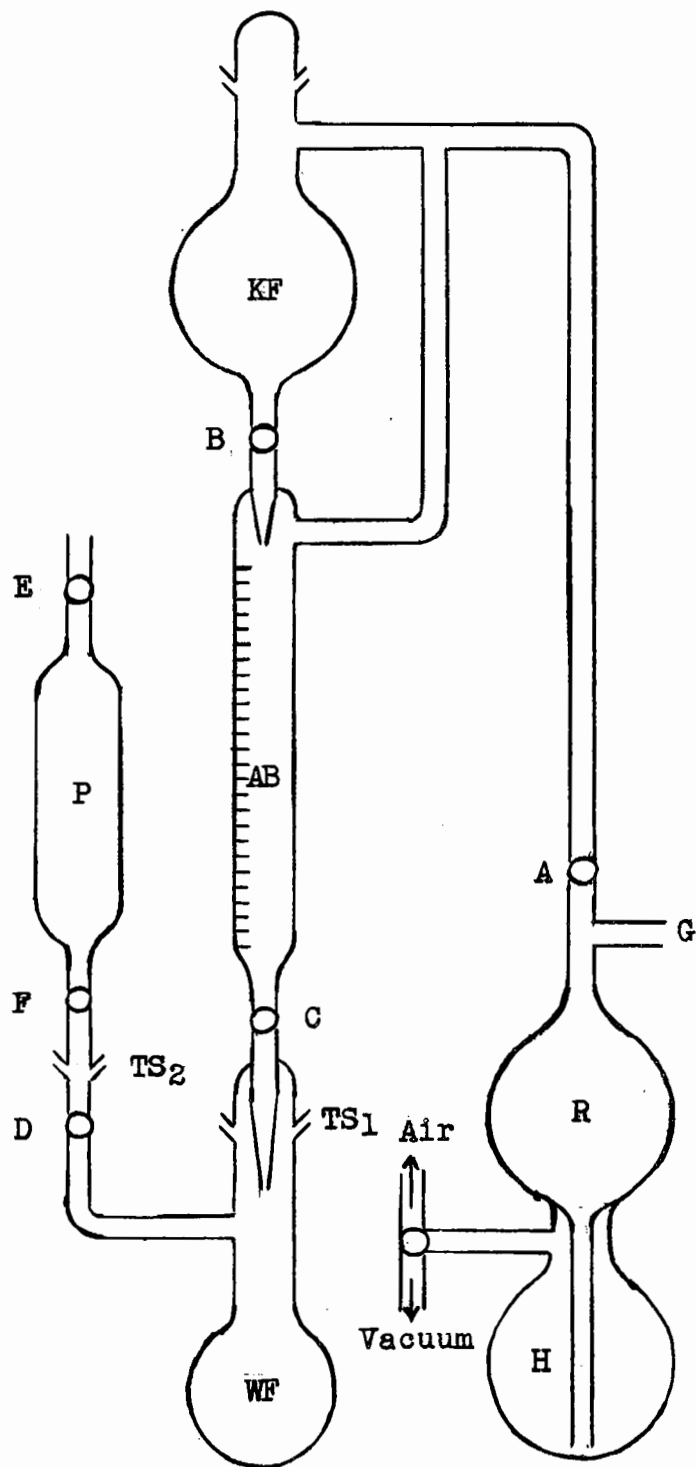
ANALYTICAL APPARATUS AND TECHNIQUE

Water Analysis

Analysis for water was carried out by the Karl Fischer titration method. In order to obtain the best possible accuracy a completely isolated system was set up as shown in Figure 8. The main feature of this apparatus was that the reagent never came into contact with the air even through tubes of standard dessicants.

The reagent was delivered to the water flask WF, which contained one of the product aliquots, from the calibrated burette AB. The pressure in the system was kept at atmospheric by forcing mercury from the reservoir

FIGURE 8
Water Analysis Apparatus



H into bulb R with stopcock A open. The relation between the internal and atmospheric pressure was given by a small differential manometer attached at G. The positive pressure that would have developed in the flask WF was reduced to atmospheric by opening stopcocks D, E and F periodically and letting the gases escape through the vessel P, filled with P_2O_5 . This vessel was provided with a stopcock at each end so that when removed from the system it would not be left open to the air. When the apparatus was not in use the mercury could be isolated from the reagent by closing stopcock A, and the lower end of the burette was protected by a dummy joint. The burette was filled by letting the reagent from the reservoir flask KF flow into it through stopcock B. All stopcocks were lubricated with silicone grease to prevent reaction with the reagent.

The Karl Fischer reagent was prepared by dissolving 25.4 g. of iodine in 500 cc. of dry methanol, adding 79 g. of pyridine and bubbling sulfur dioxide through the solution until 19.2 g. had dissolved. The volume was then made up to one liter with dry methanol. Under these conditions there was a marked change in color at the end point upon the addition of one drop of reagent. The reagent was standardized against a standard water-in-methanol solution supplied by Fisher Scientific Company,

and some standard sodium tartrate dihydrate supplied by Merck and Co. Ltd. The agreement between both standards was better than 0.5%. By using the above apparatus the reagent could be kept for months without change.

The analysis was carried out using the following procedure. Flask WF was attached to the sampling manifold by means of the standard taper joint TS_2 . The other joint on the flask, TS_1 , was closed by a matching dummy joint. After the sample had been frozen in the flask, stopcock D was closed and the flask removed from the manifold. The P_2O_5 tube P was then attached to TS_1 . The sample was allowed to warm up slowly and was prevented from exceeding atmospheric pressure by manipulating stopcocks D, E and F.

In the case of dimethyl ether the flask was not allowed to warm up above $0^\circ C$ for fear of losing some of the water which might escape along with the ether which evaporated completely.

When the sample was warmed up the dummy joints at TS_1 were quickly removed and the flask and burette joined. During the titration the solution was continuously agitated by means of a magnetic stirrer. Blank titrations were performed on the methanol and dimethyl ether. These were never larger than 0.1 cc.

Hydrogen Cyanide Analysis

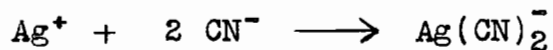
The sample aliquot used for hydrogen cyanide analysis

was collected in a pyrex tube, 4 cm. in diameter and 40 cm. long, sealed at one end and having a standard taper joint of the other. This vessel fitted into the matching joint of an adapter which was equipped with a stopcock and a standard taper joint which matched the one at A_2 on the sampling manifold.

Ten milliliters of 1 N potassium hydroxide was placed in the vessel which was then connected by means of the adapter to A_2 . The vessel was evacuated, immersed in liquid nitrogen and the sample aliquot then forced to condense on the surface of the frozen potassium hydroxide by lowering the liquid nitrogen below this level. The stopcock was closed and the vessel detached from the manifold. The vessel was then partially immersed in boiling water in such a way that the potassium hydroxide at the bottom melted and flowed over the still frozen products above it. This procedure was repeated once and the vessel was finally shaken to assure complete solution of the hydrogen cyanide.

The potassium cyanide thus formed in the KOH solution was poured into a 250-ml. erlenmeyer flask. Five milliliters of 6 N ammonia were added and the cyanide was titrated with 0.1 N silver nitrate using 0.2 g. of potassium iodide as the indicator. The appearance of a permanent turbidity of silver iodide was taken as the

end point. The initial reaction:



was followed by the formation of AgI at the end point (88).

Analysis of Other Products

Those that could not be condensed were only estimated qualitatively by mass spectrometric analysis since they never constituted more than a few parts per thousand of the nitrogen. Analysis for these were carried out on samples taken from the nitrogen flow at A₁ and A₂. The other condensible products which were liquid at room temperature and had extreme low vapor pressures were estimated from the amounts of liquid remaining after the water, hydrogen cyanide and excess reactant had boiled off. These were identified by transposing them to bulbs connected at A₁ or A₂ under prolonged distillation with subsequent analysis with the mass spectrometer.

RESULTS

REACTION OF ACTIVE NITROGEN WITH METHANOL

Characteristics of the Reaction

This reaction was carried out with active nitrogen produced by a high frequency, electrodeless discharge at three different nitrogen flow rates chosen to give a weak, moderate and strong afterglow. For comparative purposes the reaction was also carried out with active nitrogen produced by a condensed discharge, but at only one flow rate chosen to give an afterglow of comparable intensity to the brightest one obtained by the electrodeless method.

Qualitative observations indicated that the reaction took place in a blue to violet coloured zone of fairly high luminosity. Since the reaction zone flames varied in intensity and characteristics for the four series of experiments mentioned above they will be described in detail below.

Series I - Electrodeless discharge, activating nitrogen flowing at a rate of 3×10^{-4} mole/sec and at a pressure of 4.7 mm Hg. Under these conditions the afterglow was very weak and only a faint bluish flame at the alcohol inlet was observed. The afterglow was completely extinguished even at the lowest alcohol flow rate. The

intensity and extent of the flame did not appear to vary with the alcohol flow rate. The flame was approximately one to two centimeters in length.

Series II - Electrodeless discharge, activating nitrogen flowing at a rate of 5.7×10^{-4} mole/sec and at a pressure of 7.4 mm Hg. The afterglow was now moderately intense, but the introduction of the alcohol even at the lowest flow rate quenched it completely. The reaction flame was violet at the lowest alcohol flow rate, 3.6×10^{-6} mole/sec, and filled the reaction vessel completely. The flame was only 3 cm. long at a flow rate of 8×10^{-6} mole/sec, but was more intense. Upon further increasing the alcohol flow rate, the flame decreased to about 2.5 cm. in length and increased in intensity.

Series III - Electrodeless discharge, activating nitrogen flowing at a rate of 7.1×10^{-4} mole/sec and at a pressure of 8.7 mm Hg. The afterglow was now very intense; nevertheless, introduction of the alcohol still quenched it completely. The reaction flame was reddish-blue and filled the reaction vessel completely at the lowest alcohol flow rate of 2.9×10^{-6} mole/sec. At a flow rate of 7×10^{-6} mole/sec the flame was violet and only 5 cm. in length. As the flow rate was further increased the intensity of the flame increased markedly and its length decreased to 2 cm.

Series IV - Condensed discharge, activating nitrogen flowing at a rate of 5.2×10^{-5} mole/sec and at a pressure of 1.6 mm Hg. In this case the afterglow was also very intense and comparable to the one obtained in series III. The reaction flame was lavender and filled the reaction vessel completely up to alcohol flow rates of 8.4×10^{-6} mole/sec. In this case some afterglow persisted in the reaction vessel. As the alcohol flow rate was increased the flame receded in the tube leading to the discharge vessel and disappeared in the reaction vessel. When the flame was in the tube it was about 7 cm. in length. At flow rates of 20×10^{-6} mole/sec the top of the flame had receded 12 cm. in the tube and at 35×10^{-6} mole/sec it had backed up 15 cm. Again, the flame increased markedly in intensity with the alcohol flow rate.

In none of the experiments was there any indication of a trap reaction: no reaction glow was observed in this region. This was supported by the fact that no brown, nitrogeneous polymer was ever detected, as was reported to be formed in experiments using hydrocarbons (38) (39) (40).

Qualitative observations were relied upon to determine whether some of the methyl alcohol diffused back into the discharge tube. In the three series of experiments with the electrodeless discharge the afterglow was

always visible to the top of the reaction chamber and a sharp demarkation line existed there between the afterglow and the reaction flame. Under normal operating conditions the electrodeless discharge appeared to be continuous due to the high frequency of the oscillator. Its peach colour was approximately the same as that of the afterglow. If, on the other hand, the discharge was interrupted by ~~keying~~ keying the exciter two to ten times per second while the reactant was flowing, back diffusion was indicated by the change in colour of the discharge to blue. Under these conditions the afterglow was found to disappear. Therefore, when the discharge did not change in colour, and the afterglow produced by it did not decrease in intensity, it was concluded that no back diffusion had taken place.

In the fourth series of experiments, with the condensed discharge, there was some back diffusion in the tube leading to the discharge vessel. This back diffusion never proceeded more than 15 cm. in the tube and at the worst never came closer than 15 cm. from the outlet of the discharge tube. There was always a sharp demarkation line between the afterglow and the reaction zone, which suggested that back diffusion proceeded no further. Moreover, no carbon deposits were formed in the discharge tube whereas it is well known that such deposits occur

readily when carbon containing compounds are fed through an electric arc (89). Thus, although the evidence is not as conclusive as in the experiments with the electrodeless discharge, there appeared to be no large back diffusion.

The reaction temperatures were not measured since it was apparent that the reaction flames changed in intensity and size as the alcohol flow rate was varied. Thus the temperature of the reaction would be to a large extent dependent on the location of the measuring device. Furthermore, there was a marked increase in the temperature of the vessel walls due to dielectric heating from the discharge, which rendered thermocouple readings impracticable. In addition, since the present work had to be carried out without the use of wall poisoning agents, the introduction of any device in the reaction zone would have resulted in serious wall catalytic effects and made their results questionable.

Products of the Reaction

Quantitative experiments showed the major reaction products to be hydrogen cyanide, water and residual methyl alcohol. Repeated mass spectrometric analyses of the trapped products failed to yield any other constituents. Such analyses were carried out periodically in each series of experiments.

The presence of noncondensable products was detected

by sampling the gas flow beyond the traps, followed by mass spectrometric analysis. They consisted of hydrogen and oxygen. Since these were present in amounts less than 0.1% of the sample taken (the rest being nitrogen) no accurate estimates could be obtained. In addition some methane and possibly ethane were detected. The results on these last two compounds were erratic and inconclusive.

The results of the hydrogen cyanide and water analyses for Series I, II and III are shown in Tables I, II and III respectively. The hydrogen cyanide data for these three series are plotted in Fig. 9 and the water data in Fig. 10. The hydrogen cyanide values do not take into account any cyanides that might be present in the white solid generally obtained in the first trap. This amount, however, was always extremely small and could therefore not change the data by more than a few percent.

The hydrogen cyanide yield increased with increasing alcohol flow rates up to a critical flow rate, above which it remained constant. In Series II and III the initial rise seems to consist of two linear portions, the intersection of these linear portions occurring at about the same alcohol flow rate in the two cases. The horizontal portions of these curves indicate complete consumption of active nitrogen over the range of alcohol flow rates above the critical flow rate.

TABLE I

Hydrogen Cyanide, Water and Condensable Products Yield
with Various Methanol Flow Rates - Series I

Methanol mole/sec x 10 ⁻⁶	Products mole/sec x 10 ⁻⁶	Hydrogen Cyanide mole/sec x 10 ⁻⁶	Water mole/sec x 10 ⁻⁶	Gain mole/sec x 10 ⁻⁶
2.90	2.97	0.24	0.21	0.07
7.07	7.22	0.39	0.37	0.15
9.83	9.98	0.39	0.39	0.15
12.17	12.40	0.39	0.42	0.23
18.40	18.67	0.39	0.42	0.27

TABLE II

Hydrogen Cyanide, Water and Condensable Products Yield
with Various Methanol Flow Rates - Series II

Methanol mole/sec x 10 ⁻⁶	Products mole/sec x 10 ⁻⁶	Hydrogen Cyanide mole/sec x 10 ⁻⁶	Water mole/sec x 10 ⁻⁶	Gain mole/sec x 10 ⁻⁶
3.56	3.66	0.46	0.52	0.10
7.86	8.17	0.81	0.94	0.31
10.64	10.96	0.88	1.01	0.32
13.36	13.78	0.99	1.15	0.42
15.97	16.42	1.11	1.23	0.45
19.23	19.77	1.25	1.34	0.54
22.81	23.30	1.29	1.45	0.49
25.97	26.60	1.31	1.46	0.63
32.32	32.79	1.29	1.44	0.47

TABLE III

Hydrogen Cyanide, Water and Condensable Products Yield
with Various Methanol Flow Rates - Series III

Methanol mole/sec x 10 ⁻⁶	Products mole/sec x 10 ⁻⁶	Hydrogen Cyanide mole/sec x 10 ⁻⁶	Water mole/sec x 10 ⁻⁶	Gain mole/sec x 10 ⁻⁶
2.88	2.81	0.71	0.63	-0.07
7.07	7.18	1.25	1.27	0.11
12.56	12.56	1.49	1.51	0.00
12.38	12.46	1.49	1.56	0.08
12.45	12.59	1.48	1.55	0.14
18.44	18.55	1.76	2.02	0.11
25.81	25.92	1.78	2.10	0.11
32.23	32.32	1.77	2.07	0.09

FIGURE 9

Plot of Hydrogen Cyanide Yield as a Function of Methanol
Flow Rate — Series I, II and III

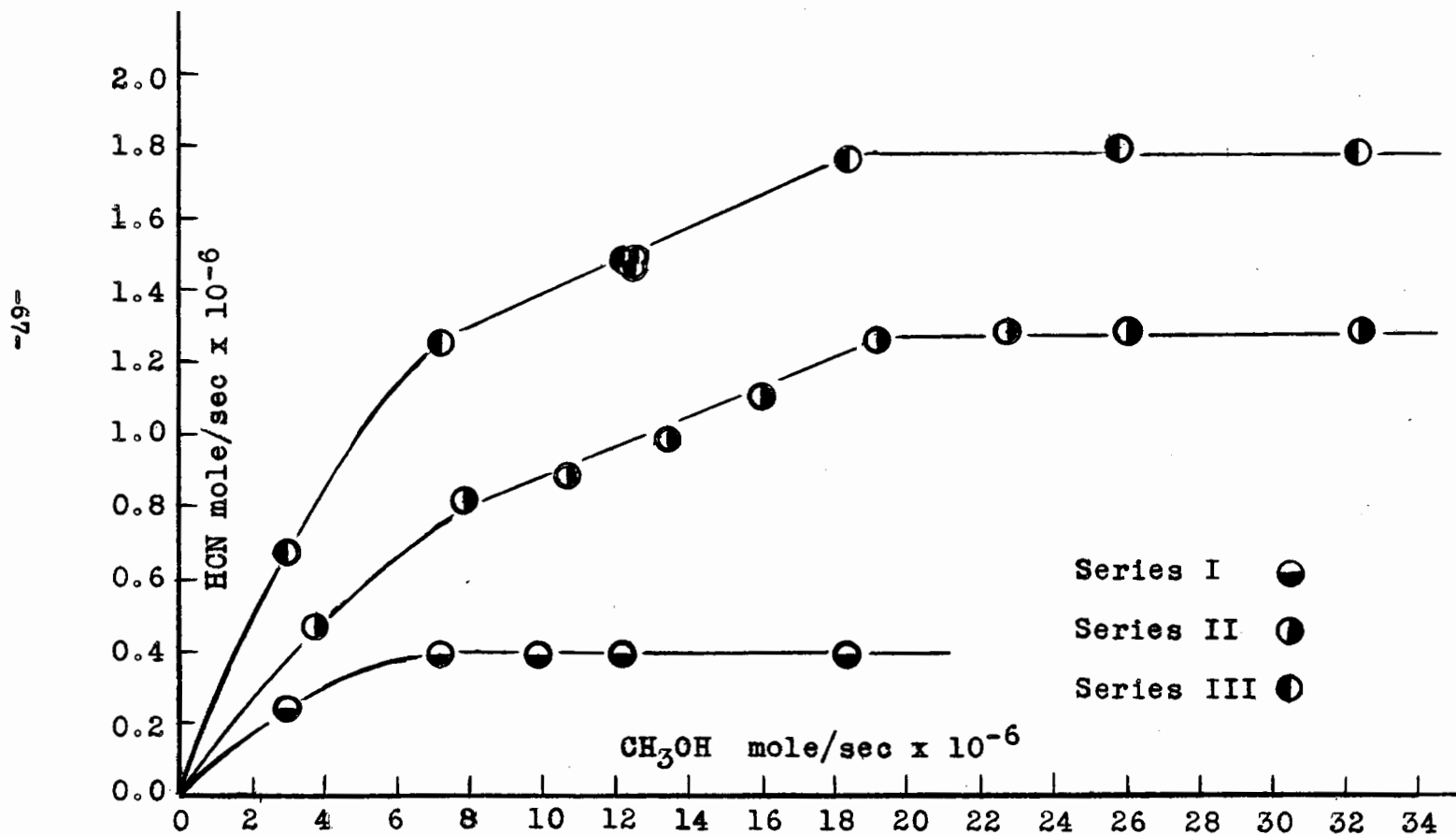
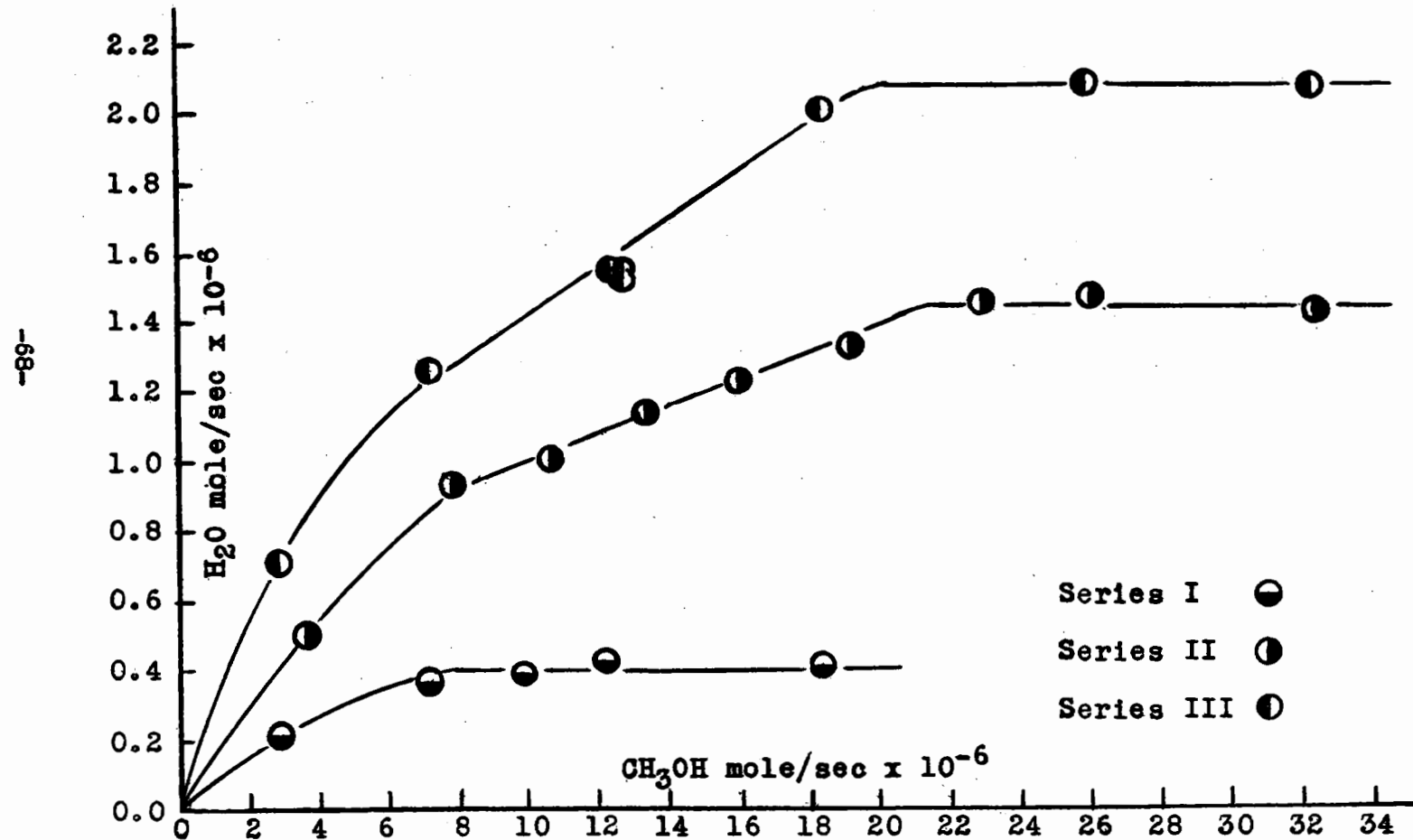


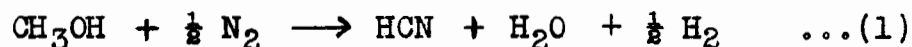
FIGURE 10

Plot of Water Yield as a Function of Methanol
Flow Rate - Series I, II and III



The water yield followed the hydrogen cyanide yield pattern. The intersections of the linear portions in the water curves for Series II and III occurred at the same alcohol flow rate. This alcohol flow rate is also the one at which the linear portions of the corresponding hydrogen cyanide curves intersected. In addition, in all three series, both the water and hydrogen cyanide yields remained constant above the same, critical alcohol flow rate.

The similarity in the behavior of the hydrogen cyanide and water curves suggests that these products are formed mole per mole of methanol reacted, and that the major portion of the reaction can be represented stoichiometrically as



However, if comparisons are made between the maximum amount of water and hydrogen cyanide produced the agreement is by no means perfect. Table IV gives these maximum yields for the three series, and Fig. 11 shows them plotted as a function of the nitrogen flow rate. It will be seen that the maximum amount of water produced is in excess of the maximum hydrogen cyanide and that the difference increases with the nitrogen flow.

Further evidence that the stoichiometric equation does not adequately describe the reaction is provided by

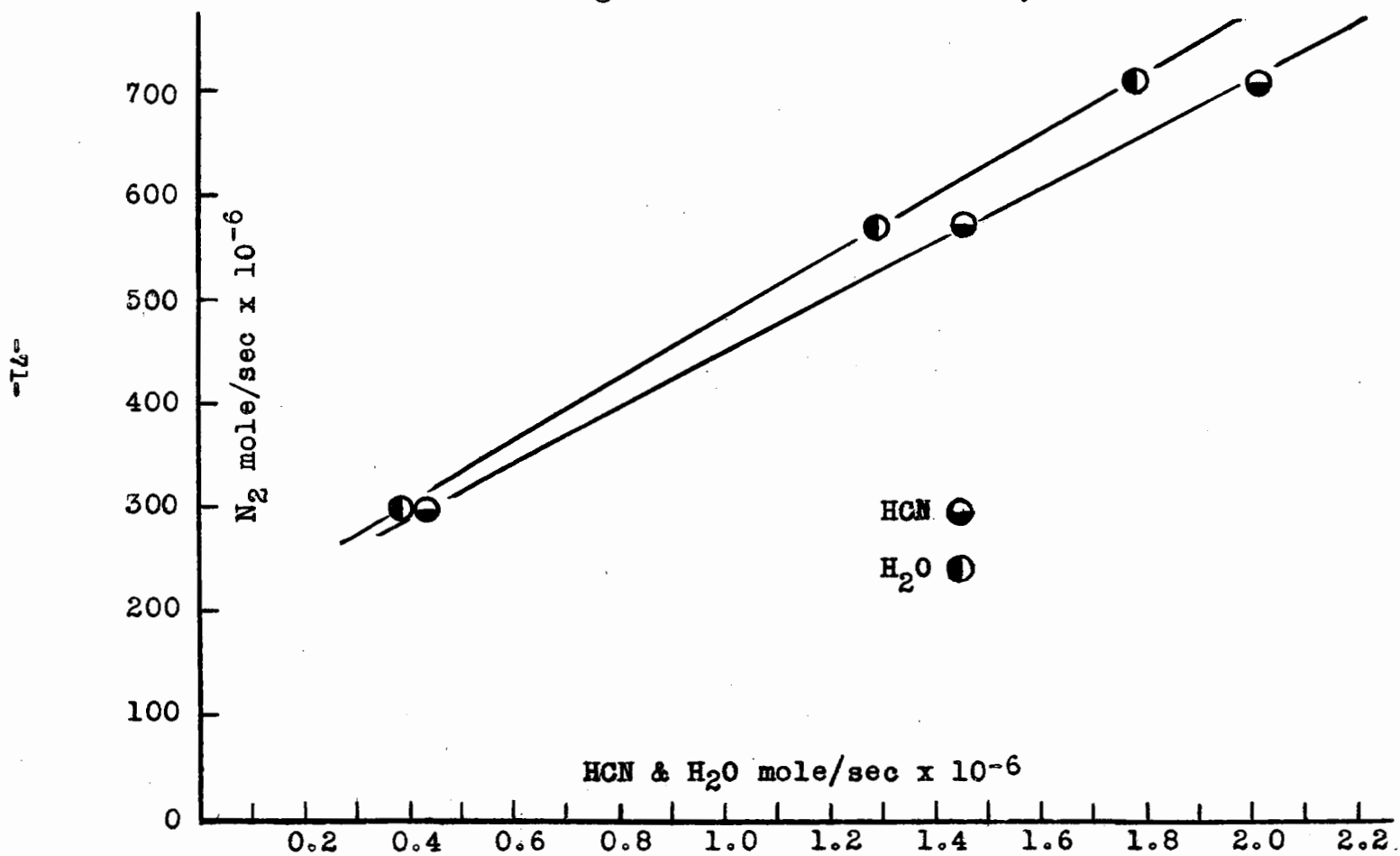
TABLE IV

Maximum Hydrogen Cyanide and Water Yield
with Various Nitrogen Flow Rates

Series	Nitrogen Flow Rate mole/sec x 10 ⁻⁶	Maximum Yield	
		Hydrogen Cyanide mole/sec x 10 ⁻⁶	Water mole/sec x 10 ⁻⁶
I	300	0.39	0.42
II	570	1.29	1.45
III	710	1.77	2.07

FIGURE 11

Plot of Maximum Hydrogen Cyanide and Water Yield as a Function of Nitrogen Flow Rate - Series I, II and III



a consideration of the mass balance. Thus according to reaction (1) the number of moles of condensible products (column 2 in Tables I, II and III) should be greater than the amount of methanol introduced into the reaction (column 1) by an amount equal to the number of moles of hydrogen cyanide or water formed (columns 3 and 4). The actual, measured gain (column 5) was always smaller than this. Some of this discrepancy is undoubtedly due to the use of the perfect gas law on these readily condensible mixtures to determine the total amount of products formed in the reaction. However, since noncondensable products other than hydrogen were detected, other reactions must also occur.

The extent to which the failure of the perfect gas law is, or the alternate reactions are responsible for these discrepancies cannot be evaluated quantitatively. However, from the order of magnitude of these discrepancies it is apparent that a fair amount of noncondensable carbon containing compounds such as methane and probably ethane also must be produced since no polymer was detected.

The results of the hydrogen cyanide and water analyses for Series IV are given in Table V. The hydrogen cyanide and water data for this series are plotted in Fig. 12.

In this case the hydrogen cyanide and water yields

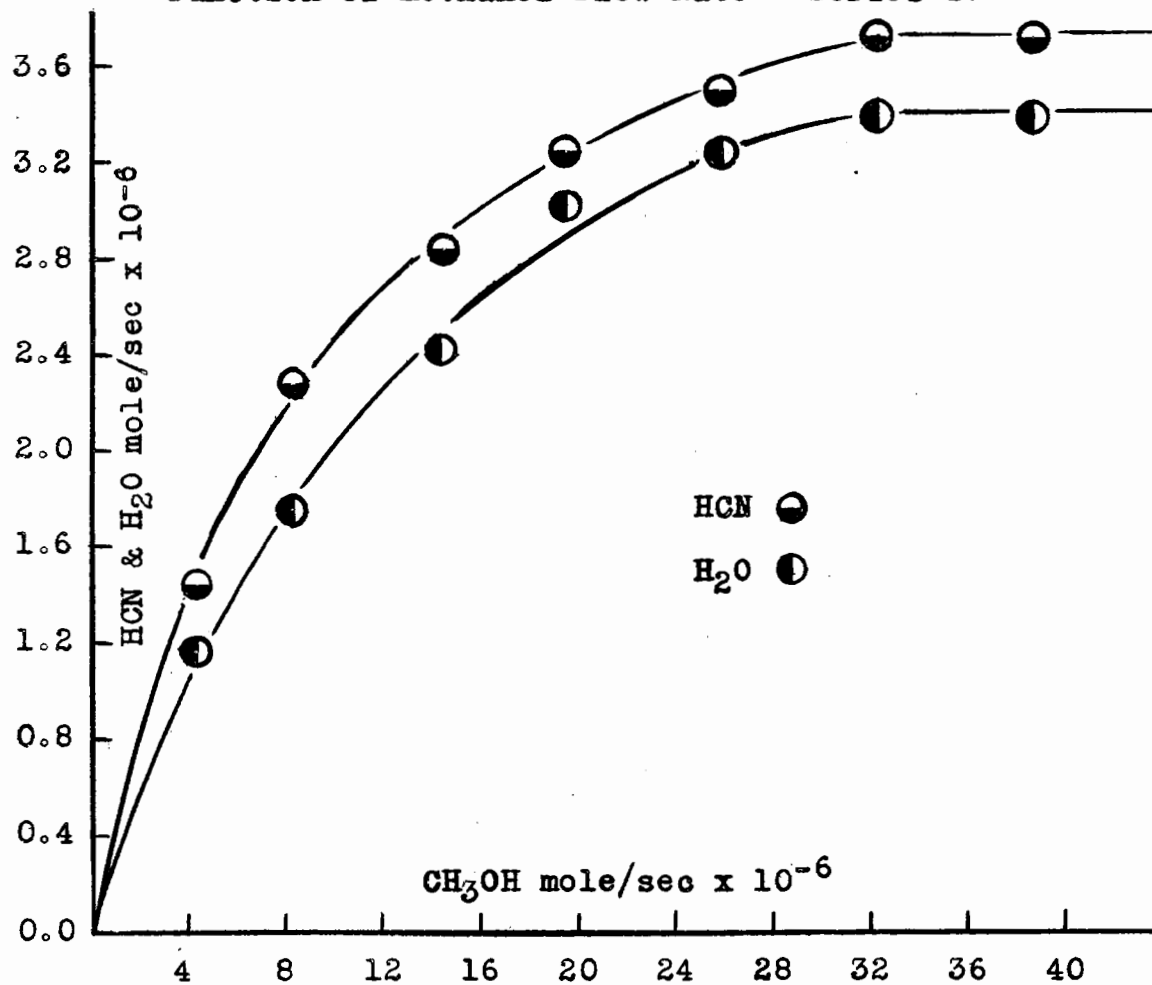
TABLE V

Hydrogen Cyanide, Water and Condensable Products Yield
with Various Methanol Flow Rates - Series IV

Methanol mole/sec x 10 ⁻⁶	Products mole/sec x 10 ⁻⁶	Hydrogen Cyanide mole/sec x 10 ⁻⁶	Water mole/sec x 10 ⁻⁶	Gain mole/sec x 10 ⁻⁶
4.15	3.83	1.44	1.13	-0.32
8.39	8.86	2.31	1.77	0.47
14.36	14.92	2.86	2.42	0.56
19.57	20.84	3.25	3.04	1.27
26.16	28.04	3.51	3.24	1.88
32.42	34.72	3.71	3.39	2.30
39.10	41.40	3.70	3.38	2.30

FIGURE 12

Plot of Hydrogen Cyanide and Water Yield as a
Function of Methanol Flow Rate - Series IV



increased gradually and did not level off until the methyl alcohol flow rate was 80% of the nitrogen flow rate. Experiments at much higher alcohol flow rates could not be performed since the reaction zone would have been too near the discharge. The critical flow rate phenomenon in this case is much less pronounced, but nevertheless still present.

The reaction also differed in some degree from that with the electrodeless discharge in that the water yield is lower than the hydrogen cyanide yield. More oxygen was liberated as indicated by the colour of the reaction flame, which was much bluer than in the first three series, and by quantitative estimates obtained by mass spectrometric analyses. There was also more white solid formed in this series than in the previous ones. This amount was approximately doubled, but was still very small.

The noncondensable products were similar to those obtained with the electrodeless discharge, namely hydrogen, oxygen, traces of methane and possibly ethane.

In Table V the number of moles of products and the gain in moles of material are also recorded. Again, from a consideration of the mass balance it is indicated that the stoichiometric equation does not adequately describe the reaction. The same difficulties being encountered in this series as in the first three series of experiments.

REACTION OF ACTIVE NITROGEN WITH DIMETHYL ETHER

Characteristics of the Reaction

Two series of experiments were carried out with dimethyl ether. One with the electrodeless discharge under the same conditions as in Series III and one with the condensed discharge as in Series IV of the methanol experiments.

Qualitative observations indicated that this reaction also proceeded with a blue to violet reaction zone of fairly high luminosity. Since the reaction flames showed marked variations in the two series of experiments they will be described separately.

Series V - Electrodeless discharge, activating nitrogen flowing at a rate of 7.1×10^{-4} mole/sec and at a pressure of 8.7 mm Hg. As in series III the afterglow was very intense and the introduction of the ether destroyed it completely even at the lowest flow rate. At ether flow rates up to 13×10^{-6} mole/sec the reaction flame was reddish blue and about 4 to 5 cm. in length. As the ether flow rate was further increased the flame increased in intensity and decreased in length. It was only 2.5 cm. at flow rates above 24×10^{-6} mole/sec.

Series VI - Condensed discharge, activating nitrogen flowing at a rate of 5.2×10^{-5} mole/sec and at a pressure of 1.6 mm Hg. At the lowest ether flow rate there were

two distinct reaction zones. A reddish flame appeared in the tube between the reaction vessel and the discharge and extended from 3 to 15 cm. above the reaction vessel. A similarly coloured flame with its upper edge 2 cm. below the connecting tube extended outwards until it filled half of the reaction vessel. The two reaction zones were thus separated by a 5 cm. dark space. At higher ether flow rates only the upper flame could be detected. Its lower end retreated up to about 8 cm. above the reaction vessel at the highest flow rate, while its upper end remained stationary. The intensity of the flame simultaneously increased and its colour deepened to a blue violet.

Products of the Reaction

Hydrogen cyanide, water and residual dimethyl ether were identified among the condensible products of the reaction. The mass spectra of the condensible fraction showed mass numbers below 45 which could not be assigned to any of the above products. When these were removed from the samples by distillation a colourless, viscous liquid remained which had the same mass spectrum as the unaccountable portion of the total sample. Since mass numbers above 45 were absent an addition product between hydrogen cyanide and formaldehyde was suspected. This addition compound, glycollic acid nitrile $\text{HO}\cdot\text{CH}_2\text{CN}$, was prepared and analyzed mass spectrometrically. The

spectrum obtained was identical to the one for the liquid fraction of the sample. Moreover, the vapor pressures, colours, and viscosities were similar and agreed with those listed in the literature for this compound. In either case the addition compound decomposed on standing in air with the evolution of hydrogen cyanide while it turned brown in colour and then black. Under vacuum it was stable and could be transposed by prolonged distillation.

The noncondensable products consisted of hydrogen and traces of methane and ethane. In addition, very little oxygen was obtained in the series of experiments with the electrodeless discharge, while for the condensed discharge more oxygen was detected. An amount of white solid comparable to that in the methanol reaction was also obtained.

The results of the hydrogen cyanide and water analyses for Series V and VI are shown in Tables VI and VII respectively. The data for Series V and VI are plotted in Figures 13 and 14 respectively.

The hydrogen cyanide yield attained its maximum value very rapidly. The portion of the curve between the lowest flow rate of ether and the critical flow rate corresponding to a decrease in size of the reaction zone. In the case of the condensed discharge the hydrogen cyanide yield increased more gradually after the sharp, initial

TABLE VI

Hydrogen Cyanide, Water and Condensable Products Yield
with Various Dimethyl Ether Flow Rates - Series V

Dimethyl Ether mole/sec x 10 ⁻⁶	Products mole/sec x 10 ⁻⁶	Hydrogen Cyanide mole/sec x 10 ⁻⁶	Water mole/sec x 10 ⁻⁶	Gain mole/sec x 10 ⁻⁶
3.86	4.81	1.90	0.80	0.95
8.02	8.90	1.97	0.82	0.88
12.93	13.17	2.12	0.89	0.24
18.47	18.83	2.21	0.88	0.36
24.20	24.24	2.20	0.87	0.04
30.32	30.66	2.19	0.85	0.34
36.22	36.33	2.16	0.85	0.11

FIGURE 13

Plot of Hydrogen Cyanide and Water Yield as a Function of Dimethyl Ether Flow Rate - Series V

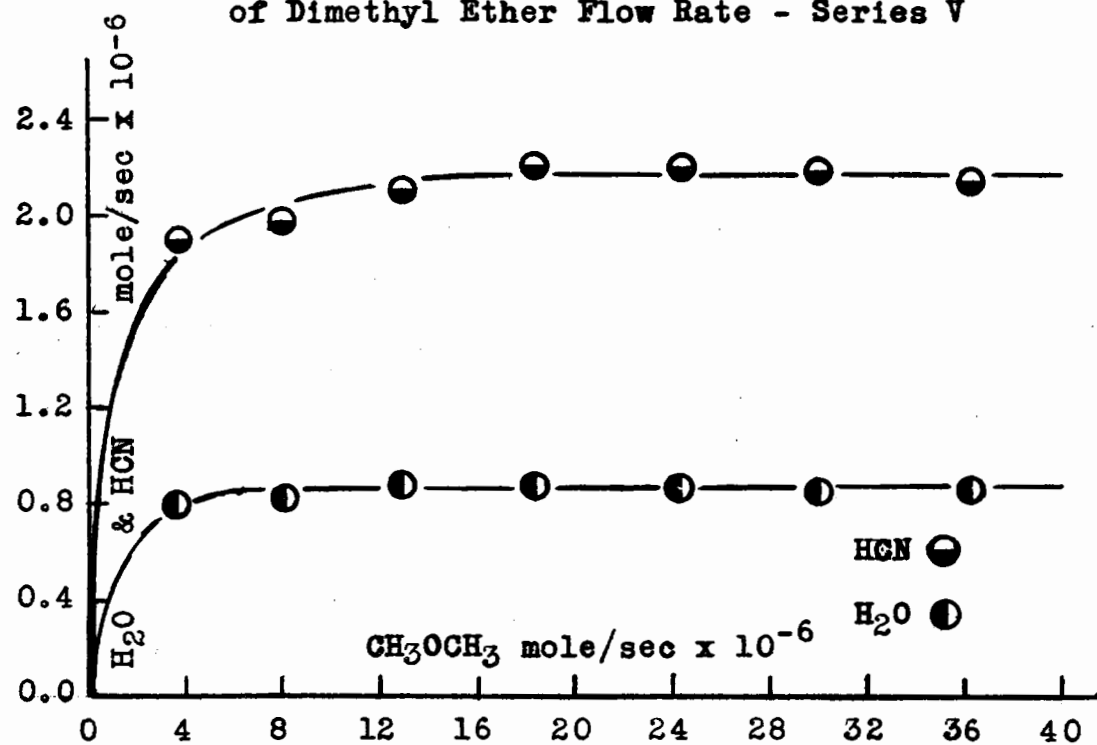


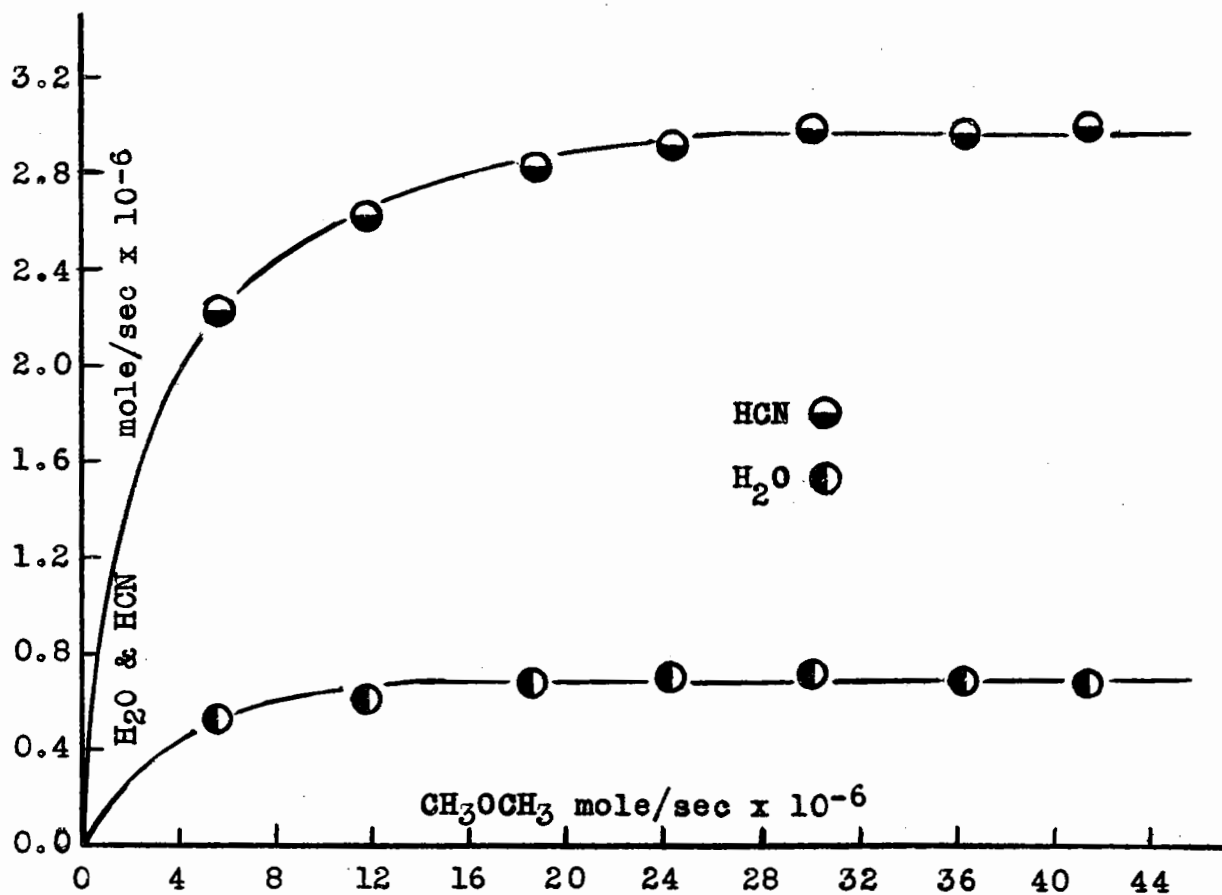
TABLE VII

Hydrogen Cyanide, Water and Condensable Products Yield
with Various Dimethyl Ether Flow Rates - Series VI

Dimethyl Ether mole/sec x 10 ⁻⁶	Products mole/sec x 10 ⁻⁶	Hydrogen Cyanide mole/sec x 10 ⁻⁶	Water mole/sec x 10 ⁻⁶	Gain mole/sec x 10 ⁻⁶
5.74	6.64	2.22	0.53	0.90
11.74	13.55	2.61	0.62	1.81
18.63	20.56	2.82	0.69	1.93
24.30	26.64	2.92	0.71	2.34
30.45	33.02	2.99	0.75	2.57
36.35	38.76	2.96	0.74	2.41
41.53	44.16	3.00	0.74	2.63

FIGURE 14

Plot of Hydrogen Cyanide and Water Yield as a Function of Dimethyl Ether Flow Rate — Series VI



rise and attained a maximum value at a higher critical ether flow rate. This was approximately the flow rate at which the reaction zone stopped receding towards the discharge.

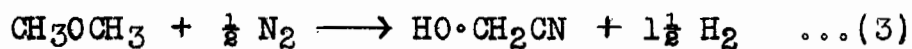
The water yield followed the hydrogen cyanide yield pattern, attaining its maximum value at the same critical ether flow rate.

As in the case of the methanol reaction this suggests that the products are formed mole per mole of dimethyl ether reacted. The stoichiometry of the reaction is illustrated by the equation



which gives a value of two for the ratio of hydrogen cyanide to water. However, in the case of the electrodeless discharge the ratio was 2.5, while for the condensed discharge it was 4.0. It is therefore evident that the stoichiometric equation does not adequately describe the reaction.

Furthermore, the formation of glycollic acid nitrile does not account for the difference between the stoichiometric ratio and the obtained ratio since two carbon atoms are present for every oxygen atom in this compound. This is illustrated by the stoichiometric equation



The difference must then be due to other reactions as

witnessed by the formation of noncondensable products. The extent of these reactions can only be inferred from the variations in this ratio since it was impossible to estimate the amounts of noncondensable products.

The glycollic acid nitrile was formed at approximately the same rate as the hydrogen cyanide in the case of the electrodeless discharge as indicated by the amount of liquid formed. For the condensed discharge it was lower by at least a factor of two. This is reflected in the observed gain in moles recorded in Tables VI and VII.

REACTION OF ACTIVE NITROGEN WITH ACETONE

Characteristics of the Reaction

This reaction was carried out to determine whether other hydrogen cyanide addition compounds could be obtained. Only one series of experiments were carried out using the condensed discharge type of activation.

Series VII - Condensed discharge, activating nitrogen flowing at a rate of 5.2×10^{-5} mole/sec and at a pressure of 1.6 mm Hg. At the two lowest acetone flow rates two reaction zones were obtained somewhat similar to those obtained at the lowest dimethyl ether flow rate in Series VI. The reaction zone in the tube leading to the discharge was red or lavender and extended from 10 to 15 cm. above the reaction vessel, while that in the reaction vessel filled the entire volume and was very faint.

Unlike the ether case however, the two zones were separated by a 10 cm. region of intense nitrogen afterglow, and some afterglow was visible up to the first trap where a blue glow was visible. At an acetone flow rate of 19×10^{-6} mole/sec the glow in the trap was no longer detected and the lower reaction zone had almost disappeared completely. The nitrogen afterglow was almost completely destroyed by the first reaction zone. As the acetone flow rate was further increased the reaction flame in the tube increased in intensity and changed in colour from red to violet.

Products of the Reaction

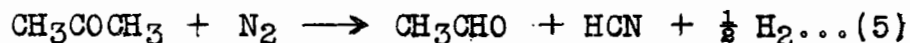
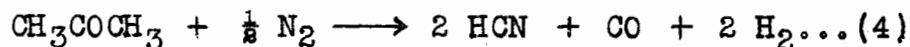
Only hydrogen cyanide could be analysed by titration. Mass spectrometric analyses of the condensible products showed the presence of unreacted acetone and acetaldehyde in considerable quantities and also confirmed the absence of water. Analysis of the noncondensable products only revealed the presence of hydrogen, although carbon monoxide, which has the same mass as nitrogen, might have been present in small quantities.

For the three lowest flow rates, which showed two reaction zones, an oil was obtained in small amounts. This oil had similar physical properties to the liquid obtained in the dimethyl ether reaction. However, it was decomposed upon heating into acetaldehyde and HCN.

The results of the hydrogen cyanide analyses are shown in Table VIII. This table is divided into two parts; the first part gives the hydrogen cyanide values obtained without decomposing the oil by heating, and the second part gives the hydrogen cyanide values obtained when this decomposition was carried out. The two sets of data are plotted in Fig. 15.

From these curves it is seen that the hydrogen cyanide yield increased rapidly at first and leveled off sharply when the critical acetone flow rate was reached, and remained constant afterwards. This indicated that maximum reactivity was also attained here.

The stoichiometric equations capable of explaining the production of acetaldehyde and hydrogen cyanide are:



In both cases an increase of one mole of condensable products should result for each mole of acetone consumed. Failure to do so was caused by the fact that some of the acetaldehyde polymerized during distillation to the sample bulb. When the addition product, lactic acid nitrile $\text{CH}_3\text{CH}(\text{OH})\text{CN}$, was obtained the mass balance deficits were large and remained larger than in the other cases after decomposition of the nitrile since this decomposition was accompanied by polymerization.

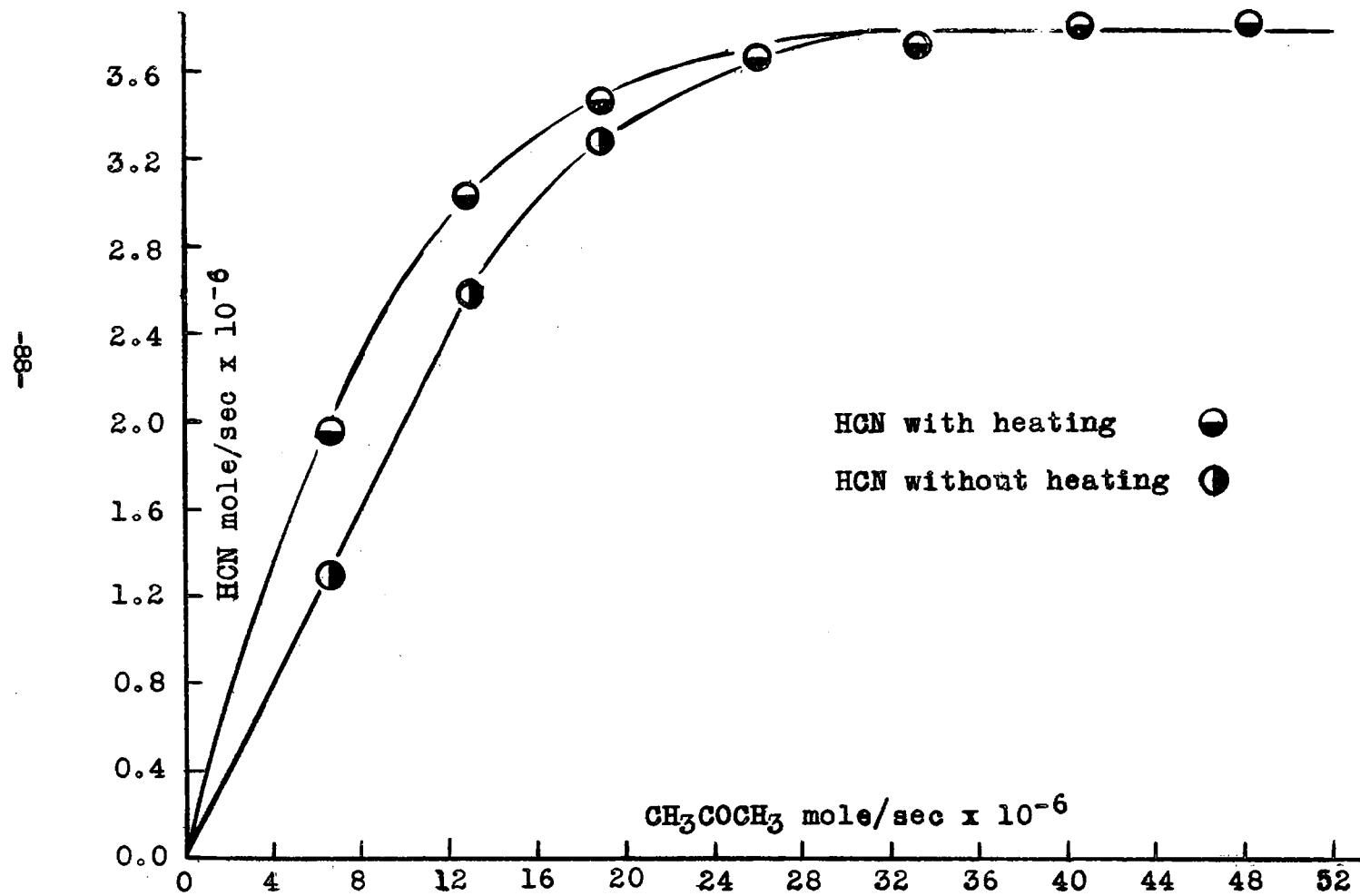
TABLE VIII

Hydrogen Cyanide and Condensable Products Yield
with Various Acetone Flow Rates - Series VII

Comments	Acetone mole/sec x 10 ⁻⁶	Products mole/sec x 10 ⁻⁶	Hydrogen Cyanide mole/sec x 10 ⁻⁶	Gain mole/sec x 10 ⁻⁶
Oil, not heated	6.67	5.43	1.27	-1.24
Oil, not heated	12.58	13.79	2.62	1.21
Oil, not heated	19.01	21.03	3.29	2.02
No oil	26.12	28.47	3.68	2.35
No oil	33.51	35.77	3.73	2.26
No oil	40.84	43.22	3.85	2.38
No oil	48.16	50.53	3.84	2.37
Oil, heated	6.61	6.55	1.95	-0.06
Oil, heated	12.85	14.24	3.07	1.39
Oil, heated	19.00	21.02	3.48	2.02

FIGURE 15

Plot of Hydrogen Cyanide as a Function of
Acetone Flow Rate — Series VII



DISCUSSION

GENERAL COMMENTS

In most investigations of reactions involving reactants produced by electrical discharges collision yields are calculated. The collision yield is defined as

$$\frac{\text{the rate of the primary process}}{\text{the number of collisions per cc. per sec.}}$$

The numerator is determined experimentally on the assumption that the initial process is rate determining. The denominator, the collision number, may be calculated from the kinetic theory. However, this calculation requires some knowledge of the concentration gradient down the reaction tube, and of the reaction time. In previous investigations of active nitrogen two alternative assumptions have been employed. First, the reactant gases were assumed to be thoroughly mixed over the entire reaction zone which was then taken to be the volume of the reaction vessel. Alternately, complete streamline flow was assumed. The results of both these alternatives were reported and the true results were assumed to correspond to an intermediate condition.

However, for the investigation reported here it is very doubtful whether either assumption is applicable for the following reasons:

1:- The reaction time cannot be calculated simply from the flow rate and the volume of the reaction vessel. At low flow rates of reactants the reaction flame filled the entire vessel, while at high flow rates it was confined to a ten centimeter region of the connecting tube in the case of the condensed discharge, or to a 2-3 cm. region at the jet in the case of the electrodeless discharge.

2:- There is some suggestion that part of these reactions proceeds heterogeneously on the walls, which invalidates collision yield calculations.

3:- Two reaction zones separated by a dark space were observed in the dimethyl ether reaction at low flow rates. In the acetone reaction the two zones were separated by a region of intense afterglow.

These observations suggest that the reactions do not proceed with uniform consumption of the reagents down the flow path. This behaviour is somewhat reminiscent of the cool-flame reactions in which alternate zones of high reactivity occur. If induction periods and possibly "whale-sardine" mechanisms are also involved in these active nitrogen reactions the usual collision yield calculations can not be applied.

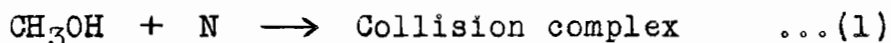
Although quantitative estimates of collision yields and activation energies can not be made it might be pointed out that complete consumption of the reactant gas was

never obtained with the conditions employed. These conditions in the case of the condensed discharge were similar to those used by Winkler and co-workers (38) (39) (40) for hydrocarbon reactions. Complete consumption of the hydrocarbons at low flow rates was reported in the case of olefins but not in the case of paraffins. It would therefore appear that the substances used in this work are less reactive towards active nitrogen than the olefins and more comparable to the paraffins.

REACTION OF ACTIVE NITROGEN WITH METHANOL

Since this reaction was the one most thoroughly investigated it will be discussed first.

The initial attack of active nitrogen can occur in at least two ways. If the activity resides in dissociated nitrogen a reaction complex could be formed as postulated in the reactions with the hydrocarbons



The point of union of the nitrogen atom is probably the carbon atom since the only nitrogen containing product found was hydrogen cyanide.

The decomposition of the collision complex might then proceed by splitting off of the OH radical



followed by

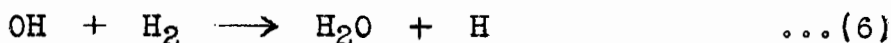


the hydrogen probably coming off as atomic rather than molecular hydrogen. The alternate decomposition of the NCH_3 fragment



was ruled out in the studies of the reaction of active nitrogen with ethane since the formation of a large amount of methane, to be expected from methyl radical reactions, did not occur. For that reaction it was concluded that the complex formed HCN exclusively and that the rearrangement proceeded rapidly.

The water could then be formed by the reaction of OH radicals with atomic or molecular hydrogen

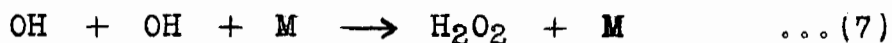


The breakdown of the initial complex into NCH_3 and OH fragments would occur rapidly and to a large extent if the collision complex has a reasonable lifetime. Geib and Harteck (90) have presented evidence that the atomic nitrogen-hydrocarbon complexes have a reasonable stability. However, complexes in which a polar group, such as OH is present might not be expected to have as great a stability.

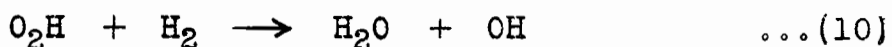
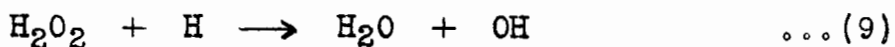
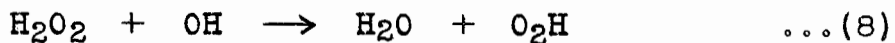
If the reaction proceeds by the above mechanism exclusively the main products should be hydrogen cyanide and water in equal proportions. However, in the experi-

ments with the high frequency discharge more water than hydrogen cyanide was formed even though some of the oxygen appeared as molecular oxygen. The ratios of the rates of water to hydrogen cyanide formation became larger as the activity increased, being 1.0, 1.1 and 1.2 respectively at maximum reactivity in each series of experiments. The mechanism as outlined above is incapable of explaining this observation.

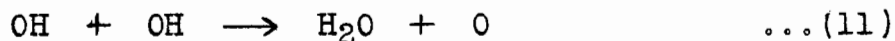
On the other hand in the case of the condensed discharge the water yield was actually lower than the hydrogen cyanide yield, the ratio being 0.95 at maximum reactivity. However, in this case more molecular oxygen was formed, perhaps as the result of an increased amount of wall reaction. According to Oldenberg and Rieke (91) OH radicals react more readily with hydrogen than with themselves. Even if the reaction between OH radicals



were to proceed in the gas phase, the formation of water would still be the main product since the peroxide is readily destroyed by the reactions:



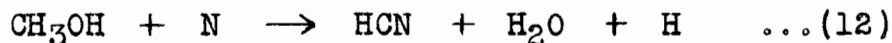
According to Rodebush, Wende and Campbell (92) the reaction



does not occur. Reaction (11) or decomposition of the peroxide radicals to form molecular oxygen could, however, occur at the unpoisoned walls in this reaction. All attempts to detect the presence of peroxides in the products were unsuccessful.

The role of the walls in this reaction is well illustrated by the difference in the results obtained from the two methods of activation. For the electrodeless discharge the reaction zone was always in the center of the flask and wall reactions were minimized. Under such conditions most of the oxygen originally present in the reacted methanol appears as water. On the other hand the reaction zone for the condensed discharge, at all flow rates, was always in contact with a large wall area and more molecular oxygen was obtained. This then may be the explanation for the lower rate of formation of water than hydrogen cyanide in the condensed discharge reaction.

Further evidence for the failure of the mechanism outlined above to adequately explain the overall reaction is provided by a consideration of the number of moles of HCN and H₂O formed compared to the possible maximum formation of these as given by the stoichiometric equation



corresponding to the mechanism.

The rate at which the methanol reacted was obtained by taking the difference between the methanol input and the calculated methanol recovery. The latter was arrived at by taking the difference between the number of moles of product collected and the sum of the hydrogen cyanide and water yields since no other condensible products could be detected. The ratio of the actual sum of the hydrogen cyanide and water yields to the maximum possible sum as obtained from the stoichiometric equation was also calculated. Finally the rate of formation of other products besides HCN and H₂O was calculated by taking the difference between the possible and actual sum of the hydrogen cyanide and water yields. These other products were identified qualitatively as methane, oxygen and ethane but could not be analyzed quantitatively. The results of the above calculations for series of experiments I to IV are recorded in Tables IX to XII respectively.

From these Tables it is clearly seen that the ratio of the actual to the possible sum of HCN and H₂O yields never exceeds the value of 0.75. This discrepancy is not solely due to some decomposition of OH radicals since the ratios of HCN to twice the methanol consumed are only 0.74, 0.57, 0.47 and 0.77 at maximum reactivity for series I to IV respectively.

TABLE IX

Series I - Calculated Data at Various Methanol Flow Rates

CH ₃ OH input	CH ₃ OH reacted	HCN yield	H ₂ O yield	Possible HCN + H ₂ O	Other products by difference	Ratio of actual to possible HCN + H ₂ O
2.90	0.38	0.24	0.21	0.76	0.31	0.60
7.07	0.61	0.39	0.37	1.22	0.46	0.62
9.83	0.63	0.39	0.39	1.26	0.48	0.62
12.17	0.58	0.39	0.42	1.16	0.35	0.70
18.40	0.54	0.39	0.42	1.08	0.27	0.75

All rate values are given in mole/sec x 10⁻⁶.

TABLE X

Series II - Calculated Data at Various Methanol Flow Rates

CH ₃ OH input	CH ₃ OH reacted	HCN yield	H ₂ O yield	Possible HCN + H ₂ O	Other products by difference	Ratio of actual to possible HCN + H ₂ O
3.56	0.88	0.46	0.52	1.76	0.78	0.56
7.86	1.44	0.81	0.94	2.88	1.13	0.61
10.64	1.57	0.88	1.01	3.14	1.25	0.60
13.36	1.72	0.99	1.15	3.44	1.30	0.62
15.97	1.89	1.11	1.23	3.78	1.44	0.62
19.23	2.05	1.25	1.34	4.10	1.51	0.63
22.81	2.25	1.29	1.45	4.50	1.76	0.61
25.97	2.14	1.31	1.46	4.28	1.51	0.65
32.32	2.26	1.29	1.44	4.52	1.79	0.60

All rate values are given in mole/sec x 10⁻⁶.

TABLE XI

Series III - Calculated Data at Various Methanol Flow Rates

CH ₃ OH input	CH ₃ OH reacted	HCN yield	H ₂ O yield	Possible HCN + H ₂ O	Other products by difference	Ratio of actual to possible HCN + H ₂ O
2.88	1.41	0.71	0.63	2.82	1.48	0.47
7.07	2.41	1.25	1.27	4.82	2.30	0.52
12.56	3.00	1.49	1.51	6.00	3.00	0.50
12.38	2.97	1.49	1.56	5.94	2.89	0.51
12.45	2.89	1.48	1.55	5.78	2.75	0.52
18.44	3.67	1.76	2.02	7.34	3.56	0.51
25.81	3.77	1.78	2.10	7.54	3.66	0.51
32.23	3.75	1.77	2.07	7.50	3.66	0.50

All rate values are given in mole/sec x 10⁻⁶.

TABLE XII

Series IV - Calculated Data at Various Methanol Flow Rates

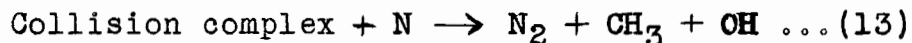
CH ₃ OH input	CH ₃ OH reacted	HCN yield	H ₂ O yield	Possible HCN + H ₂ O	Other products by difference	Ratio of actual to possible HCN + H ₂ O
4.15	2.89	1.44	1.13	5.78	3.21	0.44
8.39	3.61	2.31	1.77	7.22	3.14	0.56
14.36	4.72	2.86	2.42	9.44	4.16	0.56
19.57	5.02	3.25	3.04	10.04	3.75	0.63
26.16	4.87	3.51	3.24	9.74	2.99	0.69
32.42	4.80	3.71	3.39	9.60	2.50	0.74
39.10	4.78	3.70	3.38	9.56	2.48	0.75

All rate values are given in mole/sec x 10⁻⁶.

It will be noted that the ratios for the condensed discharge, series IV, and for the low reactivity with the electrodeless discharge, series I, are comparable. The variation in the extent of the reaction corresponding to the variation in the intensity and size of the reaction flame. In addition, for the electrodeless discharge reactions, the ratios decreased in the first three series as the activity of the nitrogen increased.

Therefore it would appear that the hydrogen cyanide formation is not exclusively associated with the initial attack of active nitrogen on the methanol molecule. In the series of experiments with the electrodeless discharge in particular the formation of other carbon containing compounds besides HCN such as methane, ethane and possibly some carbon monoxide, in amounts comparable to HCN, indicates that methyl radicals as well as other radicals might also be formed in the initial step.

A method of formation of methyl radicals might be

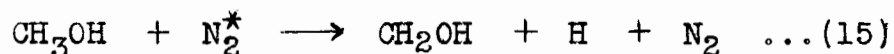
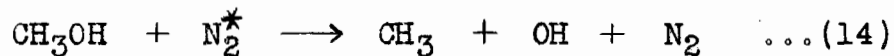


but since the atom concentration in the active nitrogen system is low it is doubtful whether the collision complex could have a sufficient lifetime to permit reaction (13) to proceed to any appreciable extent.

An alternative method of active nitrogen attack could be the transfer of energy from active nitrogen to

the methanol molecules in a manner analogous to mercury photosensitization reactions. There are several excited molecular species of nitrogen present in the afterglow with sufficient energy to break the bonds in the methanol molecules. These include the triplet states with energies of 6 to 12 volts above the ground state as well as singlet states with energies of 8 to 16 volts above the ground state.

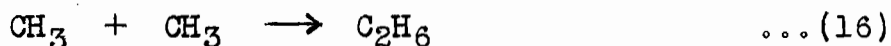
The splitting of the methanol molecules could occur in various ways such as:



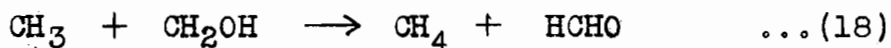
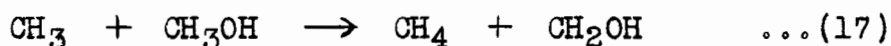
The hydrogen bond in reaction (15) would be expected to break at the carbon atom rather than the oxygen atom in view of the results of hydrogen atom and methyl radical reactions with methanol as well as the mercury photosensitization of methanol.

Of all the possible initial reactions, reaction (14) can best be made to account for the large water yield. This is in accord with the strong intensity of the OH spectrum observed in the reaction flame. If this reaction is the main initial reaction the formation of large amounts of noncondensable products - under the experimental conditions prevailing in this work - can be explained. The ethane would result from the CH_3 radical

recombinations



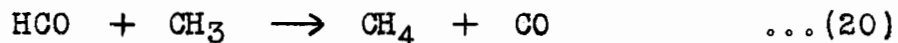
The amount of ethane would be very small, as observed, since the methyl radicals would more readily form methane by reacting with the hydrogen formed in the reaction or with the excess methanol as in the following reactions:



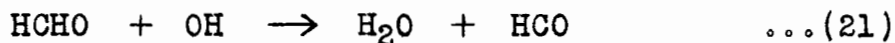
which are known to occur readily.

The CH_2OH radicals and the formaldehyde resulting from these reactions must be readily subjected to further attack since no ethylene glycol or formaldehyde were detected. Reaction (18) has been postulated to be very rapid in studies on the reaction of methyl radicals with methanol.

Decomposition of formaldehyde has been postulated to occur by the two fast reactions:



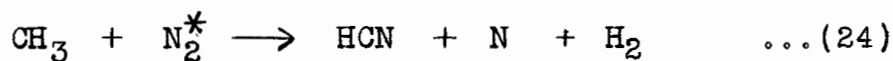
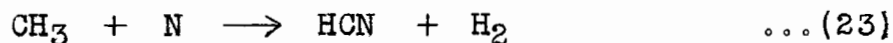
which may play important roles in this reaction due to the possible presence of a high CH_3 radical concentration. The formaldehyde might also be decomposed by the abstraction of H atoms by the OH radicals to form water:



These reactions would also lead to the loss of carbon atoms as noncondensable carbon monoxide.

The absence of even traces of formaldehyde in the products might also be due to the fact that any formaldehyde not decomposed in the reaction zone may polymerize upon solidifying in the liquid air traps. This would explain the formation of the small amount of white solid at the upper portion of the first trap just above the liquid air level. This solid was formed during the reaction and not upon melting the products in the traps since in this case a similar formation would be expected throughout the traps. The fact that the deposit occurred at or even slightly above the liquid air level and that it could not be melted without charring, suggested a polymerized material formed from a readily condensable compound such as formaldehyde. It cannot be considered to be a polymerized addition compound of formaldehyde and hydrogen cyanide since in the dimethyl ether reaction the addition product, glycollic acid nitrile, was formed in large amounts without any indication of polymerization. In addition, glycollic acid nitrile could be readily frozen, melted and distilled without any appreciable polymerization.

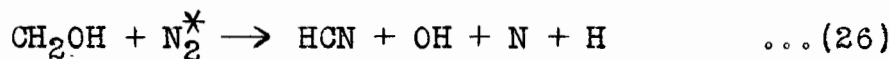
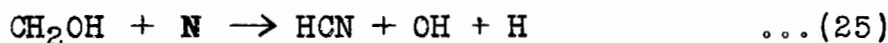
In this case the hydrogen cyanide could be formed by the reaction of active nitrogen with CH_3 radicals:



The reaction of excited molecular nitrogen, reaction (24), is just as probable as that of atomic nitrogen since several of these excited states have energies in excess of the dissociation energy of the nitrogen molecule.

Thus reaction (14) appears capable of explaining the experimental results. However, in the mercury photosensitized reaction of methanol no evidence was found for the splitting of the carbon-oxygen bond. A reaction similar to reaction (15) was preferred.

Reaction (15) could explain the hydrogen cyanide formation if it was followed by reactions:



These two reactions might occur through the formation of an intermediate stable complex such as N-CH₂-OH which rearranges by the splitting off of an OH radical and a hydrogen atom. However, it could only result in a water yield equal to the hydrogen cyanide yield, but not larger.

In addition, if a major portion of the reaction occurred in this fashion some ethylene glycol would be expected as well as formaldehyde since the CH₃ radical concentration would be much lower than if reaction (14) alone were operative. Furthermore if reaction (15) is

predominant it becomes difficult to explain the methane yield since under these conditions reaction (17), which was shown to be the major source of methane formation in the CH_3 radical reaction with methanol, would be markedly decreased.

Therefore reaction (14) must be favoured in preference to reaction (15) in order to explain the results. The active nitrogen might therefore be considered to be more effective than the $^3\text{P}_1$ mercury atoms in splitting the C-O bond due to its greater energy content. This appears a reasonable assumption considering the much larger yield of products obtained by this method of activation as compared to photosensitization. Nevertheless, reaction (15) would probably occur to some extent since it requires slightly less energy than reaction (14). The preference must be determined by the nature of the active constituents of active nitrogen.

The mechanism for the reaction, besides accounting for the different products, should be capable of explaining the behaviour of the yield curves for the different products.

In the three series of experiments with the electrodeless discharge a marked difference occurred in the HCN yield curves (Fig. 9) and the H_2O yield curves (Fig. 10) as the chemical reactivity of the active nitrogen was

increased. This increase in chemical reactivity was associated with an increase in the observed intensity of the afterglow which varied directly as the nitrogen flow rate (Fig. 11).

In all three series the reactivity increased rapidly at first up to a methanol flow rate of approximately 7×10^{-6} mole/sec. The slope of the yield curves varied with the reactivity. For the lowest reactivity, Series I, the HCN and H₂O yields remained constant above this flow rate and maximum reactivity was achieved. For the intermediate reactivity, Series II, and the highest reactivity, Series III, product formation continued to increase but at a greatly reduced rate up to a methanol flow rate of approximately 18×10^{-6} mole/sec. The slope of the yield curves, especially for H₂O, varied directly as the reactivity and the spread between the HCN and H₂O curves in each series increased. Upon further increasing the methanol flow rate the HCN and H₂O yields remained constant and maximum reactivity was achieved.

These breaks or discontinuities in the yield curves in Series II and III were carefully checked for possible experimental errors. Upon repeating the experiments in a random order for each series identical results were obtained and the experiments reported here constitute a fair sample of the experiments performed.

This behaviour suggests that there are two distinct mechanisms operative in this reaction, each leading to a series of consecutive reactions. One of the mechanisms appears to be predominant at first and the active constituent involved is rapidly consumed. This corresponds to the initial sharp rise of the yield curves up to the methanol flow rate of 7×10^{-6} mole/sec. The active constituent in this case is most likely atomic nitrogen which would react much faster due to the possibility of direct formation of HCN without passing through intermediate radical formation. This would be accounted for by the first mechanism suggested.

The second mechanism must also be operative since it shows that other compounds are formed in addition to HCN and H_2O .

Above the methanol flow rate 7×10^{-6} mole/sec the yield curves of HCN and H_2O will continue to increase as a result of the second mechanism only. The increase in reactivity will proceed until all the activity arising from the second mechanism is exhausted; this occurred at a methanol flow rate of 18×10^{-6} mole/sec.

For the first series of experiments, Series I, this second rise in activity did not occur. This can be explained by assuming that the amount of excited molecular nitrogen and the reactivity derived from these molecules

is very low and has reached its maximum as rapidly if not faster than the reactivity derived from atomic nitrogen. This is in accord with the low intensity of the afterglow observed for this series of experiments.

No discontinuity was observed in the case of the condensed discharge. This may be explained by assuming that atomic nitrogen is the predominant reactive species produced by this method of activation. Certainly the total reactivity is much greater in this case even though the afterglows are similar in intensity. The maximum percentage of the nitrogen which appears in the products as HCN was 3.6 in the case of the condensed discharge but never exceeded 0.13 for the most reactive electrodeless discharge. This figure for the condensed discharge did not correspond to a complete consumption of active nitrogen since the levelling off of the yield curve did not occur in this case before back diffusion of methanol into the discharge set in.

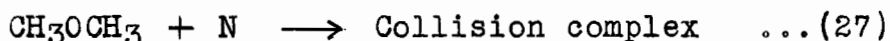
The high percentage of atomic nitrogen might also account for the difficulty in obtaining reproducible results in the case of the condensed discharge. The conditions of the walls which in these experiments were unpoisoned might be expected to be very important in this case. The failure of the second mechanism to play an important role in the condensed discharge reaction

might be due to the high percentage of products formed in this case. Deactivation of excited molecules by water and hydrogen cyanide might readily occur.

In summation then, it appears that there are two mechanisms operative in the reaction of active nitrogen with methanol, one involving atomic nitrogen and one involving excited nitrogen molecules. Both mechanisms appear to be important in the case of the electrodeless discharge reaction.

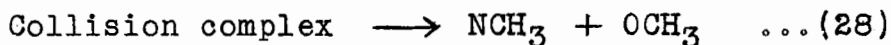
REACTION OF ACTIVE NITROGEN WITH DIMETHYL ETHER

The initial attack offers the same two possibilities as in the methanol reaction. If the activity resides in dissociated nitrogen a collision complex could be formed

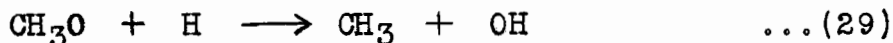


the point of union being the carbon atom in all probability.

The decomposition of the collision complex might then proceed by splitting the C-O bond, most likely at the carbon atom to which the nitrogen atom is attached



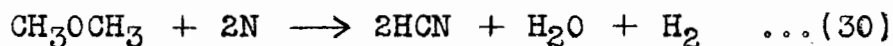
followed by reaction (3) to give hydrogen cyanide as in the methanol reaction. The water must then be formed by reactions of the OCH₃ radicals such as



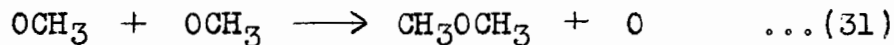
followed by reactions of OH radicals which lead to water

formation.

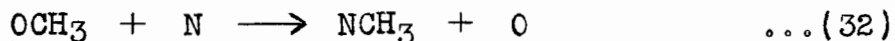
The maximum value of the ratio of the water yield to the hydrogen cyanide yield calculated from the stoichiometric equation



for the above mechanism is 0.50. The maximum value obtained from the condensed discharge experiments is 0.25 and from the electrodeless discharge experiments 0.40. The low value obtained for the condensed discharge may be due to the occurrence of wall reactions of the type



This is in agreement with the larger yields of molecular oxygen obtained from these experiments. Molecular oxygen could also be formed by the secondary reaction

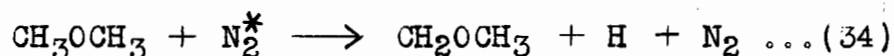
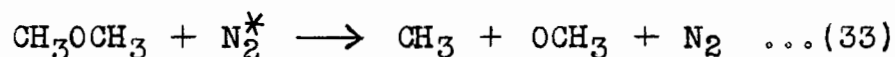


Reaction (29) appears to be the only possible secondary reaction capable of explaining the water formation. This reaction was also proposed in the investigation of hydrogen atom reactions with dimethyl ether. However, only small amounts of water were formed even though the hydrogen atom concentrations were certainly higher than those expected in the present investigation. It therefore appears that some alternative mechanism must be found to explain the large water yields.

Any alternative mechanism must also be capable of

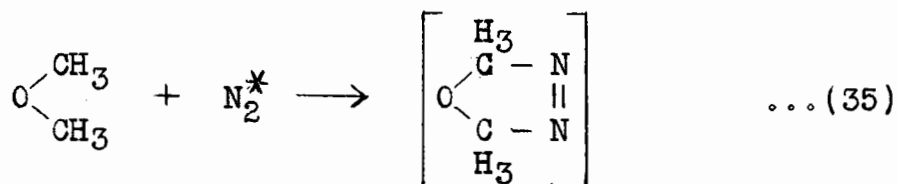
explaining the formation of glycollic acid nitrile in appreciable amounts. This compound can not be formed readily in the gas or liquid phase by simple addition of hydrogen cyanide to formaldehyde which is a possible product according to the above mechanism. Furthermore, the similar addition of hydrogen cyanide to acetaldehyde in the acetone reaction, to be discussed later, was shown to occur only to a small extent and at the lower acetone flow rates exclusively.

The energy transfer mechanism could occur in the following ways:

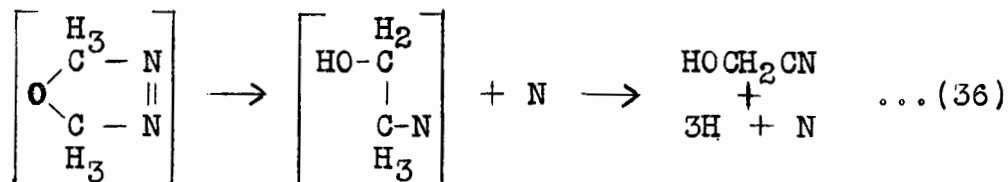


Neither reaction provides a better explanation for the water formation or for the production of the nitrile. Reaction (33) would suggest the formation of large amounts of methane which were not detected. No stable products were found to suggest the occurrence of reaction (34).

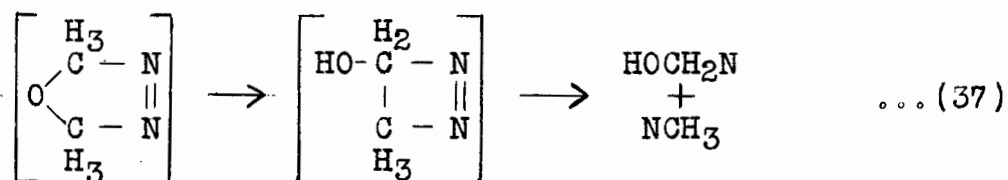
The products observed could be formed if excited nitrogen molecules attacked both carbon atoms of the dimethyl ether molecules



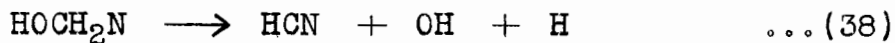
The complex could then lead to the formation of glycollic acid nitrile as follows:



Alternately the complex could decompose via:



The NCH_3 complex resulting from this reaction would lead to hydrogen cyanide formation as in reaction (3) while the HOCH_2N complex by decomposing as follows



would lead to water formation either directly or by subsequent OH radical reactions.

Thus the above mechanism can explain the formation of glycollic acid nitrile as well as water, the different yields of these two products depending on the rate at which the two rearrangements within the complex occur.

This mechanism in addition to accounting for the products should be capable of explaining the behaviour of the yield curves for the different products and should account for the differences obtained by the two methods of activation.

In contrast to the methanol reaction, the yield

curves showed no discontinuities. This suggests that in this case the two mechanisms proposed have comparable probabilities. The possible formation of a relatively stable intermediate may account for the different behaviour in the two reactions.

The fact that glycollic acid nitrile is a more important product in the electrodeless discharge reaction is in agreement with the suggestion that there are two reactive species which are produced in different proportions by the two methods of excitation.

In the case of the condensed discharge reaction the nitrile formation becomes less important compared to the gaseous products at higher flow rates. This might be due to the deactivation of the excited molecular species by the increased concentration of products in the reaction zone under these conditions.

In the case of the electrodeless discharge reaction on the other hand the amount of nitrile formed increases with increasing dimethyl ether flow rates. This could be explained by again assuming that a smaller proportion of atomic nitrogen is produced by this method of activation.

The occurrence of two reaction zones at the lower dimethyl ether flow rate in the case of the condensed discharge might be due to the incomplete removal of one

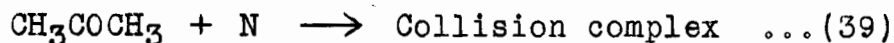
of the active constituents in the upper reaction zone which, upon coming into contact with the greater dimethyl ether concentration at the inlet jet, proceeds to react further. Since no afterglow was visible in the dark space between the two reaction zones, the active constituent cannot be one which leads directly to the production of the afterglow.

In summation then, it appears that as in the case of the methanol reaction two species must be invoked to explain the formation of the products obtained and the behaviour of the reaction. However, in the methanol reaction the excited molecules were postulated to act via an energy transfer mechanism whereas in this reaction it is suggested that they first form a relatively stable intermediate.

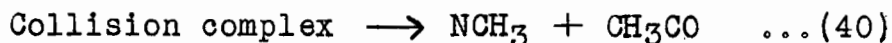
REACTION OF ACTIVE NITROGEN WITH ACETONE

This reaction was studied briefly to investigate the formation of hydrogen cyanide addition compounds with aldehydes.

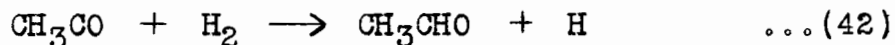
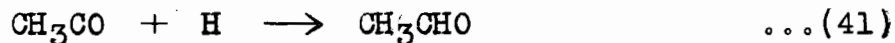
As in the two previous reactions there exist two possible modes of attack. The atomic attack which passes through the formation of a collision complex



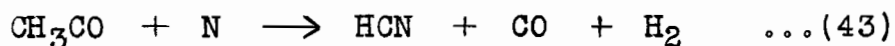
followed by its decomposition



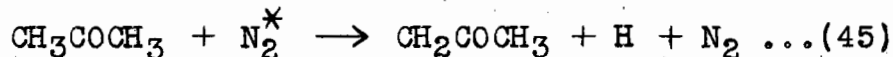
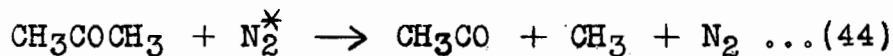
The hydrogen cyanide is then formed as in reaction (3) and the CH_3CO radicals rapidly react to form acetaldehyde by:



or can undergo further reaction with atomic nitrogen



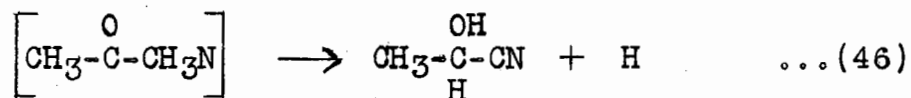
The molecular attack could proceed through energy transfer reactions as follows:



The radicals thus formed leading essentially to the same products as in the atomic attack.

The reaction was not studied in sufficient detail to permit a more comprehensive discussion of the mechanism. Suffice it to say that from the behaviour of the yield curves for hydrogen cyanide this reaction is similar to the methanol reaction, both leading to the formation of the same amount of HCN at maximum reactivity. However, the attainment of maximum reactivity is achieved at a lower flow rate of acetone than of methanol.

In this case the lactic acid nitrile could be formed by a rearrangement of the acetone-nitrogen atom complex



Its formation occurred only at low acetone flow rates, that is at flow rates below those corresponding to complete consumption of active nitrogen. This is exactly the range of flow rates at which two reaction zones were detected, one in the tube leading to the discharge vessel and one in the reaction vessel.

However, in this case the two reaction zones were separated by a region of intense afterglow as if the reaction in the upper region only removed active constituents not directly involved in the production of the afterglow. This would suggest that a different active species has been removed in this reaction as compared to the dimethyl ether reaction where no afterglow was detected between the two reaction zones. Therefore the removal of different active constituents might be an explanation for the presence or absence of an afterglow between two reaction zones.

The fact that the afterglow persisted up to acetone flow rates of 20×10^{-6} mole/sec while it was always destroyed at the lowest methanol or dimethyl ether flow rates which were about one fourth of this figure seems to indicate that in reactions where OH or OCH₃ radicals and water are present the excited molecules are rapidly deactivated by collision. In the acetone reaction where no water was formed it appears that compounds or radicals

such as CH_3CHO , CH_3COCH_3 , CO and CH_3CO are less effective in deactivating the excited nitrogen molecules.

Whether or not the above assumptions are correct the important fact remains that above acetone flow rates of 25×10^{-6} mole/sec no more lactic acid nitrile could be detected even though there was still a large amount of acetaldehyde and hydrogen cyanide formed. This is clearly shown by the values recorded in Table VIII and summarized in Fig. 15. From this it is seen that the formation of acid nitriles (whether glycollic as in the dimethyl ether reaction, or lactic as in the acetone reaction) must occur during the reaction by a rearrangement of collision complexes and not by subsequent addition of hydrogen cyanide to the respective aldehydes.

SUMMARY

- 1 - The reaction of active nitrogen with methanol was shown to lead to the formation of HCN, H₂O which were detected quantitatively and CH₄, O₂, C₂H₆ which were detected qualitatively.
- 2 - The reaction was explained by postulating two reactive species in active nitrogen. Atomic nitrogen was assumed to react by a mechanism involving the initial formation of a collision complex. A second mechanism involved the transfer of energy from excited molecular nitrogen to the methanol molecule. The first mechanism appeared to be more important in the case of the condensed discharge, the second in the case of the electrodeless discharge.
- 3 - The reaction with the condensed discharge appeared to be partly heterogeneous. The percentage of active nitrogen calculated from maximum nitrogen found in the products was 3.6 in the case of the condensed discharge and 0.13 in the case of the electrodeless discharge.
- 4 - The products of the reaction of active nitrogen with dimethyl ether were HCN, H₂O, glycollic acid nitrile, O₂ and CH₄.
- 5 - In the dimethyl ether reaction the excited molecular

nitrogen was postulated to form an addition complex with the ether molecule in order to explain the formation of large amounts of glycollic acid nitrile. The detection of two reaction zones separated by a dark space again suggested the presence of two reactive species.

- 6 - The reaction of acetone with active nitrogen produced by the condensed discharge led to the formation of HCN, CH_3CHO and in addition, to lactic acid nitrile at low acetone flow rates.
- 7 - The formation of lactic acid nitrile was assumed to result from the rearrangement of the acetone atomic nitrogen complex. Two reaction zones, in this case separated by a region of afterglow, were also observed.
- 8 - It appears that the nitrogen afterglow is readily destroyed by R-O radicals or R-OH compounds (where R stands for H or CH_3) and less readily by R-CO radicals or R-CO-R compounds.

BIBLIOGRAPHY

1. A. Morren, Ann. chim. phys. 4, 293 (1865).
2. E.P. Lewis, Ann. Physik, 2, 459 (1900).
Astrophys. J. 12, 8 (1900).
Ibid. 20, 49 (1904).
Phys. Rev. 18, 124 (1904).
3. J.B.B. Burke, Phil. Mag. 1, 342 (1901).
4. J. Kaplan, Phys. Rev. 37, 1004 (1931).
5. J. Kaplan, Phys. Rev. 42, 807 (1932).
6. H.P. Knaus and A.E. Murray, Rev. Scient. Inst. 11, 78 (1940).
7. E.J.B. Willey, Proc. Roy. Soc. (London) Ser. A 159, 247 (1937).
8. E.J.B. Willey, Nature, 119, 924 (1927).
9. R.J. Strutt, Proc. Roy. Soc. (London) Ser. A 92, 438 (1916).
10. R.J. Strutt, Proc. Roy. Soc. (London) Ser. A 88, 539 (1913).
Z. Physik, 14, 215 (1913).
Ibid. 15, 274 (1914).
11. A. Koenig and E. Elöd, Z. Physik, 14, 165 (1913).
12. E. Tiede and E. Domcke, Ber. 47, 420 (1914).
13. H.B. Baker, R.J. Strutt, E. Tiede and E. Domcke, Nature,
93, 478 (1914).
14. R.J. Strutt, Proc. Roy. Soc. (London) Ser. A 91, 303 (1915).
15. H. Sponer, Z. Physik, 34, 622 (1925).
16. G. Herzberg, Z. Physik, 46, 878 (1928).
17. B. Lewis, Nature, 121, 938 (1928).
J.A.C.S. 51, 654 (1929).
18. Lord Rayleigh, Proc. Roy. Soc. (London) Ser. A 180, 123 (1942).
19. L.H. Reinecke, Z. Physik, 135, 361 (1953).

20. Lord Rayleigh, Proc. Roy. Soc. (London) Ser. A 151, 567 (1935).
21. R. J. Strutt, Proc. Roy. Soc. (London) Ser. A 86, 56 (1912).
Ibid. 87, 179 (1912).
22. G. Cario and J. Kaplan, Nature, 121, 906 (1928).
23. J. Okubo and H. Hamada, Phil. Mag. 15, 103 (1933).
24. R.J. Strutt, Proc. Roy. Soc. (London) Ser. A 86, 262 (1912).
25. C.T. Knipp and L.N. Scheuerman, Phil. Mag. 8, 684 (1929).
26. Lord Rayleigh, Proc. Roy. Soc. (London) Ser. A 176, 1 (1940).
27. D.E. Debeau, Phys. Rev. 61, 668 (1942).
Ibid. 62, 302 (1942).
28. H.O. Kneser, Ann. Physik, 87, 717 (1928).
29. E.J.B. Willey, J. Chem. Soc. 336 (1930).
30. M.N. Saha and N.K. Sur, Phil. Mag. 43, 421 (1924).
31. E.J.B. Willey, J. Chem. Soc. 2831 (1927).
32. R.J. Strutt, Proc. Roy. Soc. (London) Ser. A 85, 219 (1911).
33. B. Lewis, J.A.C.S. 50, 27 (1928).
34. R.H. Ewart and W.H. Rodebush, J.A.C.S. 56, 97 (1934).
35. E.J.B. Willey and S.G. Foord, Nature, 128, 493 (1931).
36. E.J.B. Willey and W.A. Stringfellow, J. Chem. Soc. 153 (1932).
37. L.B. Howard and G.E. Hilbert, J.A.C.S. 60, 1918 (1938).
38. H. Blades and C.A. Winkler, Can. J. Chem. 29, 1022 (1951).
39. J.H. Greenblatt and C.A. Winkler, Can. J. Research, Sect. B,
27, 721 (1949).
40. J. Versteeg and C.A. Winkler, Can. J. Chem. 31, 1 (1953).
41. J. Okubo and H. Hamada, Science Repts. Tokoku Imp. Univ.
23, 289 (1934).
42. E.J.B. Willey, Nature, 138, 1054 (1936).

43. S.K. Mitra, *Science and Culture*, 9, 49 (1942-43).
Ibid. 10, 133 (1944-45).
Nature, 154, 212, 576, 831 (1944).
44. E.J.B. Willey and W.A. Stringfellow, *Nature*, 126, 349 (1930).
45. R.E. Worley, *J. Chem. Phys.* 16, 533 (1948).
46. J.M. Benson, *J. App. Phys.* 23, 757 (1952).
47. H. Hebb and H. Sponer, *Phys. Rev.* 59, 925 (1941).
48. G. Cario and J. Kaplan, *Z. Physik*, 58, 769 (1929).
49. G. Cario, *Z. Physik*, 89, 523 (1934).
50. A.G. Gaydon, *Dissociation Energies and Spectra of Diatomic Molecules*, London, 1947.
51. N. Thomas, A.G. Gaydon and L. Brewer, *J. Chem. Phys.* 20, 369 (1952).
52. G.B. Kistiakowsky, H.T. Knight and M.E. Malin, *J.A.C.S.* 73, 2972 (1951).
53. G. Herzberg, *Z. Physik*, 49, 512 (1928).
54. Z. Bay and W. Steiner, *Z. Elektrochem.* 35, 733 (1929).
55. P.K. Kichlu and S. Basu, *Nature*, 123, 715 (1929).
56. W.S. Herbert, G. Herzberg and G.A. Mills, *Can. J. Research, Sect. A*, 15, 35 (1937).
57. L.C. Jackson and L.F. Broadway, *Proc. Roy. Soc. (London) Ser. A* 127, 678 (1930).
58. B.M. Anand, P.N. Kalia and M. Ram, *Indian J. Physic*, 17, 69 (1943).
59. E. Inn, private communication.
60. D.S. Jackson and H.I. Schiff, *J. Chem. Phys.* 21, 2233 (1953).
D.S. Jackson, McGill University Thesis.
61. E. Wrede, *Z. Physik*, 54, 53 (1929).
62. Lord Rayleigh, *Proc. Roy. Soc. (London) Ser. A* 102, 453 (1922).
63. M. Duffieux, *Nature*, 117, 302 (1926).

64. J. Kaplan, Proc. Nat. Acad. Sci. 14, 258 (1928).
65. J. Kaplan, Phys. Rev. 53, 189 (1929).
66. J. Kaplan, Phys. Rev. 45, 675 (1934).
67. E.E. Muschlitz Jr. and J. Goodman, J. Chem. Phys. 21, 2213 (1953).
68. J. Janin, Compt. rend. 223, 321 (1946).
69. R.E. Worley, Phys. Rev. 64, 207 (1943).
70. R. Meyerott, Phys. Rev. 71, 133 (1947).
71. R.W. Nicholls, Nature, 162, 231 (1948).
72. R.W.B. Pearse and A.G. Gaydon, The Identification of Molecular Spectra, London, 1950.
73. G. Herzberg, Phys. Rev. 69, 362 (1946).
74. G. Herzberg and L. Herzberg, Nature, 161, 283 (1948)
75. R.W. Nicholls, Nature, 167, 31 (1951).
76. R. Herman, C. R. Acad. Sci. Paris, 217, 141 (1943).
Ann. de Phys. (11) 20, 241 (1945).
77. K.H. Geib, Ergeb. exakt. Naturw. 15, 44 (1936).
78. E.W.R. Steacie, Atomic and Free Radical Reactions, New York, 1946.
79. B de B Darwent, E.W.R. Steacie and A.F. van Winckel, J. Chem. Phys. 14, 551 (1946).
80. R.A. Marcus, B de B Darwent and E.W.R. Steacie, J. Chem. Phys. 16, 987 (1948).
81. M.K. Phibbs and B de B Darwent, J. Chem. Phys. 18, 495 (1950).
82. W.R. Trost, B de B Darwent and E.W.R. Steacie, J. Chem. Phys. 16, 353 (1948).
83. Shinjiro Kodama, Yoshimasa Takezaki and Joji Yoshida, J. Chem. Soc. Japan, Pure Chem. Sect. 71, 173 (1950).
84. M.K. Phibbs and B de B Darwent, Can. J. Research, Sect. B, 28, 395 (1950).

85. P.J. Le Roy, Can J. Research, Sect. B, 28, 492 (1950).
86. The Radio Amateur's Handbook, American Radio Relay League, Concord, N.H. 1952, page 159.
87. The Radio Amateur's Handbook, American Radio Relay League, Concord, N.H. 1952, page 200.
88. I.M. Kolthoff and E.B. Sandell, Textbook of Quantitative Inorganic Analysis, The Macmillan Co. New York, 1943.
89. C.L. Thomas, G. Egloff and J.C. Morrell, Chem. Rev. 28, 1 (1941).
90. K.H. Geib and P. Harteck, Ber. 66B, 1815 (1933).
91. O. Oldenberg and F.F. Rieke, J. Chem. Phys. 7, 485 (1939).
92. W.H. Rodebush, C.W.J. Wende and R.W. Campbell, J.A.C.S. 59, 1924 (1937).

